

Transport of  
reactive carriers and contaminants  
in groundwater systems

*a dynamic competitive happening*

Promotoren: dr. ir. W. H. van Riemsdijk,  
hoogleraar in de bodemscheikunde en chemische bodemkwaliteit

dr. ir. A. Leijnse,  
hoogleraar in de grondwaterkwaliteit

Transport of  
reactive carriers and contaminants  
in groundwater systems

*a dynamic competitive happening*

H. van de Weerd

**Proefschrift**

ter verkrijging van de graad van doctor  
op gezag van de rector magnificus  
van Wageningen Universiteit,  
dr. ir. L. Speelman,  
in het openbaar te verdedigen  
op maandag 23 oktober 2000  
des namiddags te vier uur in de Aula

The research presented in this thesis has been carried out at the Department of Environmental Sciences, sub-department of Soil Quality of Wageningen University. The research was partly funded by this sub-department and by the National Institute of Public Health and the Environment (RIVM).

Financial support for the publication of this thesis by Wageningen University and the Hanneke van Holk Fonds is gratefully acknowledged.

CIP-DATA KONINKLIJKE BIBLIOTHEEK, DEN HAAG

van de Weerd, Hendrika.

Transport of reactive carriers and contaminants in groundwater systems: a dynamic competitive happening / Hendrika van de Weerd.-[S.1.: s.n.]  
Thesis Wageningen University, The Netherlands. - With ref. - with summary in Dutch  
ISBN 90-5808-290-3

Subject headings: transport processes/ adsorption/ contaminants/ organic matter/  
groundwater/ simulation models

Cover: Detail of a groundwater system with carriers and contaminants

Printing: Grafisch bedrijf Ponsen & Looijen BV, Wageningen

# Abstract

Van de Weerd, H. 2000. **Transport of reactive carriers and contaminants in groundwater systems: a dynamic competitive happening**. Doctoral Thesis, Wageningen University, Wageningen, The Netherlands, 152 pages.

Transport of contaminants constitutes a potential threat for public health and ecosystems. One of the potential pathways for contaminant transport in groundwater systems is transport adsorbed to carriers (colloidal particles, large molecules). In this thesis adsorption and transport models for carriers and contaminants are developed and applied in order to increase the understanding of the behavior of carriers and the behavior of contaminants in a system with carriers. Emphasis is put on mobile natural organic matter (NOM), which is a major carrier for contaminants in soil and groundwater systems.

The first part of this thesis considers the behavior of contaminants in a system with a constant concentration of carriers. Using a model for coupled carrier and contaminants transport (COLTRAP) the effect of reaction rates and non-linearity on contaminant transport is studied. Varying the reaction rates of carrier-solid matrix and contaminant-carrier reactions, it is shown that a range exists in which time dependent reactions determine the transport of contaminants. Transport processes within this range can only be described and understood using models considering dynamic sorption, like COLTRAP. Transport at and beyond the limits of this range can be calculated with equilibrium models. Simulation of a column experiment under natural conditions shows that time dependent contaminant-carrier and carrier-solid matrix interactions are important under these conditions. In this experiment, the mobility of a radioactive contaminant (americium) is dramatically increased due to the presence of mobile NOM. Both desorption of Am from NOM and interaction between mobile and immobile NOM are found to be time dependent (slow).

The second part of this thesis considers the behavior of NOM in more detail. As mobile NOM is a mixture of molecules varying from simple small molecules like citric acid to complicated large molecules like humic acid, its adsorption behavior cannot be fully understood from mono-component adsorption models. The NOMADS model (NOM adsorption) is developed in order to describe the dynamic competitive adsorption/desorption of NOM subcomponents on a homogeneous surface. Furthermore, a method to minimize the number of adaptable parameters is developed. The model allows illustrating and quantifying important features of sorption and transport of a mixture of NOM molecules, like apparent adsorption/desorption hysteresis, slow increasing sorption maxima and large tailing of NOM breakthrough curves. It is shown that experimental results over a large range of temporal and spatial scales and surface to volume ratio's can be successfully described using the same set of model parameters. The behavior of NOM is described in laboratory batch experiments with a few grams of soil and some tens of milliliters of water and also in a field experiment with large travel times, distances of some meters and large volumes of soil.

The two main mechanisms found in this research are time dependent sorption reactions and dynamic competitive sorption of a carrier mixture. It is shown that these mechanisms are relevant for contaminant and carrier transport under natural conditions. They may determine main features of contaminant and carrier transport in groundwater systems and therefore also determine potential risks for public health and ecosystems.

*Keywords:* adsorption, desorption, adsorption kinetics, transport processes, contaminant transport, facilitated transport, contaminants, radionuclide, competitive adsorption, polydispersity, natural organic matter, NOM, dissolved organic matter, DOM, DOC, humic substances, colloids, colloidal particles, modeling, simulation, groundwater, porous media, soil



*Pro Deo*

*energiek bezig, rusteloos op zoek,  
ontwaakt besef, niet doen maar zijn,  
rust in de tuin, de knoppen springen open*



# Contents

page

Chapter 1	General introduction	1
Chapter 2	Transport of reactive colloids and contaminants in groundwater: effect of nonlinear kinetic interactions	13
Chapter 3	Assessment of the effect of kinetics on colloid facilitated radionuclide transport in porous media	37
Chapter 4	Modeling the dynamic adsorption/desorption of a NOM mixture: effects of physical and chemical heterogeneity	53
Chapter 5	Modeling transport of a mixture of Natural Organic Molecules (NOM): effects of dynamic competitive sorption from particle to aquifer scale	75
Chapter 6	Summary and conclusions	113
	Samenvatting	123
	Nawoord	135
	Curriculum vitae	139
	List of Publications	141

# Chapter 1

## General Introduction

### Background and aim

Contaminants originating from the activities of man have entered the subsurface environment through spillage, land application and waste disposal practices, either on purpose or by accident. The presence and transport of contaminants constitute a potential threat to human health and ecosystems. Protection of public health and ecosystems rely on the ability to predict the transport and distribution of contaminants in the vadose and saturated zones. However, attempts to describe and predict contaminant transport cannot succeed if major pathways and mechanisms for transport are not understood and accounted for.

Major pathways and mechanisms for transport of contaminants may differ in the vadose and saturated zone, due to different conditions. In general, the vadose zone is characterized by the presence of oxygen, the presence of a gas-water interface, relatively high concentrations of particulate organic matter and relatively high microbial activity. Chemical conditions can be highly variable in time and place, due to dilution with rainwater or concentration due to evapotranspiration and due to large horizontal and vertical variations in the composition of the solid phase. Transport of contaminants in the vadose zone will be mainly vertical. The conditions during this vertical transport will be highly variable. The saturated zone on the other hand is in general characterized by much lower organic matter contents, much lower oxygen content and a lower sorption capacity of the solid phase. In comparison with the vadose zone, chemical conditions will be less variable in time and space because in general, the influence of dilution and evapotranspiration will be negligible, and the composition of the solid phase in horizontal and vertical direction will be less variable. Transport of contaminants in the saturated zone will be mainly horizontal.

The mobility of contaminants is dependent on their distribution between the

## CHAPTER 1

immobile solid phase and the mobile aqueous phase. Many contaminants readily sorb to immobile aquifer media and are therefore considered to be virtually immobile in the subsurface, thus presenting little danger to, e.g., groundwater supplies. For example, many metals and radionuclides bind strongly to mineral components and particulate organic matter of the solid phase, while many non-polar organic contaminants have a high affinity for binding to particulate organic matter (McCarthy and Zachara, 1989). However, these virtually immobile contaminants may present danger in the following situations. Chemical conditions may change in such a way that desorption and thus mobilization of these contaminants occurs. Further, the supply of contaminants may occur in high concentrations or over long periods, resulting in saturation of the sorption complex. In case of saturation of the sorption complex contaminant transport will be unretarded. Moreover, the liquid phase also may contain reactive surfaces in the form of small particles, colloids, or large molecules. Contaminants may bind to these "carrier" surfaces and in this way their mobility may change. This has been observed in both laboratory experiments (Dunnivant *et al.*, 1992a, Kim *et al.*, 1994a, 1994b, Saiers and Hornberger, 1996) and field situations (Von Gunten *et al.*, 1988; Buddemeier and Hunt, 1988).

In recent years the interest in, and concern about, the potential role of carriers in contaminant transport has grown. Both organic and inorganic and even mixtures of organic and inorganic carriers exist. They differ in origin and their concentration ranges from  $10^8$  to more than  $10^{12}$  particles/l (Degueldre *et al.*, 1989; Gschwend and Reynolds, 1987; Longworth and Ivanovich, 1989; Short *et al.*, 1988; Kim *et al.*, 1987). One of the major carriers for contaminants is natural organic matter that is ubiquitous present in soil solution and groundwater. Because carriers are reactive as well, they will also distribute between the immobile solid phase and mobile aqueous phase. It is not a simple task to determine the potential role of carriers. We are dealing with a complicated system in which interactions occur between contaminants and the solid matrix, between carriers and the solid matrix, and between contaminants and carriers, that may be in the aqueous phase or sorbed to the solid matrix. The relative importance of the different interactions depends on the physical and chemical conditions, the type of carrier and contaminant, the type of solid matrix and the initial and boundary conditions of the situation studied. Moreover, interactions in natural systems are often nonlinear and evidence exists that contaminant-carrier and carrier-solid matrix interactions are slow relative to other interactions in natural systems (Buffle, 1988; Dunnivant *et al.*, 1992b, Saiers *et al.*, 1994). Finally, the heterogeneity of carrier surfaces

and of the solid matrix may play a role, and we may have to deal with a heterogeneous mixture of carrier molecules instead of with "one carrier".

To identify whether, and in what situations, transport with carriers is a major pathway for contaminant transport, more knowledge is needed on the behavior of carriers and on the behavior of contaminants in a system where carriers are present. Because of the large variation in potential carriers, contaminants and conditions, it is impossible to provide a general answer. To increase knowledge, it is necessary to focus, for instance on a specific type of carrier. Focusing creates the possibility to get more insight in specific mechanisms that may have much wider implications.

The central aim of this study is to identify and describe relevant mechanisms determining the transport of reactive carriers and contaminants in groundwater systems. It does so by a process of model development and model application. Three activities can be distinguished in this process:

- 1 Available knowledge on carrier and contaminant behavior and transport is integrated, and made applicable in mechanistic models.
- 2 Using the models, phenomena reported in literature are described and experiments (in the laboratory and the field) are simulated. In this way, it is made plausible that the process descriptions in the models are appropriate (weak validation; Leijnse and Hassanizadeh, 1994). Where necessary, the models are refined or adapted.
- 3 Model simulations are performed to show potential effects and potential critical situations in the "real world".

To refine the scope of this research, emphasis is put on the behavior of mobile natural organic matter (NOM), which is a major carrier for contaminants. Understanding its behavior has appeared to be an interesting challenge.

Although this research focuses on transport of reactive carriers and contaminants in groundwater systems, the results might have a broader area of application. Mechanisms found may be relevant as well for transport in the vadose zone or in the practice of subsurface remediation and water treatment.

In the second part of this chapter some properties of NOM and its occurrence in natural situations are considered. The third part describes the modeling approach and its implication in more detail. Finally, the outline of this thesis is given.

## Mobile natural organic matter

Mobile NOM (also called dissolved organic matter, DOM) is a mixture of different molecules, varying in size from 0.5 to approximately 400 nm and in molecular weight from 200 to  $> 10^5$  g.mol<sup>-1</sup>. Small molecules can be well defined, weak organic polyacids like, e.g., citric acid, which has a molecular diameter of approximately 0.5 NM and a molecular mass of 349 g.mol<sup>-1</sup>. Low molecular weight humic molecules are more or less flexible cylinders (so-called "oblong" particles) or more compact globular particles or ellipsoids. The high molecular weight humic molecules are large enough to form random coils or gels (Hayes et al, 1989). It is not easy to attribute a size to them as the conformation of these structures may easily change as a function of the environmental conditions. The diameter of high molecular weight humic molecules generally is estimated not to be larger than 5 nm (McCarthy et al, 1993 , de Wit et al, 1992). However, Kim et al (1992) found humic colloids with diameters up to 400 nm in a saline aquifer system. Probably, these colloids are aggregates of large humic molecules. Mobile NOM molecules contain functional groups like carboxyl, alcohol and quinone groups in variable concentrations and in general are negatively charged or neutral.

In general the concentration of NOM is measured in mg C/l. Clearly, NOM mixtures with the same "concentration" can have completely different compositions. Both the distribution of chemical properties and of molecular weight may differ. As a result of this, the chemical behavior of mixtures with "equal concentration" is expected to differ as well. Therefore, apart from the "concentration" of NOM, properties like the percentage of hydrophobic and hydrophilic NOM, and the molecular weight distribution are important properties.

Mean NOM concentrations in shallow groundwater in the Netherlands as measured by different authors varied between 10 and 20 mg C/l (Groot, 1996; Van Breemen et al., 1988; Boumans and Fraters, 1993). Kim et al (1992) measured NOM concentrations in groundwater from the Gorleben aquifers system in Germany. They sampled (anaerobically) water from shallow Pleistocene sand and silt aquifers with low salt content, and from a relatively deep and saline aquifer with glacial intercalation's of lignite. NOM concentrations varied from 0.1 and 16 mg C/l in the shallow aquifers with low salt content ( I = 0.004 - 0.007 M, pH 8-9 ) to 80 and 98 mg C/l in the deep saline aquifers ( I = 0.02 -

0.05 M, pH 7.5-8.5) with lignite. In the shallow aquifer, most NOM falls in the size range from 1 to 2 nm. In the deep saline aquifer however, most NOM falls in the size range from 1 to 100 nm. McCarthy et al (1996) measured NOM concentrations of 1.8 mg C/l in a shallow sandy coastal plain aquifer ( $I=0.003$ , pH 8). 90% of this NOM had a molecular weight lower than 3000 (g/mol). Obviously, the NOM concentration and the composition of NOM may vary widely between aquifers.

## **Modeling approach**

The central aim of this study is to find and describe the relevant mechanisms determining the transport of reactive carriers and contaminants in groundwater systems. Groundwater systems are complex systems. All kinds of processes occur simultaneously and we have to deal with geologic heterogeneities. To identify the major processes that result in certain observations we have to simplify reality. Processes, heterogeneities and details that are thought to be less relevant have to be discarded. The art of modeling is to reduce the complexity of “real world” in such a measure that, on one hand the model is applicable and comprehensible and, on the other hand the relevant processes are well described. Three important aspects of a modeling approach are (1) the type of model used, (2) the simplifications or assumptions made, and (3) the validation of the model. These three aspects of the modeling approach used in this research are addressed, and conclusively their implications to the applicability of this research are described.

### *Type of model*

The intention of this study is to find rules with a broad area of application. Rules that are valid for a range of conditions, different types of systems (laboratory batch and column experiments, in the field) and hopefully also valid in other area's of research. Therefore, our modeling approach is mechanistic. We are inspired by available knowledge from different scientific fields (colloid and environmental chemistry, soil science, hydrology). This knowledge is integrated in relationships that, where possible, represent the most fundamental mechanisms that determine transport of reactive contaminants and carriers in aquifer systems. However, a certain degree of empirical descriptions is unavoidable. Where

## CHAPTER 1

empirical descriptions are used, they are based on physical chemical insight or on observations from literature.

### *Simplifications*

To promote the applicability of the models and to fully understand the processes considered it is important to keep them as simple as possible and to reduce the number of unknown parameters. Further, it is important to choose model parameters in such a way that they have a meaning and can be estimated from independent experiments. In this study simplifications are made for both the interaction mechanisms in the system, as well as for the transport processes. They are chosen in such a way that we expect that the relevant mechanisms for carrier and contaminant transport under relatively constant aquifer conditions are still described.

For the interaction mechanisms the following simplifications are made. Only adsorption/desorption processes of carriers and contaminants are assumed. Flocculation and precipitation/dissolution processes are neglected. The conditions during these sorption processes (ionic strength, pH, concentration of competing species) are assumed to be constant. Adsorption properties of carriers are assumed to be independent of contaminants sorbed to them. Further, the surface heterogeneity is neglected.

For the transport processes we made the following simplifications. It is assumed that adsorption or desorption of carrier molecules to the solid matrix, does not affect the porous structure. Water transport is assumed to be one dimensional and saturated. The dispersive mass flux is described by a Fickian type relation. Further it is assumed that the porosity, flow velocity and dispersion coefficient are constant.

### *Weak validation*

It is necessary to relate models with the "real world" and to make plausible that process descriptions in models are valid. Therefore, observations to feed and evaluate the model are necessary. Often the term validation is used for testing models against observations. However, much discussion exists about the definition of the term validation. In this study we intend to test the appropriateness of the basic equations in the model in a large variety of situations, and at different scales, regardless of parameter values and boundary and initial conditions. According to Leijnse and Hassanizadeh (1994) this is "weak validation". In this study, first data from laboratory experiments are used to feed and evaluate the model.

Because laboratory experiments are well controlled, they are appropriate to test whether the process descriptions in the model are valid. It is sensible to use data from different types of laboratory experiments to evaluate the process descriptions, because they will reveal different aspects of the occurring processes. If observations from laboratory experiments of different type and scale can be explained by the mechanisms incorporated in the model, this is strong evidence that the process descriptions are appropriate. Once the behavior at the laboratory scale is well described and understood, the validity of the model in field situations is studied. Observations from the field are scarce and are generally not easy to interpret because field situations are less controlled. We have to deal with heterogeneity and uncertainty, because boundary and initial conditions are generally not known. Moreover, the flow pattern of water is 3-D, which requires models with complicated water flow, making it more complicated to include chemistry.

#### *Implication of the chosen modeling approach*

If a model is applied, it is important to be aware of the simplifications made in the model. In this study, we aim at applying a model that is tested against laboratory experiments, in the field. Field situations will differ in scale and complexity. It is important to be aware that simplifications may not be valid anymore, or new complications or processes should be taken into account. It will be evident that not all mechanisms occurring in aquifer systems are taken into account in this study due to the simplifications (see above) we made. Further, to describe transport in aquifers we have to extrapolate the model to larger spatial scales than in experiments. By increasing the spatial scale in the field, e.g., from a field experiment over a few meters to the behavior in an aquifer, the scale of complications will increase (Van der Zee, 1999). Moreover, the composition of both solution and the solid matrix in a packed soil column is generally well known. However, our knowledge of an aquifer system is often very limited. An aquifer often is characterized using only a few samples of groundwater and/or aquifer material.

Fortunately, the mechanisms, the laws found to be valid in simplified systems under certain conditions at a certain scale will be valid as well in the real world under the same and different conditions. However, it is not possible to predict their effect because the new elements in the real world possibly will influence or even overrule the effects of the modeled mechanisms. Therefore, it is not possible to prove that certain observations in "real world" are the results of certain mechanisms. However, it is possible to make plausible that

## CHAPTER 1

this is the case, by showing that the model is in accordance, or not significantly in contradiction, with these observations and with the present state of knowledge. This is the challenge of this study.

By evaluating the models against observations it is made plausibly that the processes described in the models, are relevant. Further, using the models, potential effects and potential critical situations in "real world" are distinguished. Insight gained with the modeling can be translated in main features and trends that can be used for instance in policy making or in the practice of soil remediation. Finally, assumptions made and empirical relations used may serve as starting point for further research.

### **Outline of this thesis**

This thesis is a compilation of articles (to be) published in international scientific journals. They are included without major modifications. Because it is intended that each article can be read by itself, some overlap is unavoidable. Furthermore, the terminology used in the subsequent articles varies slightly (e.g., colloids instead of carriers, attachment/detachment instead of adsorption/desorption). This thesis does not include all the work that was carried out in the past period, but it consists of the description of the mechanisms incorporated in the models and the evaluation of models against data. Further work can be found in the list of publications.

In the next two chapters the behavior of contaminants in a system where carriers are present is addressed. In **Chapter 2** a model for carrier and contaminant transport is presented. Using this model, the effect of nonlinear and non-equilibrium interactions on contaminant transport behavior is shown. The results are qualitatively compared with results from transport experiments. In **Chapter 3**, the model presented in Chapter 2 is used to simulate transport of the radionuclide americium in an experiment. In this experiment aquifer columns are used that are in equilibrium with mobile NOM.

Chapter 4 and 5 focus on the behavior of NOM in groundwater systems. **Chapter 4** reviews experimental results of NOM adsorption/desorption to oxide surfaces. A model describing the adsorption/desorption behavior of NOM is developed and applied to experimental data. **Chapter 5** reviews experimental results of NOM transport in soil and

aquifer material. The adsorption/desorption model developed in Chapter 4 is incorporated in a transport code and transport experiments in both the laboratory and the field are simulated.

In **Chapter 6**, the main findings of this research are integrated and discussed together with their implications.

## References

- Buddemeier R.W. and Hunt J.R. 1988. Transport of colloidal contaminants in groundwater: radionuclide migration at the Nevada test site. *Appl. Geochem.*, 3, 535-548.
- Buffle J. 1988. Complexation reactions in aquatic systems: an analytical approach. In: Chalmers R.A. and Masson M.R (Eds.). Ellis Horwood Series in Analytical chemistry, Ellis Horwood Limited, Chichester, UK.
- Boumans L.J.M. and Fraters D. 1993. Cadmium, chroom, zink en arseen in het freatische grondwater van de zandgebieden van Nederland onder bos en heidevelden. RIVM report no. 71230001, Bilthoven, The Netherlands.
- Degueldre C.A., Baeyens B., Goerlich W., Riga J., Verbist J. and Stadelmann P. 1989. Colloids in water from a subsurface fracture in granitic rock, Grimsel test site, Switzerland. *Geochim. Cosmochim. Acta*, 53, 603-610.
- De Wit J.C.M., Van Riemsdijk W.H. and Koopal L.K. 1993. Proton binding to humic substances. A. Electrostatic effects. *Environ. Sci. Technol.* 27, 2005-2014.
- Dunnivant F.M., Jardine P.M., Taylor D.L. and McCarthy J.F. 1992a. Cotransport of cadmium and hexachlorobiphenyl by dissolved organic carbon through columns containing aquifer material. *Environ. Sci. Technol.*, 26(2), 360-368.
- Dunnivant F.M., Jardine P.M., Taylor D.L. and McCarthy J.F. 1992b. Transport of naturally occurring dissolved organic carbon in laboratory columns containing aquifer material. *Soil Sci. Soc. Am. J.*, 56(2), 437-444.
- Groot M.S.M. 1996. Landelijk meetnet bodemkwaliteit, resultaten 1993. RIVM report no. 714801007, Bilthoven, The Netherlands.
- Gschwend P.M. and Reynolds M.D. 1987. Monodisperse ferrous phosphate colloids in an anoxic groundwater plume. *J. Contam. Hydrol.*, 1, 309-327.
- Hayes M.H.B, MacCarthy P., Malcolm R.L., Swift R.S. (Eds.) 1989. Humic Substances II: In Search of Structure, Wiley Interscience, New York
- Kim J.I., Buckau G. and Klenze R. 1987. Natural colloids and generation of actinide pseudocolloids in groundwater. In: Come B. and Chapman N.A. (Eds.), Natural Analogues in Radioactive Waste Disposal, pp. 289-299, Graham and Trotman, London.
- Kim J.I., Delakowitz B., Zeh P., Probst T., Lin X., Ehrlicher U., Schauer C. 1992. Appendix I in: Colloid migration in groundwaters: geochemical interactions of radionuclides with natural colloids, 2nd progress report, RCM 00692, Technische universität münchen.
- Kim J.I., Delakowitz B., Zeh P., Probst T., Lin X., Ehrlicher U., Schauer C. 1994a. Appendix I. In: Colloid Migration in groundwaters: geochemical interactions of radionuclides with natural colloids, RCM 00394, Technische

## CHAPTER 1

Universitat Munchen, pp. 16-61

- Kim J.I., Delakowitz B., Zeh P., Klotz D. and Lazik D. 1994b. A column experiment for the study of colloidal radionuclide migration in Gorleben aquifer systems. *Radiochim. Acta*, 66/67, 165-171.
- Leijnse A. and Hassanizadeh S.M. 1994. Model definition and model validation. *Adv. Water Resour.* 17, 197-200.
- Longworth G. and Ivanovich M. 1989. The sampling and characterization of natural groundwater colloids: studies in aquifers in slate, granite and glacial sand, *NSS/R165*, Harwell Laboratory, Harwell, UK.
- McCarthy J.F. and Zachara J.M. 1989. Subsurface transport of contaminants. *Environ. Sci. Technol.* 23, 496-502.
- McCarthy J.F., Williams T.M., Liang L., Jardine P.M., Jolley L.W., Taylor D.L., Palumbo A.V. and Cooper L.W. 1993. Mobility of Natural Organic Matter in a Sandy Aquifer. *Environ. Sci. Technol.* (4), 667-676.
- McCarthy J.F., Gu B., Liang L., Mas-Pla J., Williams T.M. and Yeh T-C.J. 1996. Field tracer tests on the mobility of natural organic matter in a sandy aquifer. *Water Resour. Res.* 32(5), 1223-1238.
- Saiers J.E., Hornberger G.M. and Liang L. 1994. First- and second-order kinetics approaches for modeling the transport of colloidal particles in porous media. *Water Resour. Res.*, 30(9), 2499-2506.
- Saiers J.E. and Hornberger G.M. 1996. The role of colloidal kaolinite in the transport of cesium through laboratory sand columns. *Water Resour. Res.*, 32(1), 33-41.
- Short S.A., Lawson R.T. and Ellis J. 1988. Uranium-234/Uranium-238, and Thorium-230/Uranium-234 activity ratios in the colloidal phases of aquifers in lateritic weathered zones. *Geochim. Cosmochim. Acta*, 52, 2555-2563.
- Van Breemen N., Visser W.F.J. and Pape Th. (Eds) 1988. Biogeochemistry of an oak-woodland ecosystem in the Netherlands affected by acid atmospheric deposition. Pudoc Wageningen, Agricultural research reports.
- Van der Zee S.E.A.T.M. 1999. Grondgebonden residuen. Inaug. Rede, Landbouwniversiteit Wageningen.
- Von Gunten H.R., Waber U.E., Krahenbuhl U. 1988. The reactor accident at chernobyl: a possibility to test colloid-controlled transport of radionuclide in a shallow aquifer. *J. Contam. Hydrol.*, 2, 237-247.



# Chapter 2

## **Transport of reactive colloids and contaminants in groundwater: effect of non-linear kinetic interactions\***

### **Abstract**

Transport of reactive colloids in groundwater may enhance the transport of contaminants in groundwater. Often, the interpretation of results of transport experiments is not a simple task as both reactions of colloids with the solid matrix and reactions of contaminants with the solid matrix and mobile and immobile colloids may be time dependent and non-linear. Further colloid transport properties may differ from solute transport properties.

In this paper, a one-dimensional model for coupled colloid and contaminant transport in a porous medium (COLTRAP) is presented together with simulation results. Calculated breakthrough curves (BTC's) during contamination and decontamination show systematically the effect of non-linear and kinetic interactions on contaminant transport in the presence of reactive colloids, and the effect of colloid transport properties that differ from solute transport properties. It is shown that in case of linear kinetic reactions, the rate of exchange of mobile and immobile colloids have a large impact on the shape of BTC's even if the solid matrix is saturated with respect to colloids. BTC's during the contamination and decontamination phase have identical shapes in this case. Moreover, the slow reactions of contaminants and colloids may lead to unretarded breakthrough of contaminants. Independent of reaction rates, non-linear reactions lead to BTC's that are steeper during contamination than in the linear case. A characteristic aspect of non-linear sorption is that shapes of BTC's differ during the contamination and decontamination phase.

It has been observed that shapes of some of the simulated adsorption and desorption curves are similar as shapes found in experiments reported in literature. This stresses the importance of incorporating both kinetics and non-linearity in models for coupled colloid and contaminant transport and the capability of COLTRAP to interpret experimental results. Finally, to figure out whether non-linear processes play a role, it is very important to consider both contamination and decontamination in transport experiments.

---

\* by H. van de Weerd, A. Leijnse and W.H. van Riemsdijk  
published in: Journal of Contaminant Hydrology 32(1998) 313-331

## Introduction

In natural groundwater, both inorganic and organic colloids are present. They differ in origin and their concentration ranges from  $10^8$  to more than  $10^{12}$  particles/l (Degueldre *et al.*, 1989, Gschwend and Reynolds, 1987, Longworth and Ivanovich, 1989, Short *et al.*, 1988, Kim *et al.*, 1987). When these colloids are transported over large distances, they can act as a carrier for contaminants and enhance the transport of e.g. trace metals. This has been observed in both laboratory experiments (Dunnivant *et al.*, 1992a, Kim *et al.*, 1994a, b, Saiers and Hornberger, 1996a) and field situations (Von Gunten *et al.*, 1988, Buddemeier and Hunt, 1988).

Due to their size and charge, colloids may be excluded from a part of the water-filled void space and thus transport properties of colloids may differ from solute transport properties. In experiments, the average velocity of inert colloids is found to be equal or larger than the average water velocity (Enfield and Bengtsson, 1988, Puls and Powell, 1992, Small, 1974). Also, a fraction of the colloids may be immobile due to attachment to the solid matrix. Consequently, colloids may travel faster or slower than inert solutes and multiple fronts of aqueous-phase contaminants, mobile colloids and contaminants bound to mobile colloids may develop.

Sorption of contaminants to the solid matrix usually is described by non-linear equilibrium isotherms, like the Freundlich and Langmuir isotherm. Sorption of contaminants to colloids can be described by the same type of isotherms. However, often desorption of contaminants from colloids is found to be slow. According to Buffle (1988), dissociation of metal complexes is a slow process relative to other processes in nature. Attachment of colloids to the solid matrix may be non-linear and kinetic as well. Saiers *et al.* (1994) showed that colloid interaction with the solid matrix can be described well with a non-linear kinetic model. Often colloid attachment is assumed to be irreversible. However, experimental evidence shows that this is not always the case (van de Weerd and Leijnse, 1997a, Dunnivant *et al.*, 1992b, McCarthy *et al.*, 1993, Saiers *et al.*, 1994), although detachment often is a very slow process.

A model for coupled contaminant and colloid transport is based on the mass balance equations for all colloid and contaminant species and equations for the interactions between these species. In case of equilibrium between the different species, the equations can be

simplified. In case of linear interactions, the introduction of retardation factors leads to further simplification of the equations.

Different models describing coupled colloid and contaminant transport have been reported (Mills *et al.* 1991, Dunnivant *et al.*, 1992b, Corapcioglu and Jiang, 1993, Jiang and Corapcioglu, 1993, Corapcioglu and Kim, 1995, Saiers and Hornberger, 1996b). Mills *et al.* (1991) and Dunnivant *et al.* (1992a) assume colloids to be non-reactive with the solid matrix. They assume the colloid concentration to be constant in time and space and take into account the effect of contaminant colloid interaction in the equation for combined contaminant and colloid facilitated contaminant transport. Jiang and Corapcioglu (1993) and Corapcioglu and Jiang (1993) assume linear non-equilibrium attachment and Saiers and Hornberger (1996b) assume non-linear kinetic but irreversible attachment of colloids to the solid matrix. They solve equations for both mobile and immobile colloids.

All models for colloid facilitated transport account for interaction of contaminants with colloids. Jiang and Corapcioglu (1993) assume linear equilibrium sorption of contaminants to the solid matrix, and to mobile and immobile colloids. Saiers and Hornberger (1996b) assume two-site kinetic sorption of contaminants to the solid matrix and non-linear equilibrium adsorption to mobile and immobile colloids. Corapcioglu and Jiang (1993) assume the sorption of contaminants to the solid matrix to be linear and in equilibrium and to mobile and immobile colloids to be linear and kinetic. In their model, mass balance equations for contaminants bound to mobile colloids, contaminants bound to immobile colloids (i.e. colloids attached to the solid matrix) and aqueous-phase contaminants are solved. They assume adsorption of contaminants to colloids to be independent of colloid concentration (i.e. the mass of adsorbent), which is in contrast with general formulations of linear adsorption reactions.

Interpretation of transport experiments in which colloid facilitated transport of contaminants occurs is often not a simple task. It is not always possible to determine interaction processes of the different species independently. Further both reactions of colloids with the solid matrix and of contaminants with the solid matrix and mobile and immobile colloids may be time dependent and non-linear and transport properties of colloids may differ from contaminant transport properties.

The aim of this paper is to show the effect of non-linear and kinetic interactions on contaminant transport in the presence of reactive colloids and the effect of colloid transport properties different from solute transport properties.

A one-dimensional model for coupled colloid and contaminant transport (COLTRAP) has been developed. In this model, the attachment of colloids to the solid matrix and the sorption of contaminants to the solid matrix and to mobile and immobile colloids is described by non-linear kinetic interaction equations. Linear sorption and equilibrium sorption can be modelled by a proper choice of the interaction parameters.

The model has been used to simulate transport of contaminants and colloids with rates of interaction varying from high (equilibrium) to low (almost inert) and with contaminant concentrations ranging from low (in the linear part of the interaction equation) to high (in the non-linear part of the interaction equation). Simulation results show the effect of the various reaction rates, the degree of non-linearity and of various ratios of colloid velocity and average water velocity and colloid and contaminant dispersion coefficients on the transport of free contaminants and contaminants bound to colloids. Model results are qualitatively compared with experimental results from literature. In an earlier paper, model results are quantitatively compared with data from an experiment (van de Weerd and Leijnse, 1997a).

### **Model description**

Figure 1 shows the six different species which are distinguished in the model. The contaminant is distributed among four different species: (1) free contaminants in the liquid phase (S1), (2) contaminants sorbed to the solid matrix (S2), (3) contaminants sorbed to mobile colloids (S3) and (4) contaminants sorbed to immobile colloids (S4). Colloids in the porous medium are distributed among two species: (1) colloids in solution (C1) and (2) colloids attached to the solid matrix (C2). Governing equations are mass balance equations for mobile and immobile contaminant and colloid species, completed with constitutive equations for kinetic non-linear interactions between colloids and the solid matrix, colloids and contaminants and contaminants and solid matrix.

It is assumed that the properties of colloids are not affected by contaminants sorbed to them. However, the properties of colloids may change once they are attached to the solid matrix; the interaction constants for contaminant sorption to mobile and immobile colloids and the number of sites available for contaminant sorption on these colloids may differ. Furthermore, it is assumed that colloids attached to the solid matrix do not affect the porous

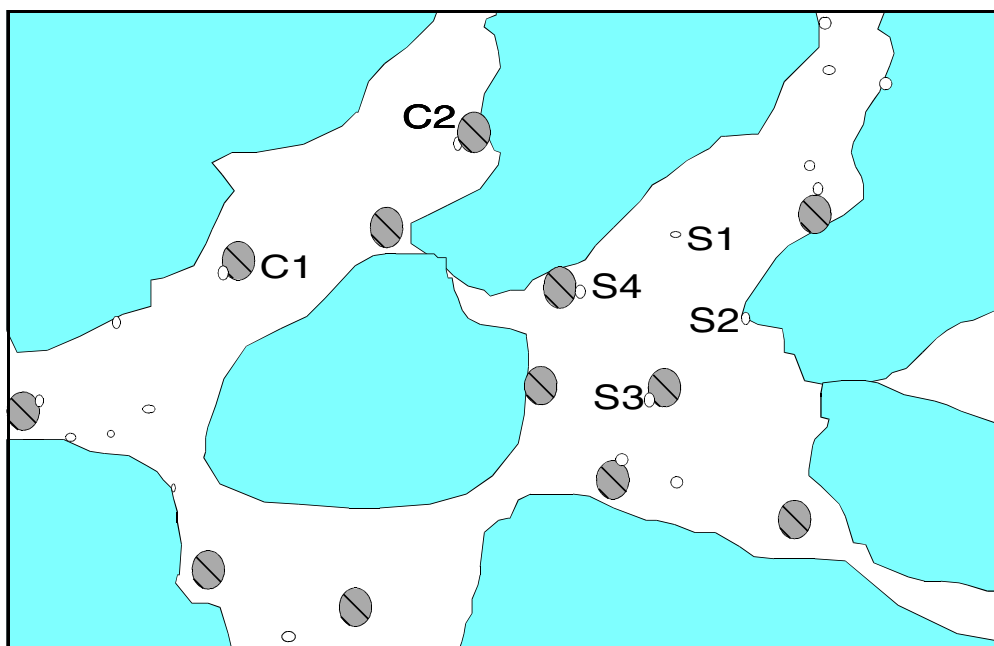


**Figure 1** Speciation of colloids (C) and contaminants (S); free contaminants in the liquid phase (S1); contaminants sorbed to the solid matrix (S2); contaminants sorbed to mobile colloids (S3); contaminants sorbed to immobile colloids (S4); colloids in the liquid phase (C1); colloids attached to the solid matrix (C2).

structure and colloid attachment does not compete with contaminant sorption to the solid matrix. Note that the term "immobile colloid" is used for colloids attached to the solid matrix, which may detach again depending on the reversibility of the interaction between colloids and the solid matrix.

In the system mobile and immobile colloid and contaminant species are present. Describing the dispersive mass flux of all species by a Fickian type relation and assuming constant porosity, velocity and dispersion coefficient, the one-dimensional mass balance equations for species W can be written as:

$$n \frac{\partial [W]}{\partial t} + n v_w \frac{\partial [W]}{\partial x} - n D_w \frac{\partial^2 [W]}{\partial x^2} = P_w \quad (1)$$

where  $t$  is time [T],  $x$  is spatial position [L],  $n$  is porosity [-] and  $v_w$  [L T<sup>-1</sup>],  $D_w$  [L<sup>2</sup> T<sup>-1</sup>] and  $P_w$  [M L<sup>-3</sup> T<sup>-1</sup>] are average velocity, dispersion coefficient and production term of species W respectively. The production term  $P_w$  is the sum of all interaction terms for species W. [W] indicates the concentration of species W per volume of pore water [M L<sup>-3</sup>]. For the aqueous-phase contaminant,  $v_w$  and  $D_w$  are the average velocity of water  $v$  and the contaminant dispersion coefficient  $D$  respectively. For contaminants sorbed to mobile colloids and for mobile colloids,  $v_w$  and  $D_w$  are given by the average velocity of colloids  $v_c$  and the

dispersion coefficient for colloids  $D_c$  respectively. For the immobile species, both  $v_w$  and  $D_w$  are zero. In this paper the mass balance equations are divided by the relative molecular or colloidal mass to obtain concentrations in mole rather than in mass per volume of pore water.

Interaction processes considered are: contaminant sorption to mobile colloids ( $P^{scm}$ ), contaminant sorption to immobile colloids ( $P^{sci}$ ), contaminant sorption to the solid matrix ( $P^s$ ) and colloid attachment to the solid matrix ( $P^c$ ). It is assumed that for all sorbing species a limited number of homogeneous binding sites exists and that variable electrostatic potential effects and other interactions between adsorbed species can be neglected. In that case the sorption reaction is given by an ideal Langmuir kinetic reaction and can be described by the following reaction equation:



where  $[S]$  is the activity of available binding sites for species A,  $[A]$  is the activity of species A and  $[SA]$  is the activity of occupied binding sites. The activity equals the concentration times an activity constant. The activity coefficient is assumed to be 1 which implies that we consider low concentrations only. Note that both SA and A are species and that their concentration is given in mole per liter pore water  $[L^{-3}]$ .  $k_a [L^3T^{-1}]$  and  $k_d [T^{-1}]$  are the forward and backward reaction rate constants, respectively. When reaction rates are high compared to the time scale of other processes in the system the forward and backward reaction may be in equilibrium.

The equilibrium constant  $K [L^3]$  is defined as follows:

$$K = \frac{k_a}{k_d} = \frac{[SA]}{[S][A]} = \frac{[SA]}{(1 - \theta)[S_t][A]} \quad (3)$$

Where  $[S_t] [L^{-3}]$  is the total concentration of binding sites and  $\theta [-]$  is the fraction of binding sites which are occupied. Without competition  $\theta S_t = [SA]$ . A kinetic Langmuir interaction equation of the following form can be derived from Equation 3:

$$\frac{\partial^i [SA]}{\partial^i t} = - \frac{\partial^i [A]}{\partial^i t} = k_a^i [A] (1 - \theta) [S_t] - k_d^i [SA]. \quad (4)$$

The superscript  $i$  is used to indicate that the change in concentration due to interaction  $i$  is considered. The interaction equation consist of an adsorption term, representing the forward

reaction rate, and a desorption term, representing the backward reaction rate. In the model COLTRAP all interaction equations have the following form:

$$P^i = n \left( k_a^i [A] (1 - \theta) [S_t] - k_d^i [SA] \right). \quad (5)$$

$P_w$  is the sum of all  $P^i$  that include species  $W$ . Other source or sink terms such as decay can also be included in  $P_w$ .

Often sorption of contaminants is assumed to be linear. This is true only if the fraction of binding sites occupied,  $\theta \ll 1$ . If equilibrium is assumed between sorption sites and the aqueous solution, the forward and backward reaction are in equilibrium and a linear sorption isotherm can be defined:

$$[SA] = K_d [A] \quad (6)$$

where  $K_d = k_a/k_d \cdot S_t = K \cdot S_t$  is the equilibrium distribution constant.

The equilibrium assumption can be investigated by using the Damkohler number. This dimensionless characteristic is given by:

$$D_k^i = k_d^i \frac{L}{v} \quad (7)$$

and gives insight in the degree of (non-)equilibrium in a certain system during a certain (dimensionless) time after a change in the influent concentration. For each kinetic reaction a Damkohler number exist. If Equation 4 is rewritten in the following way:

$$\frac{\partial^i [SA]}{\partial t} = k_d^i \left( k_a^i / k_d^i [A] (1 - \theta) [S_t] - [SA] \right) \quad (8)$$

it is evident that the rate of adsorption or desorption is determined by  $k_d^i$  times the difference between what should have been adsorbed if the system was in equilibrium and what is really adsorbed. For all reactions, a range in the value of the Damkohler number exists where the reaction changes from being insignificant (lower limit of the range) to being in equilibrium (upper limit of the range) in the system. Above and below this range, variations in Damkohler number will not change the effect of the reaction on the system. Note that the degree of non-equilibrium also influences the net adsorption or desorption rate. As the degree of non-equilibrium can change in time and place it can not be included in the Damkohler number. Further note that the Damkohler number, like e.g. the Peclet number is a characteristic of a certain system. Therefore Damkohler numbers of different experiments can not be compared without further research.

*Complete set of governing equations*

Under the assumptions given above, the mass balance equations for mobile and immobile colloids are given by:

$$n \frac{\partial C^c}{\partial t} + nv_c \frac{\partial C^c}{\partial x} - nD_c \frac{\partial^2 C^c}{\partial x^2} = -P^c \quad (9)$$

$$n \frac{\partial S^c}{\partial t} = P^c \quad (10)$$

where  $C^c$  and  $S^c$  [ $L^{-3}$ ] are the mobile and immobile colloid concentration. The interaction equation for colloid attachment to the solid matrix is given by:

$$P^c = n(k_a^c C^c (S_t^c - S^c) - k_d^c S^c) \quad (11)$$

where  $S_t^c$  [ $L^{-3}$ ] is the total number of sites available for colloid attachment. Note that in case of no competition Equation 11 is equivalent to Equation 5. Mass balance equations for free contaminants, and contaminants bound to the solid matrix are given by:

$$n \frac{\partial C^s}{\partial t} + nv \frac{\partial C^s}{\partial x} - nD \frac{\partial^2 C^s}{\partial x^2} = -P^s - P^{scm} - P^{sci} \quad (12)$$

$$n \frac{\partial S^s}{\partial t} = P^s \quad (13)$$

where  $C^s$  and  $S^s$  [ $L^{-3}$ ] are the contaminant concentration and the contaminant concentration bound to the solid matrix. Contaminant sorption to the solid matrix is given by:

$$P^s = n(k_a^s C^s [S_t^s - S^s] - k_d^s S^s) \quad (14)$$

where  $S_t^s$  [ $L^{-3}$ ] is the total number of sites available for contaminant sorption. The mass balance equations for contaminants bound to mobile and immobile colloids are given by:

$$n \frac{\partial C^{scm}}{\partial t} + nv_c \frac{\partial C^{scm}}{\partial x} - nD_c \frac{\partial^2 C^{scm}}{\partial x^2} = P^{scm} - P^{sc} \quad (15)$$

$$n \frac{\partial S^{sci}}{\partial t} = P^{sci} + P^{sc} \quad (16)$$

where  $C^{scm}$  and  $S^{sci}$  [ $L^{-3}$ ] are the concentration of contaminants bound to mobile and immobile colloids.  $C^{scm}$  and  $S^{sci}$  are products of the concentration of contaminants adsorbed per mole of colloids and the concentration of the colloids. Note that the dispersion of contaminants bound to colloids is determined by the dispersion coefficient of the colloids. In case of constant colloid concentration in space, dispersion of colloids is irrelevant for colloid transport. However, it is relevant for transport of contaminants bound to colloids as

concentration of contaminants bound to colloids may vary in space. In contrast with this, Corapcioglu and Jiang (1993), Jiang and Corapcioglu (1993) and Corapcioglu and Kim (1995) assume that the gradient of the colloid concentration is the driving force for dispersion of contaminants bound to colloids. For constant colloid concentration in space, they find dispersion of contaminants bound to colloids to be zero.

$P^{sc}$  in Equations 15 and 16 is a term accounting for mobilization or immobilization of contaminants bound to colloids due to interaction of colloids with the solid matrix. This interaction term can be given by:

$$P^{sc} = n \left( k_a^c C^{scm} [S_t^c - S^c] - k_d^c S^{sci} \right). \quad (17)$$

Contaminant sorption to mobile and immobile colloids is given by:

$$P^{scm} = n \left( k_a^{scm} C^s [C_t^{scm} C^c - C^{scm}] - k_d^{scm} C^{scm} \right) \quad (18)$$

$$P^{sci} = n \left( k_a^{sci} C^s [S_t^{sci} S^c - S^{sci}] - k_d^{sci} S^{sci} \right) \quad (19)$$

where  $S_t^{sci}$  and  $C_t^{scm}$  [-] are the total number of sites available per immobile and mobile colloid, respectively. Note that the term for adsorption to mobile or immobile colloids in Equations 18 and 19 increases if the mobile or immobile colloid concentration increases. In contrast, Corapcioglu and Jiang (1993) assume that sorption of contaminants to colloids is independent of the colloid concentration.

### *Solution method*

The governing equations together with boundary conditions for mobile species and initial conditions for all species are solved numerically by a standard Galerkin finite element method where the time derivative is approximated by a backward finite difference. Initial conditions for all species and boundary conditions for only the mobile species need to be defined. The resulting algebraic equations are solved simultaneously. A solution is obtained for the unknown concentrations  $C^c$ ,  $S^c$ ,  $C^s$ ,  $S^s$ ,  $C^{scm}$ ,  $S^{sci}$ . Non-linearities are solved by a Newton-Raphson iteration scheme.

In order to reduce round-off errors due to spatial discretization, an adaptive method is implemented where the finite element grid is dynamically refined in areas with large concentration gradients.

The code has been verified by comparing numerical results with analytical solutions (van de Weerd and Leijnse, 1997b).

## The simplified case of linear equilibrium sorption

In case of equilibrium between all sorption sites and the aqueous solution, linear sorption of contaminants and linear attachment of colloids to the solid matrix is described by:

$$S^c = K_d^c C^c \quad (20)$$

$$S^s = K_d^s C^s \quad (21)$$

with  $K_d^c = k_a^c/k_d^c \cdot S_t^c$  and  $K_d^s = k_a^s/k_d^s \cdot S_t^s$ . Sorption of contaminants to mobile and immobile colloids is described by:

$$C^{scm} = K_d^{scm} C^c C^s \quad (22)$$

$$S^{sci} = K_d^{sci} S^c C^s = K_d^{sci} K_d^c C^c C^s \quad (23)$$

with  $K_d^{scm} = k_a^{scm}/k_d^{scm} \cdot C_t^{scm}$  and  $K_d^{sci} = k_a^{sci}/k_d^{sci} \cdot S_t^{sci}$ . Combining Equations 12, 13, 15, 16, 21, 22 and 23, the mass balance equation for contaminant can be written as:

$$\begin{aligned} n \frac{\partial}{\partial t} \left( C^s (1 + K_d^s + K_d^{scm} C^c + K_d^{sci} K_d^c C^c) \right) = \\ -nv \frac{\partial C^s}{\partial x} + nD \frac{\partial^2 C^s}{\partial x^2} - nv_c \frac{\partial}{\partial x} \left( K_d^{scm} C^c C^s \right) + nD_c \frac{\partial^2}{\partial x^2} \left( K_d^{scm} C^c C^s \right). \end{aligned} \quad (24)$$

The terms at the left hand side reflect respectively: free contaminants, contaminants bound to the solid matrix, contaminants sorbed to mobile colloids and contaminants sorbed to immobile colloids. Combining Equations 9, 10 and 20, the mass balance for colloids is given by:

$$\left( 1 + K_d^c \right) n \frac{\partial C^c}{\partial t} = -nv_c \frac{\partial C^c}{\partial x} + nD_c \frac{\partial^2 C^c}{\partial x^2}. \quad (25)$$

Equation 24 can be rewritten as:

$$\begin{aligned} \left( 1 + K_d^s + K_d^{scm} C^c + K_d^{sci} K_d^c C^c \right) n \frac{\partial C^s}{\partial t} + \left( K_d^{scm} + K_d^{sci} K_d^c \right) n C^s \frac{\partial C^c}{\partial t} = \\ - \left( 1 + v_c/v K_d^{scm} C^c \right) nv \frac{\partial C^s}{\partial x} + \left( 1 + D_c/D K_d^{scm} C^c \right) nD \frac{\partial^2 C^s}{\partial x^2} + \\ K_d^{scm} C^s \left( -nv_c \frac{\partial C^c}{\partial x} + nD_c \frac{\partial^2 C^c}{\partial x^2} \right) + 2nD_c K_d^{scm} \frac{\partial C^s}{\partial x} \frac{\partial C^c}{\partial x}. \end{aligned} \quad (26)$$

If the colloid concentration is constant in time and space, Equation 26 reduces to:

$$R^* n \frac{\partial C^s}{\partial t} = -nv \frac{\partial C^s}{\partial x} + \frac{1 + D_c/D K_d^{scm} C^c}{1 + v_c/v K_d^{scm} C^c} nD \frac{\partial^2 C^s}{\partial x^2} \quad (27)$$

where the retardation factor  $R^*$  is given by:

$$R^* = \frac{1 + K_d^s + (K_d^{scm} + K_d^{sci} K_d^c) C^c}{1 + v_c/v K_d^{scm} C^c}. \quad (28)$$

Equation 27 is the conventional advection/dispersion equation with an adapted retardation factor and dispersion term. The factor multiplying the conventional dispersion term is due to the contribution of contaminants bound to colloids to the dispersion. Corapcioglu and Jiang (1993) do not consider dispersion of contaminants bound to colloids in case of constant colloid concentration in time and space. Therefore, the dispersion term in their equation is given by:

$$\frac{nD}{1 + v_c/v K_d^{scm} C^c} \frac{\partial^2 C^s}{\partial x^2}. \quad (29)$$

With this definition, the dispersion of contaminants decreases with increasing colloid concentration. In Equation 27, however, dispersion of contaminants decreases or increases depending on the ratio of  $D_c/D$  and  $v_c/v$ . If  $D_c/D > v_c/v$  the dispersion term increases if contaminants bound to colloids are present. If  $D_c/D < v_c/v$  the dispersion term decreases in these circumstances. It can be shown that for  $v_c/v = D_c/D$  Equation 27 reduces to the conventional advective/dispersion equation with an adapted retardation factor.

For equal colloid and contaminant velocities the retardation factor  $R^*$  reduces to:

$$R^* = \frac{1 + K_d^{scm} C^c + K_d^s + K_d^{sci} K_d^c C^c}{1 + K_d^{scm} C^c} = 1 + \frac{K_d^s + K_d^{sci} K_d^c C^c}{1 + K_d^{scm} C^c} \quad (30)$$

If the distribution coefficient for sorption of contaminants to immobile colloids and sorption of contaminants to mobile colloids are the same ( $K_d^{scm} = K_d^{sci}$ ) and the distribution coefficients for attachment of colloids to the solid matrix equals the coefficient for sorption of contaminants to the solid matrix ( $K_d^c = K_d^s$ ), the retardation factor  $R^*$  equals the conventional retardation factor  $R = 1 + K_d^s$ .

## Modeling results and discussion

COLTRAP has been used to investigate the effect of non-linearity, reaction rates and the effect of varying ratios of colloid and contaminant velocities and dispersion coefficients on the breakthrough curves (BTC) of contaminants in a column experiment. In all simulations the following assumptions have been made:

- We consider transport of 10 pore volumes of contaminated water with colloids (in equilibrium) through a clean soil column saturated with colloids, followed by transport of uncontaminated water with colloids. Note that in Figure 2, 3 and 4 only a part of the breakthrough curve is shown.
- Interactions of contaminants with the solid matrix is assumed to be in equilibrium.
- The interaction constants for sorption of contaminants to mobile and immobile colloids are assumed to be equal in all simulations.

Interaction parameters are chosen in such a way that in equilibrium and in the linear part of the sorption isotherm the distribution of colloids among the solution and the solid matrix is in a ratio of 1:1. The distribution of contaminants among solution (free contaminants), mobile colloids, immobile colloids and the solid matrix is in the ratio 1:1:1:2. The standard choice of model parameters and initial conditions are listed in Table 1. If deviant model parameters or conditions are used this will be noted explicitly.

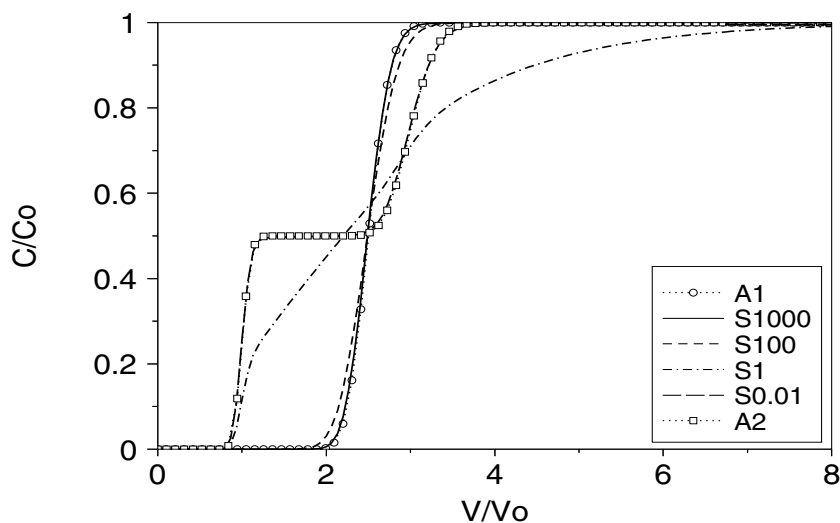


**Figure 2** Simulated breakthrough curves varying the Damkohler numbers for interaction between contaminants and colloids ( $D_k^{scm} = D_k^{sci}$ ) between 0.01 (S0.01) and 1000 (S1000) together with analytical solutions for the extreme cases: equilibrium interaction between contaminants and colloids (A1), no interaction between contaminants and colloids (A2).

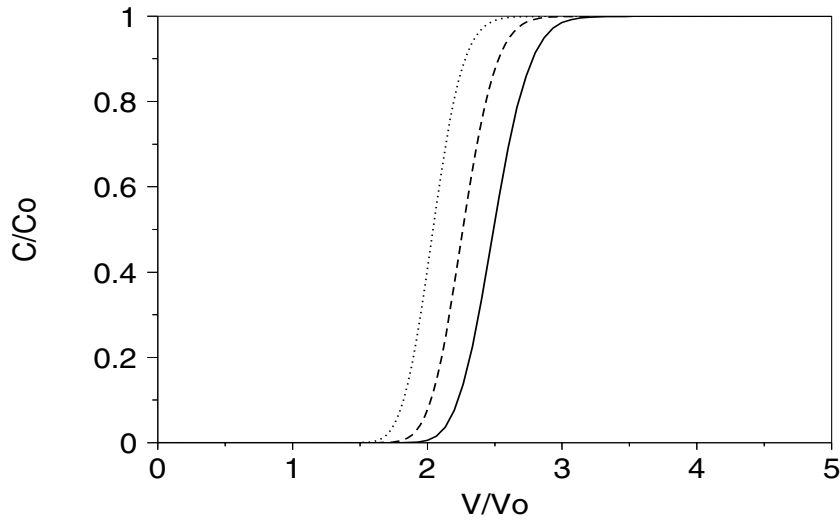


**Figure 3** Simulated breakthrough curves varying simultaneously the ratio of colloid and contaminant velocity and dispersion coefficient.  $v_c/v = D_c/D = 1$  (—), 1.2 (---), 1.4 (····).

### Linear sorption

First we will focus on the equilibrium situation. As was previously derived, in case of equilibrium, a BTC calculated with COLTRAP should be identical to a BTC calculated with the conventional advection dispersion equation using parameters from Table 1 and Equation 28 for the retardation factor (analytical solution A1 in Figure 2, Parker and Van Genuchten, 1984). From Figure 2 it is obvious that equilibrium exists if the Damkohler numbers for contaminant colloid interaction ( $D_k^{\text{scm}} = D_k^{\text{sci}}$ )  $\geq 1000$ . Note that the exchange rate between mobile and immobile colloids does not affect simulation results if equilibrium exists between contaminants and colloids. Figure 3 shows the effect of varying ratios of

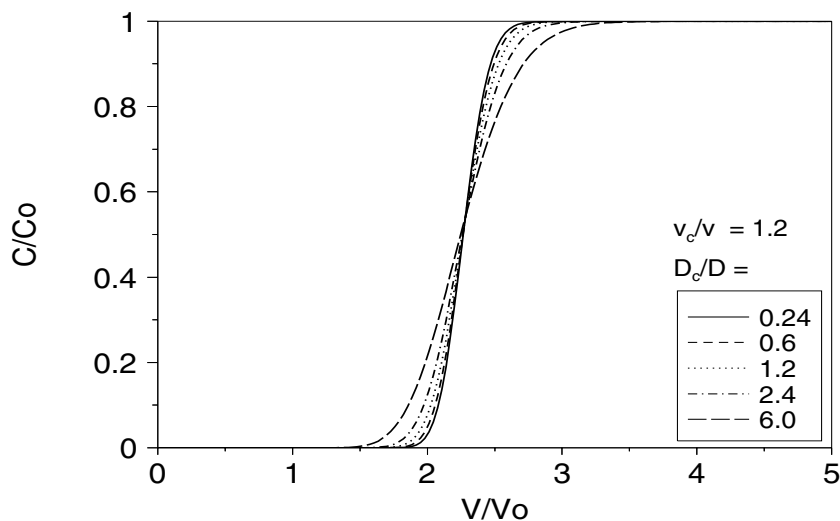


**Figure 4** Simulated breakthrough curves with a constant ratio of colloid and contaminant velocity ( $v_c/v$ ) of 1.2, varying the ratio of colloid and contaminant dispersion coefficient ( $D_c/D$ ) from 0.24 to 6.

**Table 1** Non-zero boundary and initial conditions and default parameters used for model simulations

$C^s$ - $[D/(nv)][\partial C^s/(\partial x)]$	$x=0,t$	$0 \leq t \leq t_{pulse}$	$1.0 \times 10^{-6}$	M	$S_t^s$	$2.0 \times 10^{-3}$	mol/l
$C^{sem}$ - $[D_c/(nv_c)][\partial C^{sem}/(\partial x)]$	$x=0,t$	$0 \leq t \leq t_{pulse}$	$1.0 \times 10^{-6}$	M	$k_a^s/k_d^s$	$1.0 \times 10^{+3}$	l/mol
$C^c$ - $[D_c/(nv_c)][\partial C^c/(\partial x)]$	$x=0,t$	$t \geq 0$	$1.0 \times 10^{-10}$	M	$D_k^s$	$1.0 \times 10^{+3}$	-
$C^c$ ( $x,t=0$ )		$0 \leq x \leq L$	$1.0 \times 10^{-10}$	M	$S_t^c$	$1.0 \times 10^{-7}$	mol/l
$S^c$ ( $x,t=0$ )		$0 \leq x \leq L$	$1.0 \times 10^{-10}$	M	$k_a^c/k_d^c$	$1.0 \times 10^{+7}$	l/mol
$L$			25	cm	$D_k^c$	$1.0 \times 10^{-3}$	-
$n$			0.33	-	$C_t^{sem} = S_t^{sci}$	$1.0 \times 10^{+7}$	mol/mol
$v = v_c$			2.62	cm/h	$k_a^{sem}/k_d^{sem}$	$1.0 \times 10^{+3}$	l/mol
$D = D_c$			0.22	cm <sup>2</sup> /h	$k_a^{sci}/k_d^{sci}$	$1.0 \times 10^{+3}$	l/mol
$t_{pulse}$			95.4	h	$D_k^{sem} = D_k^{sci}$	$1.0 \times 10^{+3}$	-

colloid and contaminant velocities and dispersion coefficients. According to Equation 27 and 28, the retardation factor changes from 2.5 ( $v_c/v = D_c/D = 1$ ) to 2.08 ( $v_c/v = D_c/D = 1.4$ ) but the shape of the curves remains identical. Figure 4 shows the effect of varying the ratio of the colloid and contaminant dispersion coefficient with a constant ratio of the colloid and contaminant velocity. As can be expected from Equations 27 and 28, the retardation factor remains the same but the overall dispersion coefficient increases from 0.56 ( $D_c/D = 0.24$ ,  $v_c/v = 1.2$ ) to 3.18 ( $D_c/D = 6$ ,  $v_c/v = 1.2$ ) times the contaminant dispersion coefficient. Hence, for colloid facilitated transport, the colloid dispersion coefficient affects contaminant transport even if colloid concentrations are constant in time and place.

The opposite of equilibrium between contaminants and colloids is that contaminants does not adsorb to or desorb from colloids which leads to uncoupled transport of contaminants and colloids. For uncoupled transport in the assumed model system, an analytical solution can be constructed by adding the analytical solution for inert transport of colloids ( $R=1$ ) and the transport of contaminants with the conventional retardation factor ( $R=3$ ) (analytical solution A2 in Figure 2). From Figure 2 it is obvious that transport of colloids and contaminants is uncoupled with Damkohler numbers for contaminant colloid interaction ( $D_k^{scm} = D_k^{sci}$ )  $\leq 0.01$ . If the interaction rate and thus the Damkohler number increase, transport becomes more and more coupled, the BTC becomes more symmetrical around the center of mass ( $C/Co = 0.5$ ) and in the neighborhood of equilibrium slower reaction rates have the same effect as diffusion/dispersion. The intermediate BTC has a larger tail than the extreme BTC's. This is due to contaminant adsorption on immobile colloids. In case this is negligible (i.e. very slow) the breakthrough of contaminants is dominated by the equilibrium sorption of contaminants to the solid matrix. Increasing rates of contaminant sorption to immobile colloids results in an increasing effect of immobile colloids on breakthrough of contaminants. As long as equilibrium is not reached between immobile colloids and contaminants, the concentration is affected and a tailing effect results. From Figure 2 we can conclude that very slow desorption of contaminants from colloids may result in inert transport of contaminants bound to colloids. Note that for all simulations in Figure 2 the exchange rate of mobile and immobile colloids is assumed to be negligible ( $D_k^c = 0.01$ ). Results of experiments performed by Kim *et al.* (1994b) show unretarded breakthrough of europium, americium, neptunium and protactinium (Pa) in the presence of humic colloids. Breakthrough curves of experiments with neptunium and protactinium show a plateau followed by breakthrough of a second front. Since in these

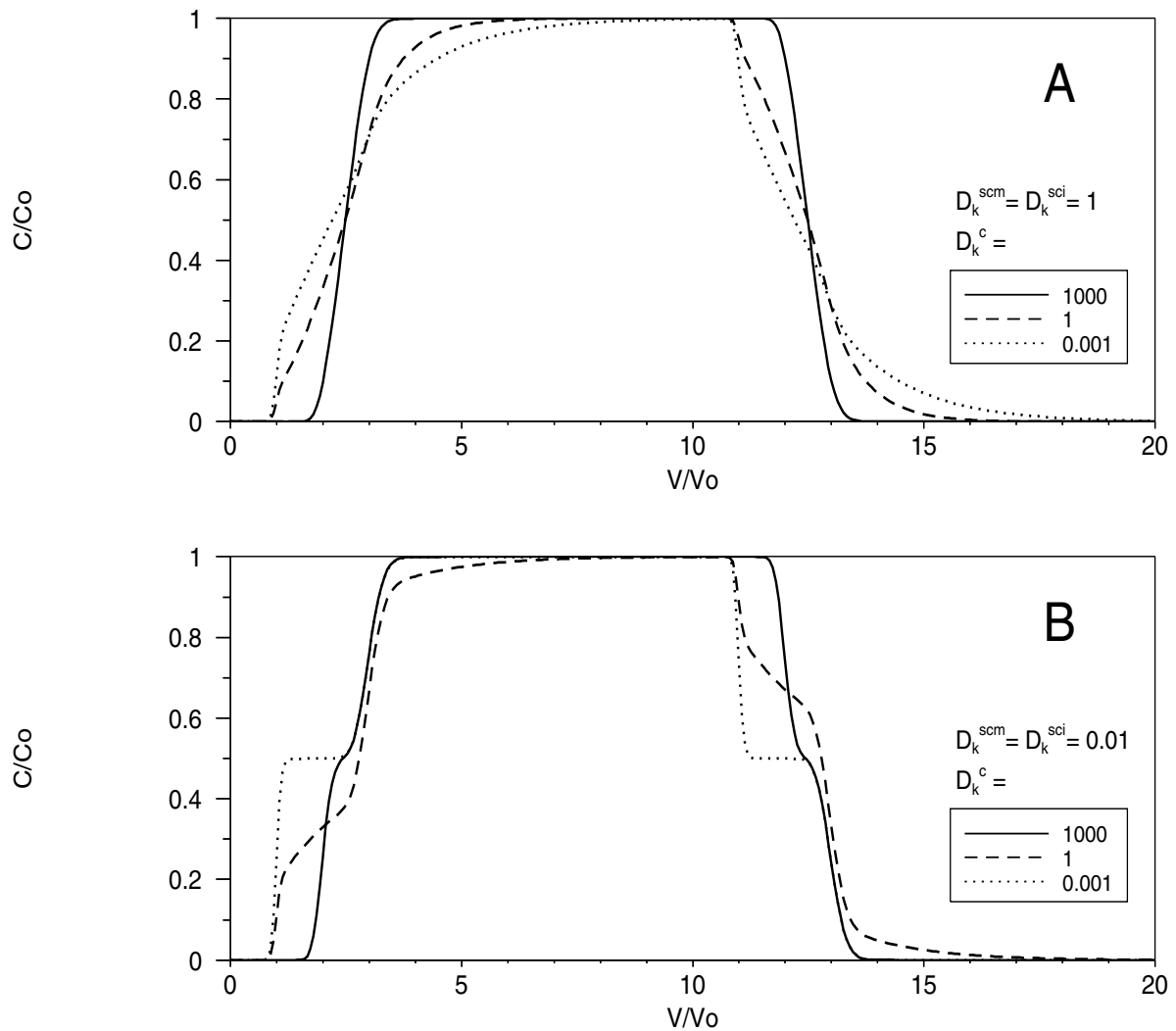


**Figure 5** Simulated breakthrough curves during contamination and decontamination, varying the Damkohler number for colloid solid matrix interaction ( $D_k^c$ ) from 0.001 to 1000, for intermediate (5A) and low interaction rates between colloids and contaminants (5B).

experiment a pulse is injected, it is not easy to interpret results. Results of experiments of Saiers and Hornberger (1996a) show unretarded breakthrough followed by a plateau and breakthrough of a second front of cesium in the presence of kaolinite colloids. The height of the plateau increases with increasing colloid concentration. This indicates that kinetic interaction of contaminants and colloids may play an important role in practice.

Figure 5 shows the effect of various exchange rates of mobile and immobile colloids. The BTC's show the breakthrough of contaminated water followed by the breakthrough of uncontaminated water. Note that the simulation in Figure 5A and 5B with  $D_k^c = 0.001$  are the same simulations as S1 and S0.01, shown in Figure 2, only now the breakthrough of uncontaminated water is shown as well. From Figure 5 we can conclude that the exchange

rate between mobile and immobile colloids has a high impact on the simulation result. With increasing exchange rate, equilibrium between mobile and immobile colloids is reached faster and thus the effect of kinetics on the simulation results will be more and more limited to non-equilibrium between colloids and contaminants. Figure 5B with intermediate exchange ( $D_k^c = 1$ ) shows extensive tailing both during breakthrough of contaminated and uncontaminated water. This is due to the slow exchange between immobile and mobile colloids. During contamination mobile colloids with contaminants exchange slowly with clean immobile colloids, during decontamination (breakthrough of uncontaminated water) the immobile colloids with contaminants exchange slowly with the clean mobile colloids. Van de Weerd and Leijnse (1997a) showed that these exchange processes may be responsible for the extensive tailing of low contaminant concentrations and the incomplete recovery within the timeframe of the experiment, found in an experiment with americium and humic colloids performed by Kim *et al.* (1994b). Extensive tailing like this is also found in an experiment performed by Grolimund *et al.* (1996). Possibly the exchange process may play a role in this experiment. However, since the colloid concentration in that experiment is not constant, this is not totally evident. The results of Figure 5 show clearly that even if the solid matrix is saturated with respect to colloids, the assumption of colloids being non-reactive with the solid matrix is only true in case of very slow exchange of mobile and immobile colloids (i.e. irreversible attachment).

Figure 5A and 5B also show that the shape of the BTC during decontamination after reflection in the time-axis (x-axis) is the same as the shape of the BTC during contamination. This is generally the case when all sorption reactions are linear and the column is in equilibrium with the contaminated water before decontamination starts. Figure 6 shows that when equilibrium is not reached before decontamination starts, this is not always the case. In Figure 6 it is shown that the shape of the reflected BTC's during decontamination does not equal the shape of the BTC during contamination if the duration of contamination pulse is decreased. However, a steep initial breakthrough of contaminated water will be followed by a steep initial breakthrough of uncontaminated water in all cases. The results of Saiers and Hornberger (1996a) show difference in shape between the BTC during contamination and the reflected BTC during decontamination. Even the initial steep breakthrough of contaminated water is not followed by a steep initial breakthrough of uncontaminated water.

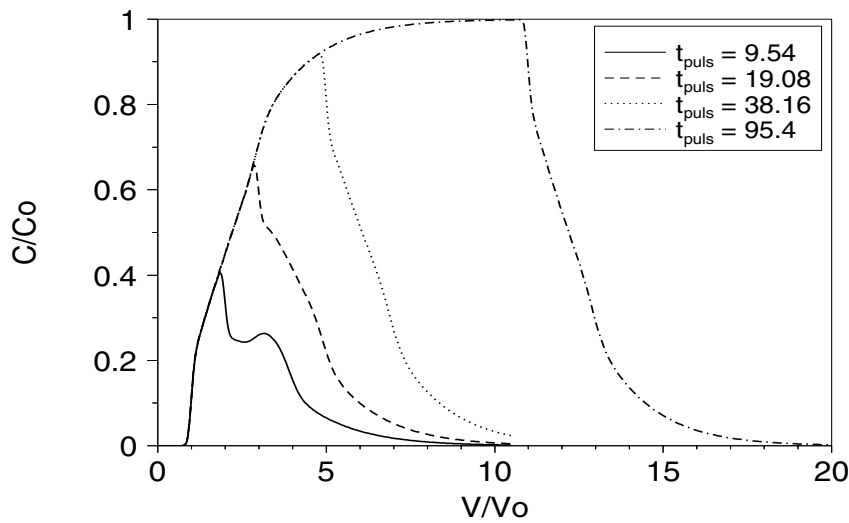


**Figure 6** Simulated breakthrough curves during contamination and decontamination varying the duration of the injected pulse.  $D_k^{scm} = D_k^{sci} = 1$ .

### *Non-linear sorption*

To show the effect of non-linearity, simulations with higher total contaminant influent concentrations are compared with simulations with lower concentrations. Figure 7 shows that the ratios between the contaminant species are equal up to a total contaminant concentration around  $2 \times 10^{-5}$ . Above this concentration, the ratios change with increasing concentration and we have non-linear sorption. We define the concentration of maximum non-linearity to be that concentration where the difference between the displacement velocity of the influent concentration and the mean front velocity is maximal. Non-linearity is found to be highest around a total concentration of  $2 \times 10^{-3}$ . Therefore, simulations with a total contaminant influent concentration of  $2 \times 10^{-6}$  are compared with simulations with influent concentrations of  $2 \times 10^{-4}$  and  $2 \times 10^{-3}$ . Figure 8 shows the effect of non-linearity on the BTC's with equilibrium (8A), almost no interaction (8C) and intermediate interaction (8B) between free contaminants and contaminants bound to colloids. Figure 8A shows that with increasing degree of non-linearity the front is more steep during contamination. With increasing non-linearity high concentrations tend to travel faster than low concentrations (but this is physically impossible) and thus the effect of dispersion will be decreased and the front will tend to be a block front. During decontamination high concentrations will travel faster than low concentrations and thus the front will be flatter with increasing non-linearity. Further, with increasing total contaminant concentration, the mean retardation factor will decrease.

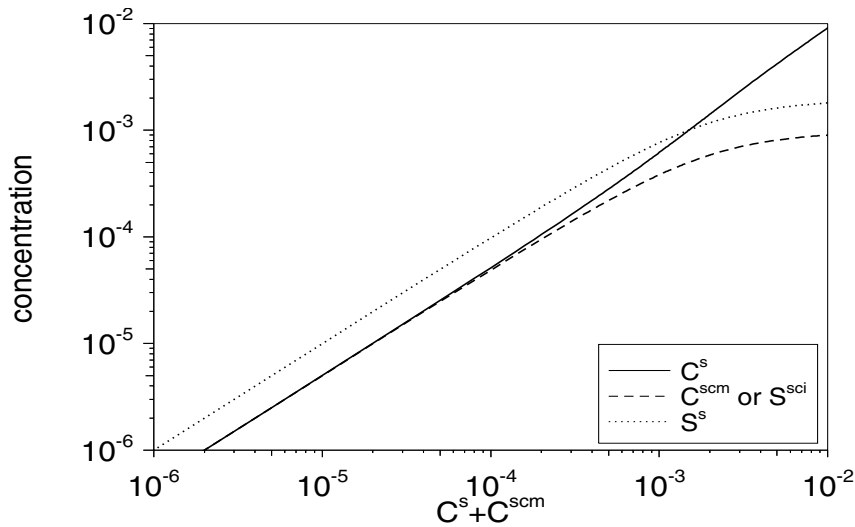


**Figure 7** Contaminant species concentration as a function of the total contaminant concentration; free contaminants ( $C^s$ ), contaminants sorbed to the solid matrix ( $S^s$ ), on mobile ( $C^{scm}$ ) and immobile colloids ( $S^{sci}$ ).

At low reaction rates, part of the contaminants bound to colloids do not desorb in the time frame of the experiment and non-linearity does not affect their inert transport. In Figure 8B and 8C we see a steep initial breakthrough during contamination, independent of non-linearity. During decontamination, part of the contaminant binding sites on colloids will not be occupied due to slow adsorption. This results in the steep initial breakthrough of uncontaminated water, independent of non-linearity. Due to non-linearity, the other part of the BTC's will be steeper in case of contamination and flatter in case of decontamination and the mean retardation factor will decrease as a result of higher total contaminant concentration. In the non-linear non-equilibrium case the concentration plateau disappears during decontamination and we get a dispersed front.

In case of non-linearity, the reflected part of the BTC during decontamination does not have the same shape as the BTC during contamination anymore. This might be an explanation for the differing shape of the BTC during contamination and decontamination found by Saiers and Hornberger (1996a).

In this paper, non-linear sorption is represented by a Langmuir isotherm and also certain parameters are assumed. It is not sure that the same effect of non-linearity will be found with different parameters, since the effect of changing parameters in non-linear systems is not always predictable. Often Freundlich or Langmuir-Freundlich type isotherms are used to represent sorption in situations with sorption site heterogeneity. It might be interesting to study the effect of introducing these non-linear isotherms. However, in this paper we want to show the importance and possible effects of non-linearity, we do not

intend to put general statements.

In this paper we use only mass balance equations of the contaminant and colloid species considered. It is assumed that all other conditions will stay constant. In practice, however, e.g. the pH may change upon introduction of contaminants. Meeussen *et al.*(1996) stressed the importance of multi-component sorption. They showed that a pH front may develop and lead to multiple fronts after introduction of fluoride in a soil column.

### Conclusions

A model is developed for coupled colloid and contaminant transport (COLTRAP). Model simulations show the effect of variation in the ratio's of the colloid and contaminant velocities and dispersion coefficients. Using model simulations the effect of kinetics and non-linearity on the shape of breakthrough and desorption curves is studied. Model results indicate that with slow reaction kinetics, unretarded breakthrough of contaminants facilitated by colloids may occur. As a result of non-linearity breakthrough curves become more steep during contamination.

It is very important to consider both contamination and decontamination in transport experiments as this gives insight in adsorption processes. It is shown that in case of linear sorption the BTC's during contamination have the same shape as the BTC's during decontamination (reflected in the x-axis) if complete breakthrough occurs. Different shapes indicate non-linear sorption or incomplete breakthrough. It is shown that shapes of simulated adsorption and desorption curves correspond with shapes of adsorption and desorption curves found in experiments (e.g. unretarded breakthrough followed by a plateau and a new front, asymmetrical curves, large tailings). This stresses the importance of incorporating both kinetics and non-linearity in models for coupled colloid and contaminant transport. Finally, it is shown that it is not correct to assume that colloids are non-reactive only by stating that the solid matrix is saturated with respect to colloids. Exchange between mobile and immobile colloids can have a large impact on the (shape of the) BTC during contamination and decontamination.

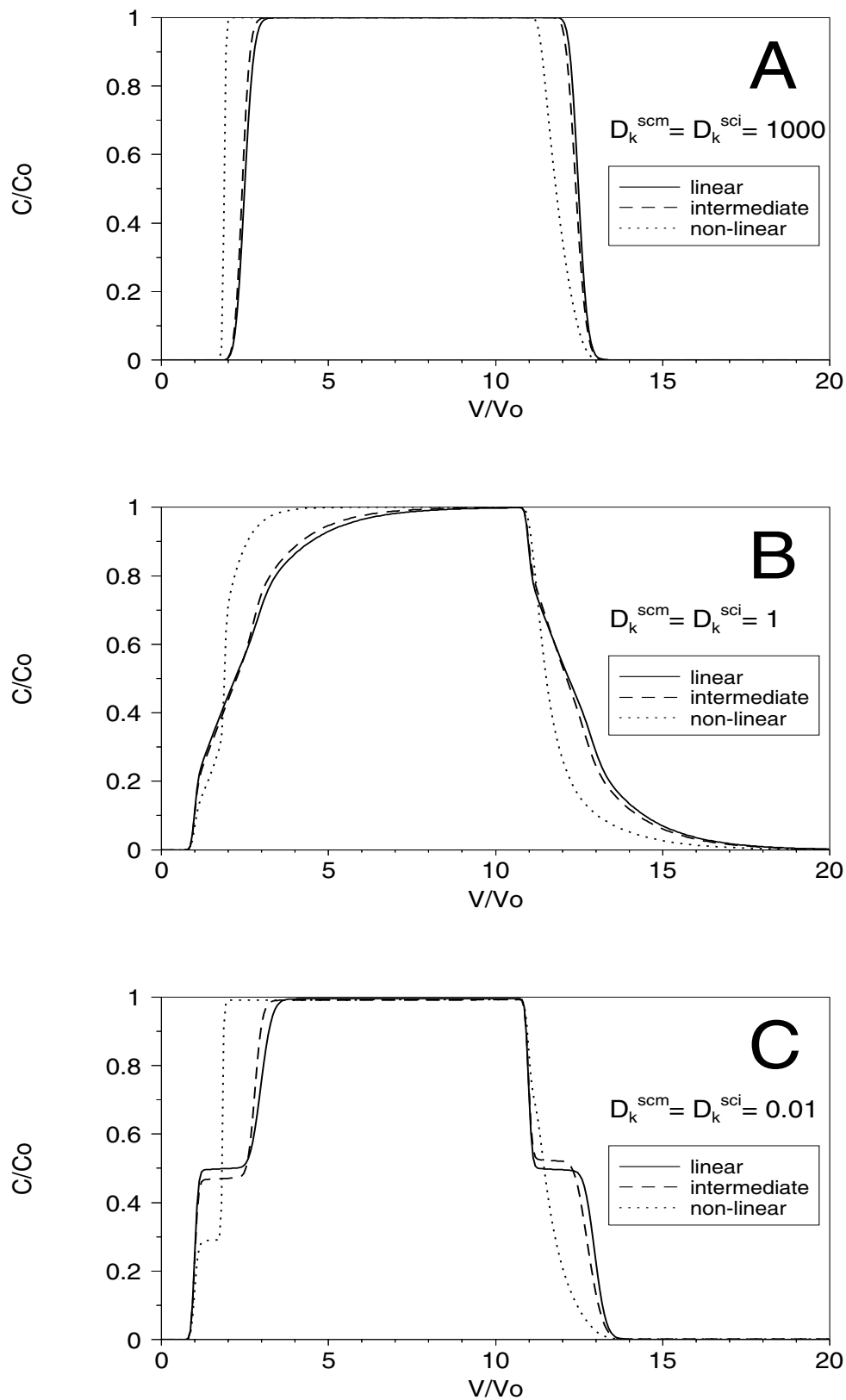


**Figure 8** Simulated breakthrough curves during contamination and decontamination with different total contaminant influent concentration  $2 \times 10^{-6}$  (linear),  $2 \times 10^{-4}$  (intermediate) and  $2 \times 10^{-3}$  M (non-linear) for 8A: high, 8B: intermediate and 8C: low interaction rates between colloids and contaminants.

## References

- Buddemeier R.W. and Hunt J.R. 1988. Transport of colloidal contaminants in groundwater: radionuclide migration at the Nevada test site. *Appl. Geochem.*, 3, 535-548.
- Buffle J. 1988. Complexation reactions in aquatic systems: an analytical approach. In: Chalmers R.A. and Masson M.R (Eds.). Ellis Horwood Series in Analytical chemistry, Ellis Horwood Limited, Chichester, UK.
- Corapcioglu M.Y and Jiang S. 1993. Colloid-facilitated groundwater contaminant transport. *Water Resour. Res.*, 29(7), 2215-2226.
- Corapcioglu M.Y. and Kim S. 1995. Modeling facilitated contaminant transport by mobile bacteria. *Water Resour. Res.*, 31(11), 2639-2647.
- Deguedre C.A., Baeyens B., Goerlich W., Riga J., Verbist J. and Stadelmann P. 1989. Colloids in water from a subsurface fracture in granitic rock, Grimsel test site, Switzerland. *Geochim. Cosmochim. Acta*, 53, 603-610.
- Dunnivant F.M., Jardine P.M., Taylor D.L. and McCarthy J.F. 1992a. Cotransport of cadmium and hexachlorobiphenyl by dissolved organic carbon through columns containing aquifer material. *Environ. Sci. Technol.*, 26(2), 360-368.
- Dunnivant F.M., Jardine P.M., Taylor D.L. and McCarthy J.F. 1992b. Transport of naturally occurring dissolved organic carbon in laboratory columns containing aquifer material. *Soil Sci. Soc. Am. J.*, 56(2), 437-444.
- Enfield, C. G. and Bengtsson G. 1988. Macromolecular transport of hydrophobic contaminants in aqueous environments. *Ground water*, 26(1), 64-70.
- Grolimund D., Borkovec M., Barmettler K. and Sticher H. 1996. Colloid-facilitated transport of strongly sorbing contaminants in natural porous media: a laboratory column study. *Environ. Sci. Technol.*, 30(10), 3118-3123.
- Gschwend P.M. and Reynolds M.D. 1987. Monodisperse ferrous phosphate colloids in an anoxic groundwater plume. *J. Contam. Hydrol.*, 1, 309-327.
- Jiang S. and Corapcioglu M.Y. 1993. A hybrid equilibrium model of solute transport in porous media in the presence of colloids. *Colloids and Surfaces A: Physicochemical and Engineering Aspects*, 73, 275-286.
- Kim J.I., Buckau G. and Klenze R. 1987. Natural colloids and generation of actinide pseudocolloids in groundwater. In: Come B. and Chapman N.A. (Eds.), *Natural Analogues in Radioactive Waste Disposal*, pp. 289-299, Graham and Trotman, London.
- Kim J.I., Delakowitz B., Zeh P., Probst T., Lin X., Ehrlicher U., Schauer C. 1994a. Appendix I. In: *Colloid Migration in groundwaters: geochemical interactions of radionuclides with natural colloids*, RCM 00394, Technische Universitat Munchen, pp. 16-61.
- Kim J.I., Delakowitz B., Zeh P., Klotz D. and Lazik D. 1994b. A column experiment for the study of colloidal radionuclide migration in Gorleben aquifer systems. *Radiochim. Acta*, 66/67, 165-171.
- Longworth G. and Ivanovich M. 1989. The sampling and characterization of natural groundwater colloids: studies in aquifers in slate, granite and glacial sand, NSS/R165, Harwell Laboratory, Harwell, UK.
- McCarthy J.F., Williams T.M., Liang L., Jardine P.M., Jolley L.W., Palumbo A.V. and Cooper L.W. 1993. Mobility of natural organic matter in a sandy aquifer. *Environ. Sci. Technol.*, 27(4), 1993.
- Meeussen J.C.L., Scheidegger A., Hiemstra T., van Riemsdijk W.H. and Borkovec M. 1996. Predicting multicomponent adsorption and transport of fluoride at variable pH in a Goethite-Silica sand system. *Environ. Sci. Technol.*, 30(2).
- Mills W.M., Liu S. and Fong F.K. 1991. Literature review and model (COMET) for colloid/metals transport in porous

- media. *Groundwater*, 29, 199-208.
- Parker J.C. and Van Genuchten M.T. 1984. Determining transport parameters from laboratory and field tracer experiments. Bulletin 84-3, Virginia Agricultural experiment Station.
- Pulse R.W. and Powell R.M. 1992. Transport of inorganic colloids through natural aquifer material: implications for contaminant transport. *Environ. Sci. Technol.*, 26(3), 614-621.
- Saiers J.E., Hornberger G.M. and Liang L. 1994. First- and second-order kinetics approaches for modeling the transport of colloidal particles in porous media. *Water Resour. Res.*, 30(9), 2499-2506.
- Saiers J.E. and Hornberger G.M. 1996a. The role of colloidal kaolinite in the transport of cesium through laboratory sand columns. *Water Resour. Res.*, 32(1), 33-41.
- Saiers J.E. and Hornberger G.M. 1996b. Modeling bacteria-facilitated transport of DDT. *Water Resour. Res.*, 32(5), 1455-1459.
- Short S.A., Lawson R.T. and Ellis J. 1988. Uranium-234/Uranium-238, and Thorium-230/Uranium-234 activity ratios in the colloidal phases of aquifers in lateritic weathered zones. *Geochim. Cosmochim. Acta*, 52, 2555-2563.
- Small H. 1974. Hydrodynamic chromatography, a technique for size analysis of colloidal particles. *J. Colloid. Interf. Sci.*, 48(1), 147-161.
- Van de Weerd H. and Leijnse A. 1997a. Assessment of the effect of kinetics on colloid facilitated radionuclide transport in porous media. *J. Contam. Hydrol.*, 26, 245-256.
- Van de Weerd H and Leijnse A. 1997b. Development of a model for coupled colloid and contaminant transport (COLTRAP). In: Development of a model for radionuclide transport by colloids in the geosphere, Nuclear Science and Technology EUR 17480 EN, Commission of the European communities (CEC) pp. 123-180.
- Von Gunten H.R., Waber U.E., Krahenbuhl U. 1988. The reactor accident at chernobyl: a possibility to test colloid-controlled transport of radionuclide in a shallow aquifer. *J. Contam. Hydrol.*, 2, 237-247.

# Chapter 3

## **Assessment of the effect of kinetics on colloid facilitated radionuclide transport in porous media\***

### **Abstract**

Binding of radionuclides to natural colloids can significantly alter their transport behaviour in porous media. Dependent on the interaction between radionuclides, colloids and the solid matrix, radionuclide transport may be enhanced or retarded as a result of the presence of colloids. Often, equilibrium models are used to describe interactions between radionuclides, colloids and the solid matrix. However, experimental results indicate that kinetic processes may be important.

In this paper, a model for coupled colloid and radionuclide transport in porous media is presented. Kinetic relationships are incorporated for the interaction between radionuclides, colloids and solid matrix. With this transport model column experiments have been simulated, and modelling results are compared with experimental data reported in literature. It appears that kinetic interaction relationships are required to adequately model the experimental data.

---

\* By H. van de Weerd and A. Leijnse  
published in: Journal of Contaminant Hydrology 26(1997) 245-256

## Introduction

Human activity may result in the introduction of heavy metals into the subsoil and/or subsurface aquifer systems, either on purpose or by accident. The presence of heavy metals constitutes a potential threat to human health and ecosystems.

In general, heavy metals are not very mobile in soil because they are sorbed very strongly on the solid matrix. However, due to binding of heavy metals with colloids in soil solution the total mobile metal concentrations in solution can be increased (Kim *et al.*, 1992). In natural groundwater both inorganic and organic colloids are present. They differ in origin and concentration (ranging from  $10^8$  to more than  $10^{12}$  particles  $l^{-1}$ , Degueldre *et al.*, 1989; Gschwend and Reynolds, 1987; Longworth and Ivanovich, 1989; Short *et al.*, 1988; Kim *et al.*, 1987). When these colloids are transported over large distances, they can act as a carrier for contaminants (Lieser *et al.* 1990) and enhance the transport of heavy metals. This has also been observed in field situations (Von Gunten *et al.*, 1988; Buddemeier and Hunt, 1988).

Different model studies to assess the effect of colloids on the transport of contaminants in porous media have been reported (Corapcioglu and Jiang, 1993; Dunnivant *et al.*, 1992a). In a model study for heavy metals Mills *et al.* (1991) showed that equilibrium binding of metals to colloids enhance the transport of metals. However, because local equilibrium is assumed, metals are stripped very fast from the colloids when colloids loaded with metal enter a "clean" part of the porous medium. The calculated enhancement of metal transport with equilibrium models seems to be insufficient to explain the increased transport distances observed in field situations.

Consequently, the assumption of equilibrium binding of heavy metals to colloids may not be valid. According to Buffle (1988), dissociation of complexes of ligands (complexing sites) and metals (from now on indicated as ML complexes) is a slow process relative to other processes in nature. This slow dissociation of ML complexes is a possible explanation for the discrepancy between model results and in situ observations. Another explanation is that relatively long time is required for metals to leave complex structures of colloids.

In this paper, a one-dimensional model for coupled colloid and contaminant transport (COLTRAP) is presented. The model is used to simulate transport of

radionuclides and colloids in a porous medium representing a natural system. Governing equations are mass balance equations for mobile and immobile radionuclide and colloid species, completed with constitutive equations for kinetic interactions between colloids and the solid matrix, colloids and radionuclides and radionuclides and solid matrix. Two types of simulations have been carried out:

- assuming no interaction between humic colloids and the solid matrix and different rates of interaction between free radionuclide and humic colloids;
- assuming constant rates of interaction between free radionuclides and humic colloids and different rates of reversible interaction between humic colloids and the solid matrix.

Modelling results have been compared with experimental data reported in literature and the importance of the kinetic nature of radionuclide-colloid interaction and colloid-solid matrix interaction has been evaluated.

## **Transport model**

A one-dimensional model for simulating transport of contaminants and colloids in porous media (COLTRAP; coupled colloid and contaminant transport) has been developed. In this paper, only the governing equations required for the simulations presented here are given.

Six different species are distinguished in the system considered (Figure 1). The radionuclide is distributed among four different species: (1) free contaminants in the liquid phase (S1), (2) contaminants sorbed on the solid matrix (S2), (3) contaminants sorbed on mobile colloids (S3), (4) contaminants sorbed on immobile colloids (S4). Colloids in the porous medium are distributed among two species: (1) colloids in solution (C1), (2) colloids sorbed directly on the solid matrix (C2).

The governing equations are the six mass balance equations for mobile and immobile radionuclide and colloid species, completed with constitutive equations for the interactions between the different species. All interactions in the system are described by non-linear, time dependent (kinetic) relations. Linear and equilibrium relations can be obtained from these by making some simplifying assumptions. System properties are assumed to be constant in space and time. Groundwater flow is assumed to be steady state.

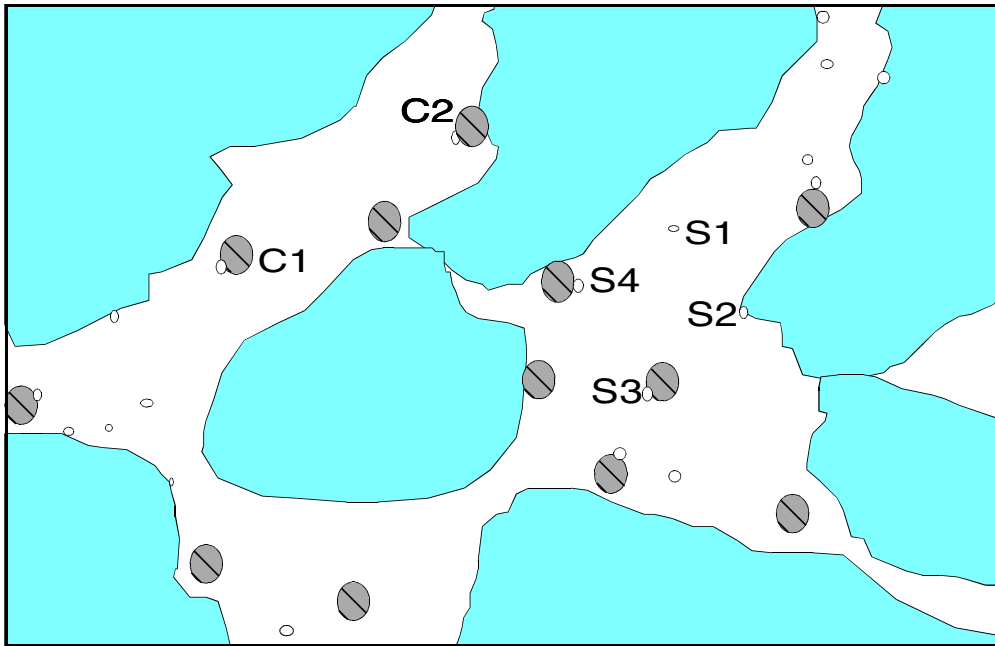


**Figure 1** Speciation of Colloids (C) and Contaminants (S): free contaminants in the liquid phase (S1); contaminants sorbed on the solid matrix (S2); contaminants sorbed on mobile colloids (S3); contaminants sorbed on immobile colloids (S4); colloids in the liquid phase (C1); colloids sorbed directly on the solid matrix (C2).

*Transport and behavior of colloids*

We will assume that the properties of the porous medium and the liquid phase are not influenced by the presence of radionuclides and colloids. Thus, neither the influence of immobile colloids on the porosity of the medium nor clogging of the porous medium by (large) colloids will be considered. For the behavior of colloids we will assume that only one type of colloid is present, or that colloids can be described by some "mean behavior". Interactions between colloids in the liquid phase are not considered, and colloids are regarded to be stable. Furthermore it is assumed that properties and mass of the colloids are not influenced by sorption of contaminants on colloids.

If the dispersive mass flux of mobile colloids is described by a Fickian type relation, the governing mass balance equation for one-dimensional colloid transport in porous media is given by:

$$\frac{\partial}{\partial t}(nC^c) + \frac{\partial}{\partial x}(nv_c C^c) - \frac{\partial}{\partial x}\left(nD_c \frac{\partial C^c}{\partial x}\right) = - Q^c \quad (1)$$

where  $C^c$  [ML<sup>-3</sup>] is mobile colloid concentration,  $t$  [T] is time,  $x$  [L] is distance,  $n$  [-] is porosity,  $D_c$  [L<sup>2</sup>T<sup>-1</sup>] is colloid dispersion coefficient,  $v_c$  [LT<sup>-1</sup>] is mean colloid velocity. Note that the dispersion coefficient for colloids and the mean colloid velocity are not necessarily

the same as dispersion coefficients for free contaminants and the mean water velocity. Due to their size and charge, mobile colloids may be excluded from a part of the water-filled porosity. The right hand side in Equation 1,  $Q^c$ , represents the binding of colloids to the solid matrix.

The mass balance equation for immobile colloids sorbed on the solid matrix is given by:

$$\frac{\partial}{\partial t}(n\underline{S}^c) = Q^c \quad (2)$$

where,  $\underline{S}^c$  [ML<sup>-3</sup>] is the concentration of immobile colloids expressed in mass per unit volume of liquid phase instead of mass per unit mass of solid matrix as is usually done (indicated by  $\underline{\quad}$ ).

The following kinetic Langmuir equation, where the maximum number of sorption sites is taken into account, is used to describe colloid solid matrix interaction:

$$Q^c = n \left( k_a^c C^c \left( f_{\max}^{ci} \underline{A} - \frac{\underline{S}^c}{M^c} \right) - k_d^c \underline{S}^c \right) \quad (3)$$

where  $k_a^c$  [L<sup>3</sup>T<sup>-1</sup>] and  $k_d^c$  [T<sup>-1</sup>] are rate constants of adsorption and desorption respectively,  $f_{\max}^{ci}$  [L<sup>-2</sup>] is the maximum sorption capacity of colloids per unit area of solid matrix (<sup>ci</sup> indicates immobile colloids),  $\underline{A}$  [L<sup>-1</sup>] is surface area per volume of pore water and  $M^c$  [M] is the molar mass of colloids. Irreversible adsorption can be described by setting the desorption rate constant  $k_d^c$  to zero.

#### *Transport and behavior of contaminants*

If the dispersive mass flux of free contaminants is described by a Fickian type relation, the governing mass balance equation for the free contaminant is given by:

$$\frac{\partial}{\partial t}(nC^s) + \frac{\partial}{\partial x}(nvC^s) - \frac{\partial}{\partial x} \left( nD \frac{\partial C^s}{\partial x} \right) = - Q^s - Q^{sfc m} - Q^{sfc i} \quad (4)$$

where  $C^s$  [ML<sup>-3</sup>] is the free contaminant concentration,  $v$  [LT<sup>-1</sup>] is the mean water velocity,  $D$  [L<sup>2</sup>T<sup>-1</sup>] is the dispersion coefficient for free contaminants and the right hand side terms represent sorption of contaminants on the solid matrix ( $Q^s$ ), sorption of contaminants on mobile colloids ( $Q^{sfc m}$ ) and sorption of contaminants on immobile colloidal particles ( $Q^{sfc i}$ ), respectively.

Contaminants sorbed on mobile colloids are subject to advection, dispersion and sorption on the solid matrix together with the colloidal particles they are sorbed on. In addition, exchange with solution occurs by sorption processes. The governing mass balance equation for contaminants bound to mobile colloids is given by:

$$\frac{\partial}{\partial t}(nC^{scm}) + \frac{\partial}{\partial x}(nv_c C^{scm}) - \frac{\partial}{\partial x}\left(nD_c \frac{\partial C^{scm}}{\partial x}\right) = Q^{sfc m} - Q^{sc} \quad (5)$$

where  $C^{scm}$  [ML<sup>-3</sup>] is the concentration of contaminants sorbed on mobile colloids and the right hand side terms represent sorption of contaminants on mobile colloids ( $Q^{sfc m}$ ) and transfer of contaminants to the immobile phase due to sorption of colloids on the solid matrix ( $Q^{sc}$ ). Note, that the velocity and dispersion coefficient in Equation (5) are those of colloids.

The mass balance equation for contaminants sorbed on the solid matrix and for contaminants sorbed on immobile colloids are:

$$\frac{\partial}{\partial t}(n\underline{S}^s) = Q^s \quad (6)$$

$$\frac{\partial}{\partial t}(n\underline{S}^{sci}) = Q^{sfc i} + Q^{sc} \quad (7)$$

where,  $\underline{S}^s$  [ML<sup>-3</sup>] is the concentration of contaminants sorbed on the solid matrix and  $\underline{S}^{sci}$  [ML<sup>-3</sup>] is the concentration of contaminants sorbed on immobile colloids.

The following kinetic Langmuir equations are used to describe interactions between contaminants and the solid matrix, mobile and immobile colloids:

$$Q^s = n \left( k_a^s C^s \left[ f_{\max}^{si} \underline{A} - \frac{\underline{S}^s}{M^s} \right] - k_d^s \underline{S}^s \right) \quad (8)$$

$$Q^{sfc m} = n \left( k_a^{sfc m} C^s \left[ f_{\max}^c \frac{C^c}{M^c} - \frac{C^{scm}}{M^s} \right] - k_d^{sfc m} C^{scm} \right) \quad (9)$$

$$Q^{sfc i} = n \left( k_a^{sfc i} C^s \left[ f_{\max}^c \frac{\underline{S}^c}{M^c} - \frac{\underline{S}^{sci}}{M^s} \right] - k_d^{sfc i} \underline{S}^{sci} \right) \quad (10)$$

where  $\underline{S}^{sci}$  [ML<sup>-3</sup>] is the concentration of contaminants bound to immobile colloids,  $k_a^s$ ,  $k_a^{sfc m}$  and  $k_a^{sfc i}$  [L<sup>3</sup>T<sup>-1</sup>] are rate constants of adsorption and  $k_d^s$ ,  $k_d^{sfc m}$  and  $k_d^{sfc i}$  [T<sup>-1</sup>] are rate constants of desorption of contaminants to the solid matrix, mobile and immobile colloids,

respectively.  $f_{max}^{si}$  [ $L^{-2}$ ] and  $f_{max}^c$  [-] are the maximum sorption capacity of contaminants per unit area of solid matrix and per mole of colloids, respectively and  $M^s$  [M] is the molar mass of contaminants.

Since colloidal particles interact with the solid matrix, the concentrations of contaminants sorbed on these (mobile or immobile) colloids are also affected by this process, resulting in the following interaction term:

$$Q^{sc} = n \left( k_a^c C^{scm} \left[ f_{max}^{ci} A - \frac{S^c}{M^c} \right] - k_d^c S^{sci} \right) \quad (11)$$

Equations (1), (2), (4), (5), (6) and (7) form the set of mass balance equations that describe the 1-dimensional transport of colloids and contaminants in a porous medium. These mass balance equations are coupled through the interaction terms as defined by Equations (3), (8), (9), (10) and (11).

#### *Numerical solution of the equations*

The governing equations are solved numerically by a Galerkin finite element method. A solution is obtained for the unknown concentrations  $C^c$ ,  $S^c$ ,  $C^s$ ,  $S^s$ ,  $C^{scm}$ , and  $S^{sci}$ . Non-linearities are solved by a Newton-Raphson iteration scheme. In order to reduce round-off errors due to spatial discretization, an adaptive method is implemented, where the finite element grid is dynamically refined in areas with large concentration gradients.

## **Simulation results and comparison with experimental data**

COLTRAP had been used to simulate the transport of Americium in a column packed with aquifer material in equilibrium with anaerobic, humic rich natural groundwater (Kim *et al.*, 1994a, 1994b). The experiment consists of injection of 2 ml prefiltered natural groundwater spiked with  $^{241}\text{Am}$  and equilibrated for three months, followed by injection of unspiked prefiltered natural groundwater. Experimental details are given in Table 1.

After equilibration, humic colloids will be sorbed on the solid matrix, and may determine surface characteristics of the solid matrix together with minerals such as hematite and alumina(hydr)oxides. From the first complexation constants of Am(III) with the ligand anions  $\text{OH}^-$ ,  $\text{CO}_3^{2-}$ , and humic acid, and the experimental conditions given in Table 1, the

## CHAPTER 3

**Table 1** Physical and chemical properties of the simulated experiment (Kim et al, 1994a; 1994b) and chemical constants used for calculations

Groundwater properties and chemical conditions		Column and hydraulic properties	
Ionic strength	0.044 M	Column length	25 cm
pH	7.6	Column diameter	5 cm
T	298 K	Effective porosity <sup>d</sup>	0.330
<sup>241</sup> Am <sup>a</sup>	8.7x10 <sup>-6</sup> mol l <sup>-1</sup>	Dispersivity <sup>d</sup>	8.4x10 <sup>-2</sup> cm
DOC	80 mg C l <sup>-1</sup>	Darcy velocity	0.864 cm h <sup>-1</sup>
HA <sup>b</sup>	7.8x10 <sup>-4</sup> eq l <sup>-1</sup>	Average flow velocity	2.62 cm h <sup>-1</sup>
CO <sub>2</sub> partial pressure	1%	Dispersion coefficient	0.220 cm <sup>2</sup> h <sup>-1</sup>
Solid matrix properties		Chemical constants	
BET surface area <sup>c</sup>	2.21 m <sup>2</sup> g <sup>-1</sup>	logK Am(OH) <sup>2-</sup> <sup>e</sup>	6.3
Bulk density <sup>c</sup>	1.81x10 <sup>6</sup> g m <sup>-3</sup>	logK Am(CO <sub>3</sub> ) <sup>-</sup> <sup>f</sup>	6.22
Main constituents <sup>c</sup>	SiO <sub>2</sub> 93.8 wt.% Al <sub>2</sub> O <sub>3</sub> 2.44 wt.% Fe <sub>2</sub> O <sub>3</sub> 0.42 wt.%	logK AmHA <sup>g</sup>	6.44

<sup>a</sup> In spiked groundwater. <sup>b</sup> Estimated on the basis of proton exchangeable functional groups (Kim *et al.*, 1994b). <sup>c</sup> Determined before equilibration with natural groundwater. <sup>d</sup> Determined with tracer tests. <sup>e</sup> Stadler and Kim, 1988. <sup>f</sup> Meinrath and Kim, 1991. <sup>g</sup> Kim et al., 1991.

**Table 2** Boundary and initial conditions and parameters used for model simulations

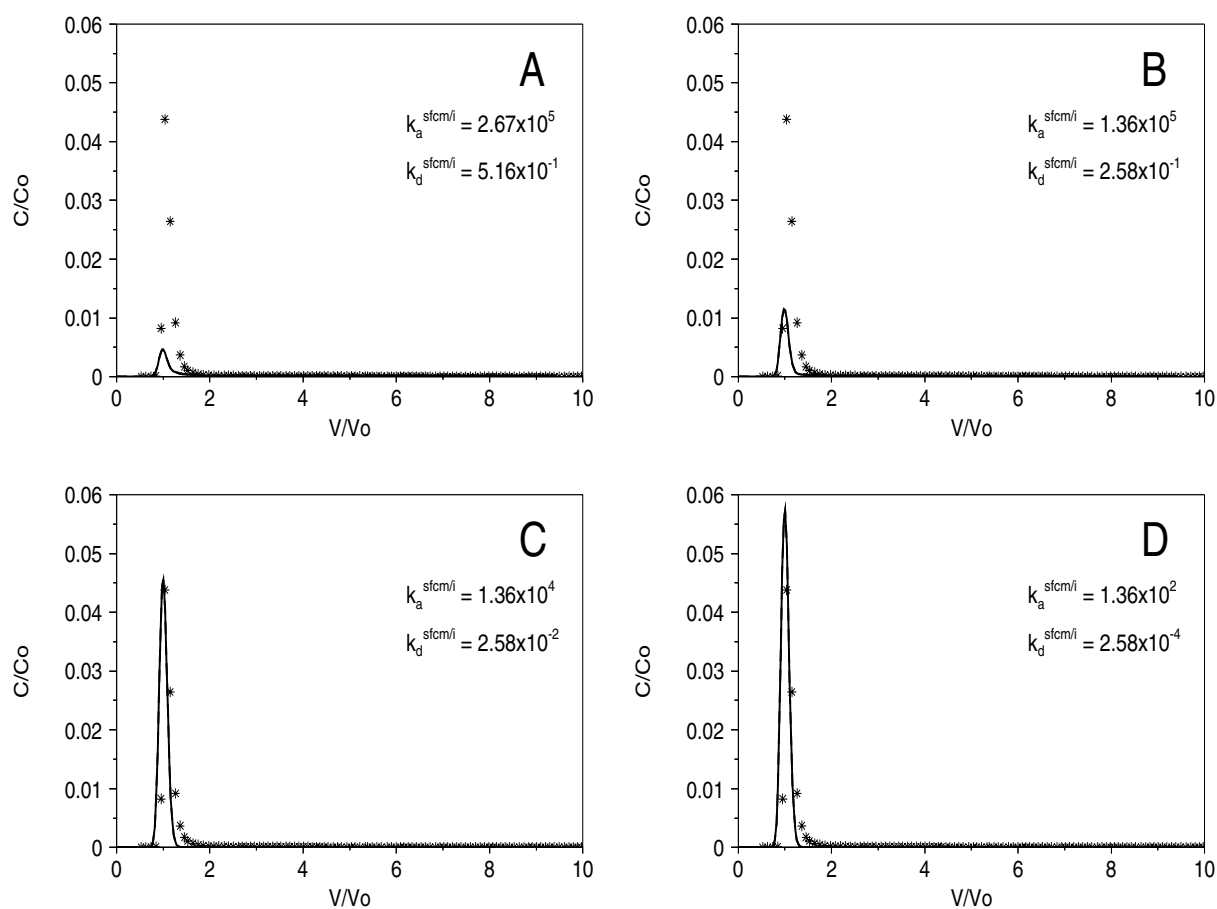
$C^s(x=0,t)$ <sup>a</sup>	$0 \leq t \leq t_{puls}$	5.04x10 <sup>-6</sup>	g l <sup>-1</sup>	$M^s$	241	g mol <sup>-1</sup>
$C^{scm}(x=0,t)$ <sup>b</sup>	$0 \leq t \leq t_{puls}$	2.09x10 <sup>-3</sup>	g l <sup>-1</sup>	$M^c$ <sup>d</sup>	2.5x10 <sup>+9</sup>	g mol <sup>-1</sup>
$C^c(x=0,t)$	$t \geq 0$	8.00x10 <sup>-2</sup>	g l <sup>-1</sup>	$A$	1.21x10 <sup>+4</sup>	m <sup>2</sup> l <sup>-1</sup>
$C^c(x,t=0)$	$0 \leq x \leq L$	8.00x10 <sup>-2</sup>	g l <sup>-1</sup>	$f_{max}^{si}$ <sup>e</sup>	1.00x10 <sup>-5</sup>	mol m <sup>-2</sup>
$\underline{C}^c(x,t=0)$ <sup>c</sup>	$0 \leq x \leq L$	2.74x10 <sup>-2</sup>	g l <sup>-1</sup>	$k_a^s/k_d^s$ <sup>f</sup>	5.01x10 <sup>+4</sup>	l mol <sup>-1</sup>
$L$		25	cm	$f_{max}^{ci}$ <sup>g</sup>	8.26x10 <sup>-9</sup>	mol m <sup>-2</sup>
$r$		2.5	cm	$k_a^c/k_d^c$ <sup>c,g,h</sup>	3.25x10 <sup>+4</sup>	l mol <sup>-1</sup>
$n$		0.33	-	$f_{max}^{ci}$ <sup>i</sup>	8.17x10 <sup>+6</sup>	mol <sup>-1</sup>
$v = v_c$		2.62	cm h <sup>-1</sup>	$k_a^{scm}/k_d^{scm}$ <sup>j</sup>	5.18x10 <sup>+5</sup>	l mol <sup>-1</sup>
$D = D_c$		0.22	cm <sup>2</sup> h <sup>-1</sup>	$k_a^{sfc}/k_d^{sfc}$ <sup>j</sup>	5.18x10 <sup>+5</sup>	l mol <sup>-1</sup>
$t_{puls}$		0.118	h			

<sup>a</sup> sum of concentrations of aqueous species (Am bound to colloids not included). <sup>b</sup> Am bound to humic colloids. <sup>c</sup> assuming immobile colloids concentration of 5x10<sup>-6</sup> g C per g solid matrix before injection. <sup>d</sup> assuming a colloid diameter of 100 nm and a colloid density of 1.2x10<sup>6</sup> g m<sup>-3</sup>. <sup>e</sup> assuming 6 binding sites per nm<sup>2</sup>. <sup>f</sup> assumed. <sup>g</sup> assuming a maximum binding capacity for humic colloids of 5.56x10<sup>-6</sup> g C per g solid matrix. <sup>h</sup> assuming equilibrium between mobile and immobile colloids in the system <sup>i</sup> assuming 3.27x10<sup>-3</sup> mol binding sites per g DOC at pH 7.6. <sup>j</sup> based on first complexation constant of Am to humic acid (Kim *et al.*, 1991) corrected for 19% of aqueous Am being Am(III).

americium speciation in spiked groundwater is calculated to be:  $[\text{Am(III)}] = 3.93 \times 10^{-9}$  mol l<sup>-1</sup>,  $[\text{Am(CO}_3\text{)}^{2-}] = 1.58 \times 10^{-8}$  mol l<sup>-1</sup>,  $[\text{Am(OH)}^-] = 1.19 \times 10^{-9}$  mol l<sup>-1</sup>, and  $[\text{AmHA}] = 8.68 \times 10^{-6}$  mol l<sup>-1</sup>. Decay can be neglected since the half-life of <sup>241</sup>Am is 458 years.

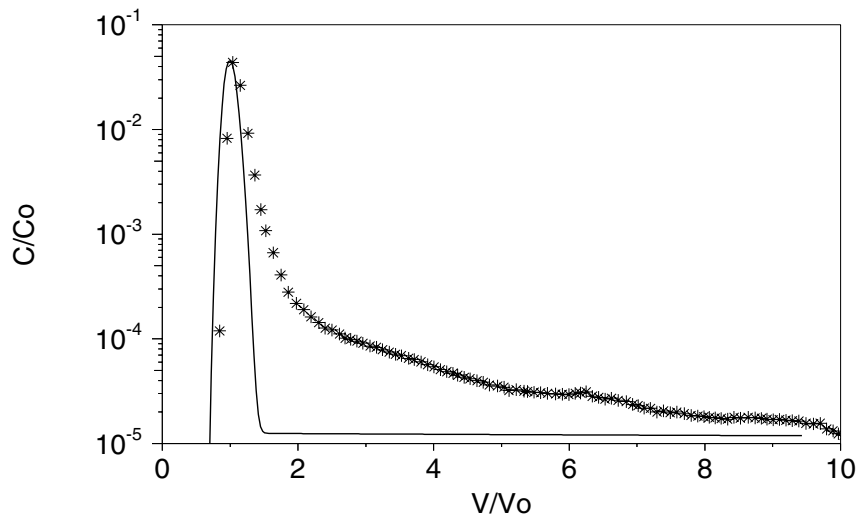
For the system considered, two types of simulations were carried out. Boundary and initial conditions and parameters used for these simulations are given in Table 2. In the first set of simulations, colloids are assumed to be non-reactive with the solid matrix which is saturated with colloids. This represents a system in which immobile colloids are sorbed irreversibly on the solid matrix. For interaction between Am and humic colloids a constant ratio between  $k_a^{sfc}$  and  $k_d^{sfc}$  is used. Adsorption and desorption rate constants are varied over a range representing almost irreversible to equilibrium Am humic colloid interaction. Interaction of Am with both mobile and immobile colloids is considered. A second set of simulation was done using the "best fit" rate constants for interaction between Am and humic colloids obtained from the first set of simulations. In these simulations, colloids were assumed to be reactive with the solid matrix. The colloid solid matrix interaction was described by a constant ratio of  $k_a^c$  and  $k_d^c$  varied over a range representing equilibrium to almost irreversible interaction.

Figure 2 shows the results for the first set of simulations together with experimental results. Decreasing the rate constants for interaction between Am and colloids changes the behaviour of Am in the column from almost quantitative sorption to almost unretarded breakthrough. For values of  $k_a^{sfc}$  and  $k_d^{sfc}$  of  $1.36 \times 10^4$  l h<sup>-1</sup> and  $2.58 \times 10^{-2}$  h<sup>-1</sup> respectively (Figure 2c), experimental results agree reasonably well with simulation results. A minor shift in breakthrough time is observed, which may be attributed to a small error in the flow rate. However, if the same breakthrough curves are plotted on a log scale (Figure 3), one can see that the tailing observed in the experiment is not observed in the simulations. The tailing in the simulated breakthrough curve at a very low concentration is the result of stripping of Am from the solid matrix by mobile colloids entering the column after the spiked groundwater has passed. As adsorption of Am to mobile colloids is the rate limiting step, variation of desorption and adsorption rate constants of the Am-solid matrix interaction does not influence simulation results. The tailing observed in the experiment cannot be explained by assuming that all Am exchange between mobile colloids and solid matrix occurs via the liquid phase, even if unrealistic low sorption of Am on the solid matrix is assumed.



**Figure 2** Mobile Am breakthrough curves: —, simulations with different rate constants for Am humic colloid (mobile and immobile) interaction; \*, experimental data.

Figure 4 shows the results for the second set of simulations together with experimental data. Increasing the colloid-solid matrix interaction rate constants decreases the height of the peak due to the increasing exchange of mobile colloids with sorbed Am and immobile colloids without sorbed Am. Increasing the rate constants also results in an increase of the relative concentration at which the tailing starts and the slope of tailing. For large values of  $k_a^c$  and  $k_d^c$ , interaction of colloids with the solid matrix is relatively quick and Am bound to immobile and mobile colloids will be equally distributed between the two phases. In that case, the location of the peak is shifted to a later time and no distinction can be made between the peak and the tail (Figure 4d). Note that in all simulations in this set the mobile concentration of Am almost equals the concentration of Am sorbed on mobile colloids. It appears that the tailing can be explained by kinetic-colloid solid matrix interaction. Figure 4b shows that rate constants  $k_a^c = 8.2 \times 10^2 \text{ l h}^{-1}$  and  $k_d^c = 0.025 \text{ h}^{-1}$  give a reasonable fit of calculated and measured breakthrough curves.



**Figure 3** Mobile Am breakthrough curve: —, simulation,  $k_a^{sfc} = k_a^{sfi} = 1.36 \times 10^4$ ,  $k_d^{sfc} = k_d^{sfi} = 2.58 \times 10^{-2}$ ; \*, experimental data.

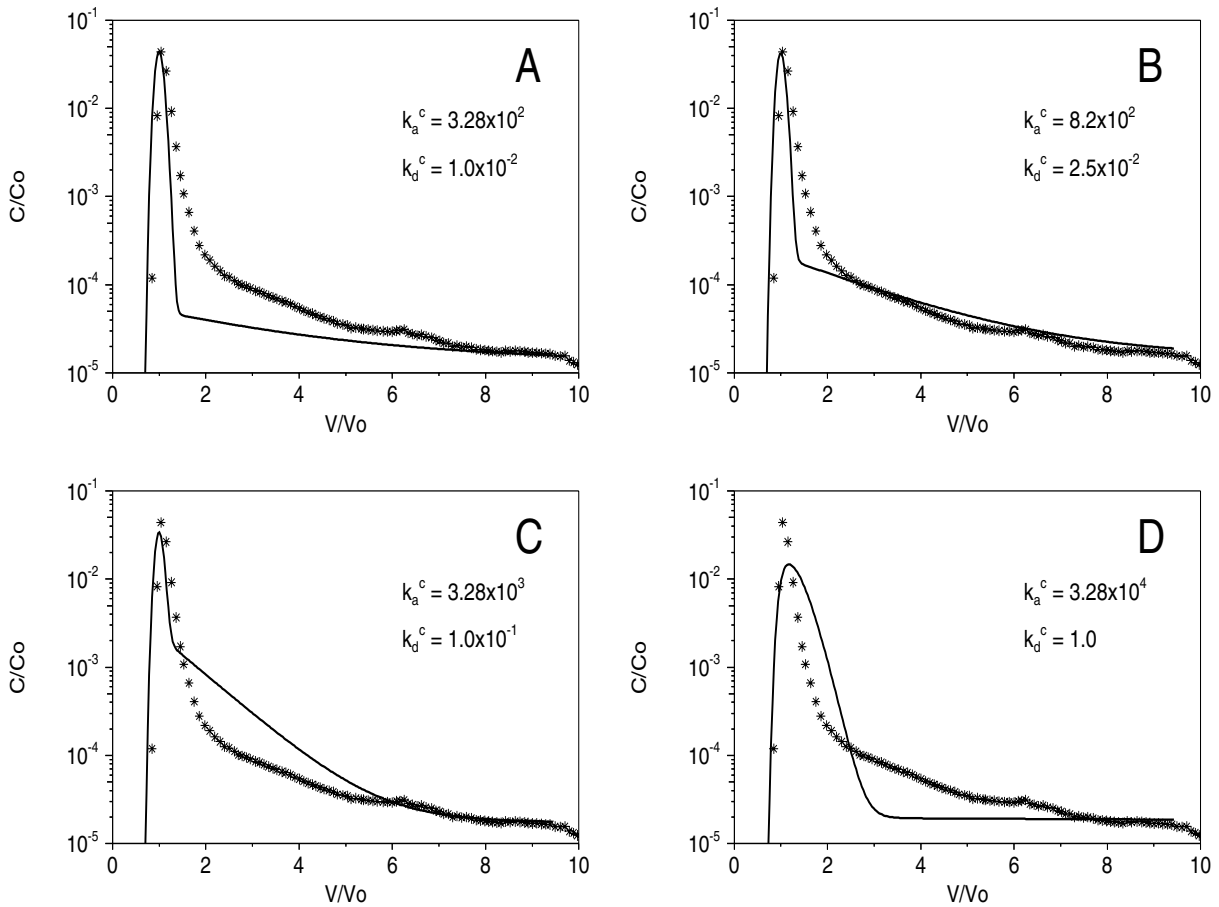


**Figure 4** Mobile Am breakthrough curves: —, simulations with different colloid-solid matrix interaction rate constants,  $k_a^{sfc} = k_a^{sfi} = 1.36 \times 10^4$ ,  $k_d^{sfc} = k_d^{sfi} = 2.58 \times 10^{-2}$ ; \*, experimental data.

## Discussion

Simulation results indicate that the process having the largest impact on the peak in the breakthrough curve calculated by the model is kinetic Am-Humic colloid interaction. Without the assumption of a kinetic interaction, it is impossible to simulate experimental results. Even the assumption of an unrealistically low sorption of Am on the solid matrix is insufficient to reproduce the peak in the breakthrough curve. The desorption rate constant as determined from the simulation results is representative for the global rate of complex dissociation in the system considered. This global rate constant may differ from the dissociation rate of Am from a humic colloid site, e.g. due to the fact that Am has to travel by diffusion from a site which is located in a complex colloid structure before it can leave the structure, or because conformational changes are needed before Am can leave the structure. A decrease in the adsorption and desorption rate constants changes the behaviour of Am in the column from almost quantitative sorption to inert transport.

To simulate the tail in the Am breakthrough curve as observed in the experiments, additional processes had to be included in the model. The tailing could be explained by reversible interaction between colloids and solid matrix. Physical nonequilibrium, as described by Brusseau (1993), does not play a role in the simulated experiment as the intraparticle porosity and thus the impact of intraparticle and film diffusion is negligible for the nonstructured aquifer material used. Dunnivant *et al.* (1992b) suggested the multisite adsorption of DOC via direct association with the solid matrix and hydrophobic binding processes between mobile and immobile organic matter. As in the simulated experiment the aquifer column is saturated with respect to DOC and DOC concentrations are high, the most probable and dominant mechanism for colloid binding is the hydrophobic binding between mobile and immobile organic matter which can be described successfully by a time dependent Langmuir equation (Jardine *et al.*, 1992). Although the simulation results do not exactly mimic the experimental data, a strong indication exists for reversible kinetic colloid solid matrix interaction being responsible for the large tailing.

In the simulations reported here, all association and dissociation rate coefficients are assumed to be constants. In reality, this may not be true. For instance, sorption of Am on humic colloids can change the properties of the colloids and thus the adsorption and desorption rate constants may depend on the amount of Am bound on the colloids. Similarly, sorption of contaminants and colloids on the solid matrix may change the surface

properties of this matrix and, hence, the association and dissociation constants related to interactions with the solid matrix. Finally, colloid sizes may increase due to adsorption of Am on the colloidal surfaces (Kim et al, 1994a).

## Conclusions

Comparison of simulation results with experimental data indicates that the model COLTRAP can successfully describe some of the important characteristics of colloid facilitated transport of radionuclides, at least under certain conditions. It has been shown that desorption of Am from humic colloids is a slow process. Without assuming kinetic interaction between Am and humic colloids it was impossible to simulate experimental data. A strong indication exists that reversible kinetic colloid solid matrix interaction is responsible for the large tailing observed in the experiment.

## Acknowledgments

This work was partly financed by the Commission of the European Communities' (CEC) 4th R&D Programme on Management and Storage of Radioactive Waste (1990-1994) Part A, Task 4: "Disposal of Radioactive Waste" under contract FI2W/CT91-0079.

## References

- Brusseau M.L. 1993. The Influence of Solute Size, Pore Water Velocity, and Intraparticle Porosity on Solute Dispersion and Transport in Soil. *Wat. Resour. Res.*, 29, 1071-1080.
- Buddemeier R.W. and Hunt J.R. 1988. Transport of Colloidal Contaminants in Groundwater: Radionuclide Migration at the Nevada Test Site. *Appl. Geochem.*, 3, 535-548.
- Buffle J. 1988. Complexation reactions in aquatic systems: an analytical approach. R.A. Chalmers, M.R. Masson, Eds, Ellis Horwood Series in Analytical chemistry. Ellis Horwood Limited, Chichester, UK.
- Corapcioglu M.Y and Jiang S. 1993. Colloid-Facilitated Groundwater Contaminant Transport. *Water Resour. Res.*, 29, 2215-2226.
- Deguedre C.A., Baeyens B., Goerlich W., Riga J., Verbist J. and Stadelmann P. 1989. Colloids in Water from a

## CHAPTER 3

- Subsurface Fracture in Granitic Rock, Grimsel Test Site, Switzerland. *Geochim. Cosmochim. Acta*, 53, 603-610.
- Dunnivant, F.M., Jardine P.M., Taylor D.L. and McCarthy J.F. 1992a. Cotransport of Cadmium and Hexachlorobiphenyl by Dissolved Organic Carbon through Columns Containing Aquifer Material. *Environ. Sci. Technol.*, 26, 360-368.
- Dunnivant, F.M., Jardine P.M., Taylor D.L. and McCarthy J.F. 1992b. Transport of Naturally Occurring Dissolved Organic Carbon in Laboratory Columns Containing Aquifer Material. *Soil Sci. Soc. Am. J.*, 56, 437-444.
- Gschwend, P.M. and Reynolds M.D. 1987. Monodisperse Ferrous Phosphate Colloids in an Anoxic Groundwater Plume. *J. Contam. Hydrol.*, 1, 309-327.
- Jardine, P.M., Dunnivant F.M., Selim H.M. and McCarthy J.F. 1992. Comparison of Models for Describing the Transport of Dissolved Organic Carbon in Aquifer Columns. *Soil Sci. Soc. Am. J.*, 56, 393-401.
- Kim, J.I., Buckau G. and Klenze R. 1987. Natural Colloids and Generation of Actinide Pseudocolloids in Groundwater. In: B. Come and N. A. Chapman (Editors.), Natural Analogues in Radioactive Waste Disposal. Graham and Trotman, London, UK, 289-299.
- Kim, J.I., Rhee D.S. and Buckau G. 1991. Complexation of Am(III) with Humic Acids of Different Origin. *Radiochim. Acta*, 52/53, 49-55.
- Kim, J.I., Zeh P., Delakowitz B. 1992. Chemical Interactions of Actinide Ions with Groundwater Colloids in Gorleben Aquifer Systems. *Radiochim. Acta* 58/59, 147-154.
- Kim, J.I., Delakowitz B., Zeh P., Probst T., Lin X., Ehrlicher U. and Schauer C. 1994a. Appendix I In: Colloid Migration in groundwaters: geochemical interactions of radionuclides with natural colloids. Institut für radiochemie, Technische Universität München, RCM 00394.
- Kim, J.I., Delakowitz B., Zeh P., Klotz D. and Lazik D. 1994b. A column Experiment for the Study of Colloidal Radionuclide Migration in Gorleben Aquifer Systems. *Radiochim. Acta*, 66/67, 165-171.
- Lieser K.H., Ament A., Hill R., Singh R.N., Stingl U. and Thybusch B. 1990. Colloids in Groundwater and their Influence on Migration of Trace Elements and Radionuclides. *Radiochim. Acta*, 49, 83-100.
- Longworth G. and Ivanovich M. 1989. The Sampling and Characterisation of Natural Groundwater Colloids: Studies in Aquifers in Slate, Granite and Glacial Sand. Harwell Laboratory, Harwell, UK, NSS/R165.
- Meinrath G. and Kim J.I. 1991. The Carbonate Complexation of the Am(III) Ion. *Radiochim. Acta* 52/53, 29-34.
- Mills W.M., Liu S. and Fong F.K. 1991. Literature Review and Model (COMET) for Colloid/Metals Transport in Porous Media. *Ground Water*, 29, 199-208.
- Short S.A., Lawson R.T. and Ellis J. 1988. Uranium-234/Uranium-238 and Thorium-230/Uranium-234 Activity Ratios in the Colloidal Phases of Aquifers in Lateritic Weathered Zones. *Geochim. Cosmochim. Acta*, 52, 2555-2563.
- Stadler S. and Kim J.I. 1988. Hydrolysis reactions of Am(III) and Am(IV). *Radiochim. Acta* 44/45, 39.
- Von Gunten H.R., Waber U.E. and Krahenbuhl U. 1988. The Reactor Accident at Chernobyl: A Possibility to Test Colloid-Controlled Transport of Radionuclide in a Shallow Aquifer. *J. Contam. Hydrol.* 2, 237-247.



# Chapter 4

## **Modeling the dynamic adsorption/desorption of a NOM mixture: Effects of physical and chemical heterogeneity\***

### **Abstract**

Because natural organic matter (NOM) can act as a carrier for contaminants, it is of great importance to understand its dynamic adsorption/desorption behavior. NOM is a mixture of organic molecules that vary both in chemical and physical properties. The adsorption/desorption behavior of a NOM mixture to the solid matrix can not be adequately described using simple equilibrium sorption isotherms, like the Langmuir isotherm. Often adsorption/desorption hysteresis is found or "adsorption maxima" keep increasing slowly.

In this paper a relatively simple model is developed to describe the kinetic adsorption/desorption of NOM. The model is calibrated using experimental data. Model simulations of experimental data show that adsorption/desorption hysteresis is an inherent property of a heterogeneous mixture of molecules. The composition and thus the properties of the mixture vary with the total amount of NOM added and with surface/volume ratio's. Therefore the relationship between the overall adsorption and the overall solution concentration is non-unique and thus a non-thermodynamic isotherm. Although adsorption in terms of mass of carbon seems to reach equilibrium relatively fast, the distribution of individual components can still be far from equilibrium. This indicates that the composition of the NOM mixture may vary with time as well.

---

\* by H. van de Weerd, W.H. van Riemsdijk and A. Leijnse  
published in: Environmental Science & Technology 33(1999) 1675-1681

## Introduction

In groundwater and pore water of soils and sediments, natural organic matter (NOM) is present in variable concentrations. Organic carbon concentration ranges from less than 1 to more than 100 mg C/l (e.g. Kim *et al.*, 1992, Gooddy *et al.*, 1995; del Castilho *et al.*, 1993). NOM can act as a carrier for solutes and may enhance transport of contaminants in soil and subsoil. Therefore, the understanding of the dynamic sorption behavior of NOM is of great importance for the understanding of carrier enhanced transport processes.

NOM is a mixture of different molecules, with sizes varying between 0.5 and about 400 nm and a molecular weight ranging from 200 to  $> 10^5$  g.mol<sup>-1</sup>. Small NOM molecules can be well defined weak organic polyacids like e.g. citric acid, which has a molecular diameter of around 0.5 nm and a molecular mass of 349 g.mol<sup>-1</sup>. Low molecular weight humic molecules are more or less flexible cylinders (so-called "oblong" particles) or more compact globular particles or ellipsoids. The high molecular weight humic molecules are large enough to form random coils or gels (Hayes *et al.*, 1989). It is not easy to attribute a size to them as the conformation of these structures may easily change as a function of the environmental conditions. The diameter of high molecular weight humic molecules generally is estimated not higher than 5 nm (McCarthy *et al.*, 1993, de Wit *et al.*, 1993). However, Kim *et al.* (1992) found humic colloids with diameters up to 400 nm in a saline aquifer system. Probably these colloids are aggregates of large humic molecules. NOM molecules contain functional groups like carboxyl, alcohol and quinone groups in variable concentrations and in general are negatively charged or neutral.

In soil, the main components for adsorption of NOM are iron- and aluminum(hydr)oxides. They can be present in crystalline form, as discrete particles or as amorphous oxide coatings on phyllosilicates (Jardine *et al.*, 1989). Under natural pH conditions (pH 3 - 8), pure iron and aluminum(hydr)oxides exhibit a positive charge, which decreases with increasing pH. Complexation of iron and aluminum(hydr)oxides with ligands like phosphate and small organic acids is relatively well understood (Balistrieri *et al.*, 1986, Hiemstra and Van Riemsdijk, 1996, Filius *et al.*, 1997, Geelhoed *et al.*, 1997ab). Sorption of NOM on Iron and aluminum(hydr)oxides is much more complicated. It is not likely that all reactive groups of NOM will interact in the same way with the surface due to steric effects, differences in the types of reactive groups and differences in the "molecular

environment" of the same type of groups. The hydrophobic nature of part of the NOM may influence the adsorption as well. Gu *et al.* (1994) provided evidence for ligand exchange reactions between NOM and iron oxide surfaces. They concluded that the sorption mechanism of NOM on oxide surfaces probably is a combination of charge neutralization and ligand exchange reactions.

In this paper we focus on the effect of the physical and chemical heterogeneity of a NOM mixture on its dynamic adsorption and desorption behavior. Therefore, we only consider sorption of NOM as a function of concentration and time. It will be evident that understanding the sorption behavior is further complicated by the fact that sorption behavior is dependent on temperature and on properties of the soil solution like pH, ionic strength and concentration of competing ions.

Studies of NOM adsorption to iron and aluminum(hydr)oxides as a function of aqueous NOM concentrations (Day *et al.*, 1994, Gu *et al.*, 1994, 1995, Parfitt *et al.*, 1977, Tipping, 1981, Wang *et al.*, 1997) show that sorption of NOM is characterized by isotherms with initially a relatively steep slope which becomes less steep upon adsorption. Often, no distinct sorption maximum is reached and a continuing slight increase of sorption density with increasing equilibrium NOM concentration is observed. Day *et al.* (1994) found different sorption isotherms for the same NOM and oxide surface at different surface to volume ratios (SV). Gu *et al.* (1994) found a profound hysteresis effect between adsorption and desorption. In contrast with adsorption data, desorption data showed high affinity behavior (a very steep initial slope followed by a plateau value).

To describe the sorption of NOM to iron oxides Tipping (1981) and Day *et al.* (1994) used the Langmuir isotherm. Part of their data could be described in an adequate way with this isotherm. Ochs *et al.* (1994) used the Frumkin Fowler Guggenheim (FFG) equation to describe sorption of humic acids to aluminum oxides in an adequate way. The FFG model takes into account lateral interaction of the adsorbed molecules. Gu *et al.* (1994,1995) could describe adsorption of NOM in an adequate way with a so-called modified Langmuir isotherm, which is essentially the same as the FFG model. To describe desorption data, a modified version of the model was used in which a hysteresis coefficient was introduced.

By using the Langmuir, modified Langmuir and FFG model, equilibrium is assumed between the NOM in solution and sorbed on the solid phase. Moreover, possible preferent binding of certain fractions of the mixture of NOM molecules is not considered explicitly in

these models. In fact one "average" NOM molecule is assumed with an "average" behavior. Sorption studies show that iron oxide and aluminum oxide adsorb different fractions of NOM with different affinity and capacity (Gu *et al.*, 1995, Ochs *et al.*, 1994). Also, UV-absorbance spectrometry observations of the NOM mixture in solution before and after adsorption differed, which indicates preferential adsorption of certain NOM fractions by iron oxides (Gu *et al.*, 1996). Sorption data of NOM to aluminum oxide (Ochs *et al.*, 1994) show that different fractions of NOM (measured in the aqueous phase with UV/VIS) respectively increase and decrease as a function of equilibration time at low SV. This indicates kinetic adsorption/desorption behavior and competition between the different NOM fractions. Equilibrium models assuming average behavior might describe sorption of NOM well under certain conditions. However, if sorption behavior is time dependent and not "average", a sorption model should take into account time dependence and the competition between the different NOM fractions.

For adsorption of polymers, it is theoretically and experimentally well established that a) monodisperse polymers have a very high initial slope of the adsorption isotherm followed by a plateau (high affinity behavior), b) the maximum amount adsorbed is a function of the molecular weight and c) large molecules adsorb preferentially over smaller ones (have a higher affinity). Thus in the equilibrium situation short chains will have been displaced by longer ones (Cohen Stuart *et al.*, 1980). Rates of diffusion and reformation will decrease with increasing molecular size, and thus the time required to exchange small polymer molecules for larger ones is governed by the rate of diffusion and reformation of the larger components (Koopal, 1981).

For NOM the same phenomena may play a role. However with NOM the situation is more complicated than with synthetic polymers: the latter are a mixture of exactly the same type of molecules, differing only in size, whereas different NOM fractions differ in average molecular weight as well as in chemical composition and structure. Hence, a replacement of one class of molecules at the surface by another class could be caused by difference in molecular weight as well as difference in chemical composition of these classes (Ochs *et al.*, 1994). Vermeer (1996) shows that using the advanced adsorption theory of Scheutjens and Fleer (Fleer *et al.*, 1993) for linear polyelectrolytes, the sorption of naturally occurring humic substances on iron oxide can be understood and that adsorbed humics can be described as a dynamic layer of polyelectrolytes, extending into the solution.

In this paper, the effect of the physical and chemical heterogeneity of NOM on its

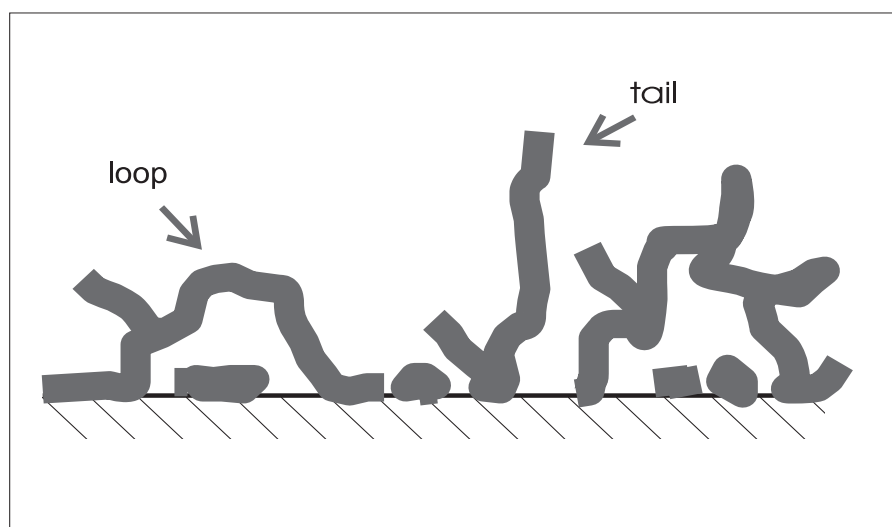


**Figure 1** Sorption of a mixture of small and large NOM molecules on the solid matrix in 2-D

dynamic adsorption and desorption behavior is studied. The sorption of NOM is imagined as the sorption of a heterogeneous mixture of polyelectrolytes. The sorption behavior of the individual molecules is a function of the chemical characteristics and the molecular weight of the molecules. A relatively simple model is developed for time dependent sorption of a mixture of NOM. Model parameters (the number of NOM fractions, affinity and maximum sorption capacity for each fraction) are determined using data and relations from literature. Using this model, experimental data are simulated and the effect of dynamic competition between different fractions (MW and chemical characteristics) is shown.

## Adsorption/Desorption Model for a NOM mixture

In our model we imagine the sorption of NOM as the sorption of a heterogeneous mixture of polyelectrolytes. The (hydr)oxide surface is heterogeneous as well. However, we assume this heterogeneity to be negligible compared to the heterogeneity in the NOM mixture. Therefore, the solid matrix is treated as a reactive surface with only one type of sorption site to which the different molecules may adsorb. Occupation of surface sites may occur by direct binding of NOM functional groups. However, due to steric hindrance, more sites than those involved in direct binding may be blocked (occupied). Small molecules will only occupy one or a few sites that are located near or close to each other. The larger molecules,

however, may cover a larger area of the surface. The occupied sites in this area are not necessarily neighboring. A fraction of the larger molecules extends in solution and may form so called "loops" and "tails", parts attached to the surface at respectively two and one side. Figure 1 shows an example of sorption of a mixture of small and large molecules. For small, rigid molecules, the number of surface sites occupied per molecule will be a constant. As the larger molecules are flexible, they can bind in different conformations, which may vary in time. Due to this, the number of surface sites occupied may be variable and is dependent on the fraction of the molecule in direct contact with the surface. In spite of this, we define an average number of surface sites occupied for every molecular weight fraction. The larger the molecule, the larger the part which is extended into the soil solution and the higher the sorption maximum expressed in  $\text{mg C/m}^2$ . This is also observed in polymer chemistry. Cohen Stuart *et al.* (1980) derived a relationship between molecular mass and the sorption maximum. Figure 2 shows a relationship between molecular mass and sorption maximum for the hydrophobic (Hb) and hydrophilic (HI) fraction of NOM as derived later in this paper, based on their work. We assume that it is always possible to saturate unoccupied sites with every molecular size. As the larger molecules are flexible, they can occupy sites that are not necessarily neighboring (See Figure 1). For simplicity, we assume that for all molecules the affinity is constant with surface coverage. However, lateral interaction may cause a variation of sorption affinity with surface coverage (Ochs *et al.*, 1994, Gu *et al.* 1994, 1995).

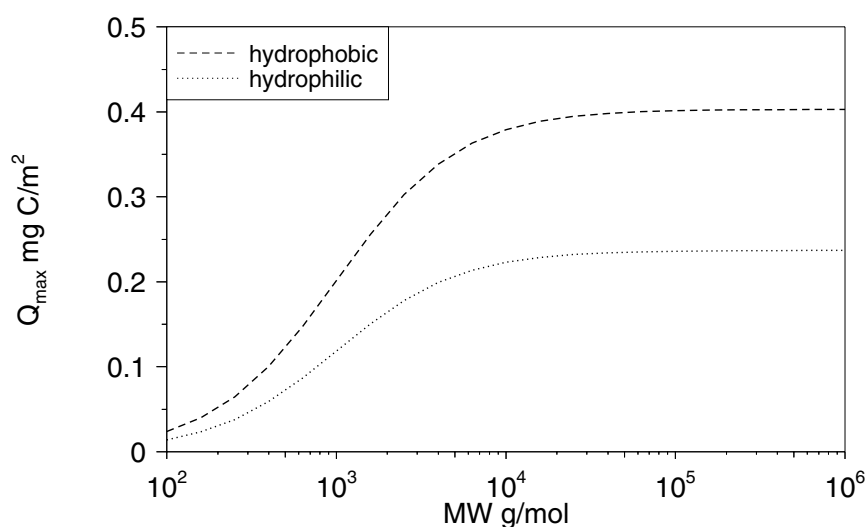


**Figure 2** Relationship between molecular mass and sorption maximum for the hydrophobic (Hb) and Hydrophilic (HI) fraction of NOM

To model a NOM mixture, it is assumed that NOM consists of a number of discrete fractions (species) that may vary in their affinity for the surface,  $K$ , adsorption rate constant  $k_a$ , desorption rate constant  $k_d$ , maximum mass adsorbed  $Q_{max}$  and the average number of surface sites occupied per molecule  $n$ . All species are assumed to compete for the same sites and their reaction with the surface may be simplified as in Equation 1, where  $S$  is a free surface site,  $A_i$  is a molecule of species  $i$  in the aqueous phase and  $S_{n_i}A_i$  is the surface complex formed.



The sorption of each individual species is described by a kinetic competitive Langmuir type equation of the form:

$$\frac{d[S_{n_i}A_i]}{dt} = k_{ai}[A_i] \frac{S_t}{n_i} (1 - \Theta) - k_{di}[S_{n_i}A_i] \quad (2)$$

in which  $t$  (s) is time,  $[S_{n_i}A_i]$  ( $\text{mol}\cdot\text{m}^{-2}$ ) is the concentration of surface complexes with species  $i$  and  $S_t$  ( $\text{mol}\cdot\text{m}^{-2}$ ) is the total number of surface sites ( $S_t = [S] + \sum_{i=1}^{i=x} n_i[S_{n_i}A_i]$ ).

$[A_i]$  ( $\text{mol}\cdot\text{l}^{-1}$ ) is the concentration of species  $i$ ,  $k_{ai}$  ( $\text{l}\cdot\text{mol}^{-1}\text{s}^{-1}$ ) and  $k_{di}$  ( $\text{s}^{-1}$ ) are the adsorption and desorption rate constant for species  $i$  and  $\Theta$  (-) is the fraction of sorption sites which are occupied, given by:

$$\Theta = \sum_{i=1}^{i=x} \Theta_i = \sum_{i=1}^{i=x} \frac{[S_{n_i}A_i]}{\frac{1}{n_i}S_t} = \sum_{i=1}^{i=x} \frac{n_i[S_{n_i}A_i]}{S_t} \quad (3)$$

where  $x$  is the number of species. Using Equation 3, Equation 2 can be rewritten in the following form:

$$\frac{d\Theta_i}{dt} = k_{ai}[A_i](1 - \Theta) - k_{di}\Theta_i \quad (4)$$

Note the difference between  $\Theta$  and  $\Theta_i$ .

For equilibrium, a thermodynamically consistent (Franses *et al.*, 1995) competitive Langmuir equation can be derived:

$$\frac{n_i[S_{n_i}A_i]}{S_t} = \Theta_i = \frac{K_i[A_i]}{1 + \sum_{i=1}^{i=x} K_i[A_i]} \quad (5)$$

in which the equilibrium constant  $K_i$  is given by:

$$K_i = \frac{k_{ai}}{k_{di}} = \frac{[S_{n_i}A_i]}{\frac{1}{n_i}[S][A_i]} = \frac{[S_{n_i}A_i]}{\frac{1}{n_i}S_t(1-\Theta)[A_i]} \quad (6)$$

It is not simple to derive forward and backward reaction rates for a mixture of polyelectrolytes consisting of large and small molecules. The reaction statistics are complicated. Larger molecules occupy more sites than small molecules and the chance of finding these sites near each other is smaller. However, large molecules are flexible and they may reach sites in a large area. In contrast with standard Langmuir behavior, in Equation 2 it is assumed that the adsorption reaction rate of a species is proportional with the number of free sites divided by the average number of sites occupied by this species. In accordance with standard Langmuir behavior we assume that the desorption reaction rate is proportional with the concentration of sorbed molecules while the adsorption reaction rate is proportional with the aqueous concentration of the species.

As both the adsorbed and aqueous concentrations of NOM are usually given in mass of carbon, it is convenient to express the model equations in these terms.  $\Theta_i$  also can be written as:

$$\Theta_i = \frac{[S_{n_i}A_i]}{\frac{1}{n_i}S_t} * \frac{M_{ci}}{M_{ci}} = \frac{Q_i}{Q_{max\ i}} \quad (7)$$

where  $M_{ci}$  is the mass of carbon per mole of species  $i$  and  $Q_i$  and  $Q_{max\ i}$  are the amount and the maximum amount of species  $i$  adsorbed ( $\text{g C}\cdot\text{m}^{-2}$ ). Note that  $n_i$  disappears by introducing  $Q_{max\ i}$ . Expressing the aqueous concentration in mass per liter, the individual mass balance equation of the species and the overall mass balance equations for organic carbon adsorbed and in the aqueous phase respectively can be given by combining Equations 3, 4 and 7:

$$\frac{dQ_i}{dt} = k_{ai}^* C_i (1-\Theta) Q_{\max i} - k_{di} Q_i \quad (8a)$$

$$\frac{dQ}{dt} = \frac{d \sum_{i=1}^{i=x} Q_i}{dt} = C(1-\Theta) \sum_{i=1}^{i=x} k_{ai}^* f_i Q_{\max i} - \sum_{i=1}^{i=x} k_{di} Q_i \quad (8b)$$

$$\frac{dC_i}{dt} = -SV \frac{dQ_i}{dt} \quad (9a)$$

$$\frac{dC}{dt} = \frac{d \sum_{i=1}^{i=x} C_i}{dt} = -SV \frac{d \sum_{i=1}^{i=x} Q_i}{dt} = -SV \frac{dQ}{dt} \quad (9b)$$

where,  $Q$  ( $\text{g C}\cdot\text{m}^{-2}$ ) and  $C$  ( $\text{g C}\cdot\text{l}^{-1}$ ) are the overall concentration of NOM adsorbed and in the aqueous phase,  $f_i$  is the fraction of the aqueous phase carbon concentration consisting of species  $i$ ,  $C_i = f_i \cdot C$  is the aqueous concentration of species  $i$  ( $\text{g C}\cdot\text{l}^{-1}$ ),  $k_{ai}^*$  is the adsorption rate constant expressed in  $\text{l}\cdot\text{g}^{-1}\cdot\text{s}^{-1}$  and  $SV$  is the surface to volume ratio ( $\text{m}^2\cdot\text{l}^{-1}$ ).

Combining Equations 3, 5 and 7 we obtain Equation 10 for the equilibrium situation.

$$Q = \sum_{i=1}^{i=x} Q_i = \sum_{i=1}^{i=x} \frac{C K_i^* f_i Q_{\max i}}{1 + C \sum_{i=1}^{i=x} K_i^* f_i} = \frac{C \sum_{i=1}^{i=x} K_i^* f_i Q_{\max i}}{1 + C \sum_{i=1}^{i=x} K_i^* f_i} \quad (10)$$

where,  $K_i^*$  is the affinity expressed in  $\text{l}\cdot\text{g}^{-1}\cdot\text{C}^{-1}$ . In situations where the amount sorbed substantially influences the composition of the aqueous phase (i.e. at low total amount of NOM added or high  $SV$ ) the fraction  $f_i$  of a species is not equal to the initial fraction of this species in solution due to preferential adsorption of certain fractions with high  $K_i \cdot Q_{\max i}$ . At high total amount of NOM added or low  $SV$ , however, the solution composition will be little influenced by the sorption and thus  $f_i$  will tend to a constant value. Using Equation 3, 7 and 10, for a system in equilibrium with constant mass fractions in solution,  $f_i$ , of the individual species, the following apparent monocomponent Langmuir equation, in terms of surface coverage can be derived:

$$\Theta = \frac{\overline{CK^*}}{1 + \overline{CK^*}} \quad (11)$$

where  $\overline{K^*} = \sum_{i=1}^{i=x} f_i K_i^*$  is the weighted average of the affinities. Note that Equation 11 is only valid under specific circumstances! Note further that Equation 11 cannot be transformed into an apparent monocomponent Langmuir equation in terms of mass adsorbed ( $Q$ ) as the values of  $Q_{max\ i}$  differ. Equations 8 and 10 simplify to the conventional kinetic Langmuir equation and its equilibrium form if the adsorption and desorption rate constant, the affinity and the values of  $Q_{max}$  are equal for the different species.

### *Program*

An adsorption program for NOM adsorption, NOMADS, is developed that, given the initial composition of the sorption complex and the solution phase and the value of SV, calculates the distribution of species in a batch system at a certain time. Equations 8a and 9a for all species considered form the set of mass balance equations that describe the dynamic adsorption and desorption of the mixture of discrete fractions of NOM. These equations constitute a set of ordinary differential equations, which is solved using a standard fourth order Runge-Kutta method.

## **Determination of model parameters**

Ideally, one should determine model parameters from independent data. As every mixture of NOM is unique, it is not possible to determine model parameters for a mixture without considering properties of the mixture itself. In this paper we simulate data measured by Gu *et al.* (1994). We try to determine model parameters as much as possible from properties that can be obtained independently from the adsorption/desorption data. However, not all parameters can be determined without fitting to these data. By finding relationships between model parameters and respectively MW and chemical composition of NOM, from theoretical consideration, literature or other experiments, the number of degrees of freedom is minimized. When parameter values are obtained by fitting this will be mentioned explicitly. Table 1 shows the distinguished fractions, which will be treated as model species, together with their attributed MW and model parameters.

**Table 1** Properties of the discrete NOM fractions distinguished, and model parameters used for these discrete fractions<sup>a</sup>

fractions		MW (g·mol <sup>-1</sup> )	<i>f</i> (-)	<i>K</i> (l·mg C <sup>-1</sup> )	<i>k<sub>a</sub></i> · 10 <sup>2</sup> (l·mg C <sup>-1</sup> ·h <sup>-1</sup> )	<i>k<sub>d</sub></i> (h <sup>-1</sup> )	<i>Q<sub>max</sub></i> (mg C·m <sup>-2</sup> )
MW < 3·10 <sup>3</sup>	HI	1.5·10 <sup>3</sup>	0.24	9.0·10 <sup>-1</sup>	1.62	1.8·10 <sup>-2</sup>	178
	Hb		0.26	1.8·10 <sup>0</sup>	3.24		252
3·10 <sup>3</sup> < MW < 10 <sup>5</sup>	HI	5.0·10 <sup>4</sup>	0.11	3.0·10 <sup>1</sup>	1.62	5.4·10 <sup>-4</sup>	284
	Hb		0.31	6.0·10 <sup>1</sup>	3.24		403
MW > 10 <sup>5</sup> (d < 1 μm)	HI	5.0·10 <sup>5</sup>	0.05	3.0·10 <sup>2</sup>	1.62	5.4·10 <sup>-5</sup>	287
	Hb		0.03	6.0·10 <sup>2</sup>	3.24		407

<sup>a</sup> Hb = Hydrophobic, HI = Hydrophilic, MW = molecular weight, d = diameter

### *Number of fractions and distribution of mass over fractions*

McCarthy *et al.* (1993) characterized the organic material used by Gu *et al.* (1994). They give the distribution of carbon of the NOM over three chemical fractions and within these fractions over four MW fractions. It is assumed that sorption behavior of the hydrophobic acid and hydrophobic neutral fraction does not differ significantly (Jardine *et al.* 1989). Further the largest MW fraction was not present in the NOM used in the adsorption/desorption experiment. Therefore, 6 fractions (2 chemical and 3 MW fractions) are distinguished. To each fraction an average MW is attributed.

### *Maximum mass adsorbed, $Q_{max}$*

In accordance with observations from polymer chemistry, it is assumed that  $Q_{max}$  is a function of MW. For sorption of polymers, Cohen Stuart *et al.* (1980) have derived an empirical equation relating  $Q_{max}$  to molecular weight. For a good solvent this empirical equation can be simplified to:

$$Q_{max} = p / (1 + (M/M_0)^{-2b}) \quad (12)$$

where M is molecular weight,  $M_0$  is the molecular weight at which the increase of  $Q_{max}$  as a function of molecular weight is maximal,  $p$  is the maximum value of  $Q_{max}$  to which Equation 12 approaches at high MW. The value of  $b$  is chosen to be 0.6 (a value taken from Cohen Stuart (1980)). Equation 12 is valid for chemically homogeneous polymer solutions. Therefore, for both the hydrophobic (Hb) and the hydrophilic (HI) fraction  $Q_{max}$  as a

function of molecular weight is derived. Figure 2 shows the derived relationships. Gu et al. (1995) derived  $Q_{max}$  values for the Hb and Hl fraction and the < 3000 MW and > 3000 MW fraction of Georgetown NOM at pH 4.3 (0.403, 0.284, 0.237 and 0.304 mg/m<sup>2</sup> respectively). For p, the values of  $Q_{max}$  for Hb and Hl NOM are taken. We assume that these values (measured at high NOM concentrations in a "chemically homogeneous" mixture of molecules of different MW) approach the  $Q_{max}$  values for the largest MW. The value of  $M_0$  is estimated by using the  $Q_{max}$  values of the two MW fractions. Assuming that the measured  $Q_{max}$  values (Gu *et al.*, 1995) can be assigned to the MW at the upper boundary of the fraction (3000 and > 100,000),  $M_0$  is estimated to be 1000, and the  $Q_{max}$  values for both MW fractions fall between the values found for the Hb and Hl fraction determined at the "upper boundary MW" with Equation 12 (See Figure 2).

*Adsorption and desorption rate constants,  $k_a$  and  $k_d$ .*

The values of  $k_{ai}$  and  $k_{di}$  vary with the size of adsorbate molecules. Rates of diffusion and reformation will decrease with increasing molecular weight and size (Koopal, 1981). Additionally, high MW polymer molecules adsorb preferentially over smaller ones at equilibrium (Koopal, 1981), which means that their affinity,  $K_i = k_{ai}/k_{di}$ , is higher. Amongst others, this might be due to the fact that larger molecules adsorb with a larger number of functional groups. We assume that the affinity of sorption is proportional to molecular weight. Results from literature (Jardine *et al.*, 1989, Gu *et al.*, 1995) show that the affinity for Hb NOM is roughly a factor 2 higher than the affinity of Hl NOM. This leads to the following relationships:

$$\begin{aligned} \text{Hl NOM} & : k_{ai}/k_{di} = \kappa MW \\ \text{Hb NOM} & : k_{ai}/k_{di} = 2\kappa MW \end{aligned} \tag{13}$$

where  $\kappa$  is a coefficient relating the affinity for Hl and Hb NOM to MW. Using the data of Gu *et al.* (1994) its values is fitted to be  $0.6 \cdot 10^{-3} \text{ l} \cdot \text{mg}^{-1} \cdot \text{C}^{-1} \cdot \text{g}^{-1} \cdot \text{mol}$ . Both the affinity and the rate of diffusion and reformation of the molecules determine the absolute values of  $k_{ai}$  and  $k_{di}$ . To distinguish between both effects  $k_{ai}$  and  $k_{di}$  are divided in a part determined by the rate of diffusion and reformation,  $k_{aiD}$ ,  $k_{diD}$  and a part determined by the affinity,  $k_{aiA}$ ,  $k_{diA}$ . The rate of diffusion and reformation is assumed to be inversely proportional with molecular weight. Further it is assumed that the diffusion related constants are equal during adsorption and desorption and equal for the Hb and Hl fractions. This leads to the following

relationships:

$$\begin{aligned}
 k_{ai} &= k_{ai_D} k_{ai_A} \\
 k_{di} &= k_{di_D} k_{di_A} \\
 k_{ai_D} &= k_{di_D} = \gamma/MW
 \end{aligned}
 \tag{14}$$

where  $\gamma$  is a coefficient relating the rate of diffusion and reconfiguration during adsorption and desorption to MW. Using the data of Gu *et al.* (1994) its value is fitted to be  $27 \text{ g}\cdot\text{mol}^{-1}\cdot\text{h}^{-1}$ . Combining Equations 13 and 14, we then get the following relationships for the affinity:

$$\begin{aligned}
 \text{Hl NOM} : \frac{k_{ai}}{k_{di}} &= \frac{k_{ai_A}}{k_{di_A}} = \kappa MW \\
 \text{Hb NOM} : \frac{k_{ai}}{k_{di}} &= \frac{k_{ai_A}}{k_{di_A}} = 2\kappa MW
 \end{aligned}
 \tag{15}$$

The affinity might change due to changes in  $k_{ai}$ ,  $k_{di}$  or both. We choose  $k_{ai_A}$  to be equal to  $\kappa MW$  and  $2\kappa MW$  for Hl and Hb NOM respectively.  $k_{ai}$  Hl and Hb then equals  $\kappa\gamma$  and  $2\kappa\gamma$  respectively.  $k_{di_A}$  then will be 1 and  $k_{di}$  will be  $\gamma/MW$  for both Hl and Hb fractions.

## Simulation results and comparison with experimental data

Figure 3 shows adsorption and desorption data measured by Gu *et al.* (1994) at pH 4.1, together with simulation results using NOMADS. Model parameters are summarized in Table 1. Adsorption data are obtained by adding an iron oxide suspension to a series of Georgetown NOM solutions with different concentrations. After about 18 hours of shaking, the supernatant was separated and the NOM concentration was measured in this separated supernatant. After the adsorption phase of the experiment, desorption was initiated by replacing 4/5 of the supernatant volume by water with the same pH and ionic composition. The suspensions were shaken for 24 hours. The desorption equilibration process was repeated five times for each sample. The NOM concentration was measured in the separated supernatant. For all adsorption and desorption experiments SV was  $20.2 \text{ m}^2/\text{l}$ .

From the adsorption and desorption data in Figure 3a it is clear that adsorption and desorption occurs via a different pathway. The desorption isotherms exhibit more high

affinity behavior than the adsorption isotherm; the slope at low concentration is steeper and a plateau is reached at much lower concentrations than in the adsorption isotherm. Simulation results show a good agreement with the adsorption and desorption data, suggesting that both adsorption and desorption data can be described with the same model, NOMADS, without changing any of the parameters. Figure 3a shows the overall adsorption and desorption while Figures 3b through 3d show the calculated contribution of the different species to the organic carbon concentration in the aqueous phase and on the solid matrix during adsorption and desorption. The calculated composition of the NOM in the aqueous phase and the adsorption complex differ significantly as was also suggested by measurements of Gu et al (1996). The high molecular weight (HMW) and hydrophobic (Hb) fractions are overrepresented on the adsorption complex and the low molecular weight (LMW) and Hydrophilic (Hl) fractions are overrepresented in solution. Figure 3b and 3c show that during adsorption, the composition of the NOM in solution resembles more and more the initial composition of NOM as the solution concentration increases. On the adsorption complex however, the Hb and the HMW fractions are overrepresented more and more with increasing concentration. During desorption (Figure 3d) the HMW and intermediate MW (IMW) fractions remain sorbed on the surface and the LMW fractions are removed selectively. During the adsorption and desorption phase of the experiment, the composition of the NOM mixture in solution changes, which is one of the reasons for the different shapes of the isotherms measured for adsorption and desorption (Figure 3a).

## Discussion

NOMADS is a relatively simple mechanistic model that describe the competitive kinetic adsorption behavior of a heterogeneous mixture of natural organic molecules. In this paper, NOM is described using 6 discrete fractions. The choice of fractions is based on experimental fractionation studies that have been done with this NOM. For every fraction we need values for  $k_a$ ,  $k_d$  and  $Q_{max}$ , leading to 18 model parameters for the simulations. However, the number of adjustable parameters is reduced to 2 by using relations between molecular weight and model parameters and values from literature. The relation between  $Q_{max}$  and molecular weight is derived from polymer chemistry (Cohen Stuart *et al.*, 1980).

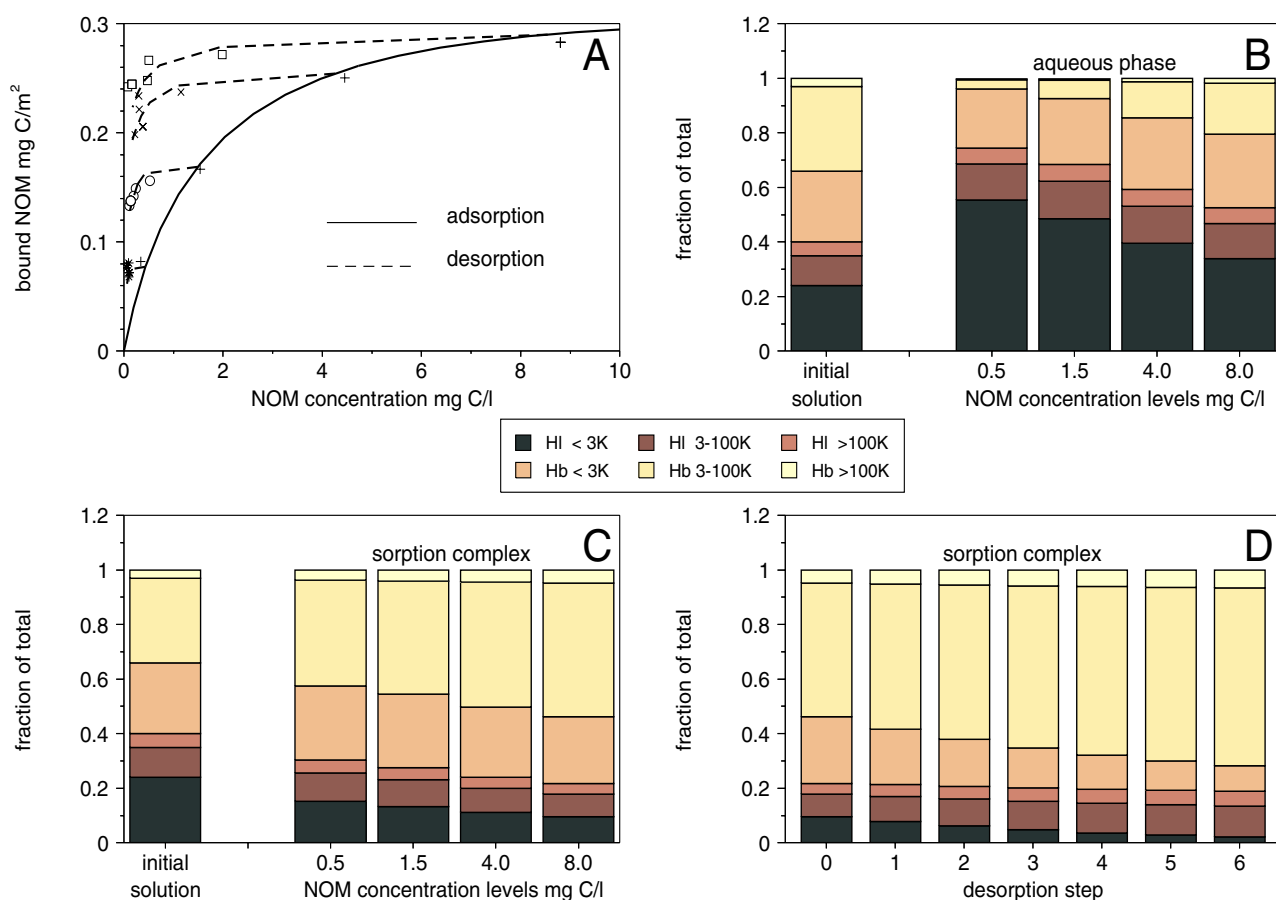


**Figure 3** Simulation and experimental results of adsorption and desorption of NOM to iron oxide at pH 4.1 (data from Gu *et al*, 1994). **3a** calculated adsorption and desorption curves together with experimental data of adsorption (+) and desorption experiments (□, x, ○, \*). **3b,c** Initial fractionation of the NOM solution together with calculated fractionation in the aqueous phase (3b) and on the sorption complex (3c) during the experiment at 4 NOM concentration levels representing roughly the adsorption data points in Figure 3a. **3d** Calculated fractionation of NOM on the sorption complex at a high NOM concentration level in the aqueous phase (~8.0 mg C/l, desorption step 0) and after the subsequent desorption steps, corresponding with the upper desorption curve in Figure 3a. HI = Hydrophilic, Hb = Hydrophobic, K = 1 Kilodalton = 1000 g/mol.

The other assumed simple linear relationships between the affinity and the rate of diffusion and reformation and molecular weight represent trends described in literature (Cohen Stuart *et al.*, 1980, Koopal, 1981). The model concept and the relations between physical and chemical properties of the NOM molecules and model parameters can be refined, once more detailed knowledge of these complex systems becomes available.

Only the values of  $\gamma$  and  $\kappa$ , which are coefficients that relate respectively the affinity and the rate of diffusion and reformation to the molecular weight, are fitted using the adsorption and desorption data from Gu *et al* (1994). Although only 6 fractions are used, experimental results indicating a different pathway for adsorption and desorption can be described well. This gives confidence that the here defined model concepts and ideas are

reasonable at least in a semi-quantitative manner. The physical and chemical heterogeneity of the NOM mixture appears to be an essential element in understanding the dynamic adsorption and desorption behavior of NOM on mineral surfaces.

During the adsorption experiment the mass fractions of the individual NOM species in the whole system (sorbed and in solution) are constant because the proportions in which the species are added to the system are constant. Simulations show, however, that the individual mass fractions in solution and on the sorption complex change, both as function of time and total amount of NOM added to the system (loading). This is due to differences in affinity and rate constants of the species. During desorption experiments performed according to Gu et al (1994) the individual mass fractions for the whole system may change as well due to selective removal of certain species from the system.

During the experiments, the composition and thus the properties of the NOM mixture change and therefore, adsorption and desorption can not be described using average properties of the mixture. The use of adsorption isotherms to describe adsorption and desorption of a mixture of NOM molecules therefore easily leads to confusion.

In adsorption isotherms usually the amount adsorbed of a certain species per unit mass or area of solid matrix is plotted against the activity of this species in solution. Other experimental conditions like pH, ionic strength, temperature and concentration of competing species will be kept constant. If adsorption of a species is given in this way, and the system is in equilibrium, the slope of the isotherm at low surface loading is a measure of the affinity. Different values of SV will not affect the thermodynamic adsorption isotherms and, adsorption and desorption experiments will result in the same curve.

In adsorption isotherms for NOM generally the mass of organic carbon per unit area or weight of solid matrix is plotted as a function of the mass of organic carbon in solutions. In fact the total adsorption of a mixture of competing species is plotted against the total concentrations of all species. In contrast with an adsorption isotherm for one species under constant conditions, sorption isotherms for a mixture are not unique. Changes in SV may affect the mass fractions of different NOM species in solution. In this way, the overall adsorption is affected and thus the adsorption isotherm of the mixture (see Equation 10 and the explanation after it). At low surface loading, the slope of the adsorption isotherm can vary strongly because differences in SV affect the composition of the mixture strongly under these conditions. It is impossible to construct desorption experiments for a mixture of molecules without either changing SV or allowing selective removal of certain species.

Both will affect the sorption isotherms of a mixture of molecules. Therefore it is almost unavoidable that adsorption and desorption experiments will result in different "sorption isotherms" for such systems. These types of isotherms are therefore from a thermodynamic point of view not meaningful.

We deal with a mixture of NOM molecules which may result in different curves for adsorption and desorption experiments; hysteresis. However, these phenomena may also occur if reactions are not in equilibrium. In the model simulation, using the "best fit" parameters, overall equilibrium is not reached in the timeframe of the adsorption and desorption experiments. However, the mixture effect is the major reason for the observed hysteresis, because simulations with increased reaction time reaching full equilibrium show that the curves change somewhat but the hysteresis is still present (results not shown).

In accordance with observations of Gu *et al.* (1994) simulations show only little increase of the amount of NOM sorbed (in terms of gC) after 18 hours (results not shown). However, this does not mean that equilibrium has been reached for the individual NOM species in the mixture. Redistribution of the different species may still occur. From Equation 8a we can derive that for the individual species at equilibrium we have:

$$\frac{Q_i}{C_i(1-\Theta)} = \frac{k_{ai}^* Q_{maxi}}{k_{di}} \quad (16)$$

The quotient at the right hand side (RHS) of Equation 16 is a constant, meaning that also the quotient at the left hand side (LHS) should be a constant at equilibrium. If equilibrium is not reached yet, the LHS quotient will vary with time. Dividing this quotient by the RHS quotient gives a good measure of the degree of equilibrium of the individual NOM species in the system that can be calculated easily. Note that the degree of equilibrium of a NOM species is influenced by its concentration in solution, its amount adsorbed and the total sorption of all species ( $\Theta$ ). Values higher and lower than 1 indicate more respectively less adsorption than at equilibrium. Figure 4 shows the simulated degree of equilibrium against time for all species at two points of the adsorption isotherm. Results show that depending on the amount of NOM added to the system (the point on the adsorption isotherm) and on the particular NOM species, the degree of equilibrium varies (if full equilibrium has not yet been reached). At low concentrations total equilibrium is reached within about a week (168 h). At high concentrations however, even after a month (720 h) equilibrium is not reached and redistribution still occurs. At high concentration we see that the smallest fractions are

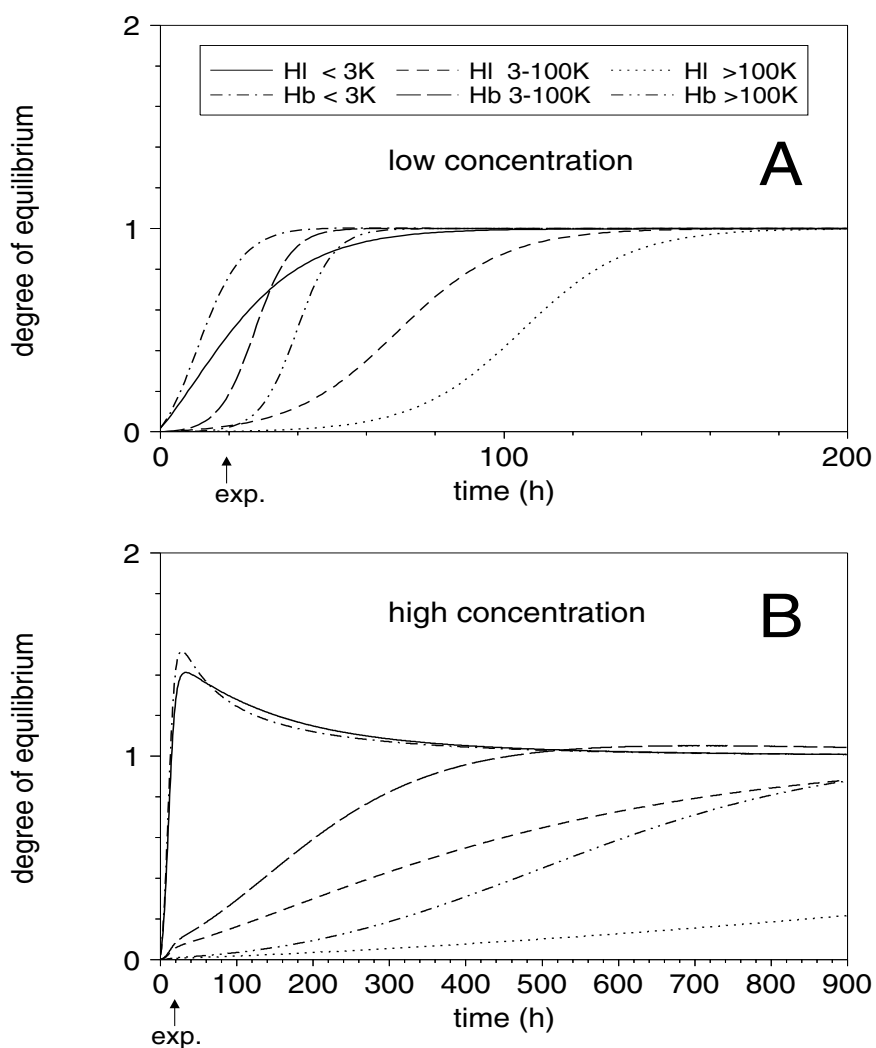


**Figure 4** Simulated degree of equilibrium of the individual species in the NOM mixture as a function of time at two NOM concentration levels. The initial concentration in the system was 2.0 mg/l (4a) and 14.4 mg/l (4b) (corresponding roughly to the initial concentrations at lower and upper point of the adsorption isotherm in Figure 3a). The arrows indicate the duration of the adsorption experiments of Gu *et al* (1994). The degree of equilibrium is given by the quotient of the LHS and RHS of equation 16.

initially overrepresented on the surface and will exchange with the larger fractions in course of time. At low concentration we see that Hb fractions reach equilibrium earlier than the HI fractions. For a mixture of NOM, the fact that the amount sorbed in time is almost constant is not a good indication for approaching equilibrium. Although the occupation of sites ( $\Theta$ ) will hardly change, the redistribution will lead to more high affinity species (with a higher  $Q_{max}$  and more carbon per site occupied) on the sorption complex. This will lead to a slow increase of the amount sorbed in terms of  $gC/m^2$  with progressing contact time.

In this paper we have shown that adsorption and desorption data showing hysteresis can be described well with a relatively simple model integrating knowledge from polymer

chemistry and environmental chemistry. The model describes all reported data without changing model parameters. It allows illustrating and quantifying important features of dynamic sorption of a mixture of NOM molecules, which are not easily understood without such a model concept.

## Acknowledgement

Mr. B. Gu is greatly acknowledged for providing the adsorption/desorption data.

## References

- Balistreri L.S. and Murray J.W. 1986. The influence of the major ions of seawater on the adsorption of simple organic acids by goethite. *Geochim. Cosmochim. Acta* 51, 1151-1160.
- Cohen Stuart M.A., Scheutjens M.M.H.M and Fleer G.J. 1980. Polydispersity effects and the interpretation of polymer adsorption isotherms. *J. Polym. Sci.* 18, 559-573.
- Day, G. McD., Hart B.T., McKelvie I.D., Beckett R. 1994. Adsorption of natural organic matter onto goethite, *Coll. Surf. A: Physicochemical and Engineering Aspects* 89, 1-13.
- de Wit J.C.M., van Riemsdijk W.H., Koopal, L.K. 1993. Proton binding to humic substances: 1. Electrostatic effects. *Environ. Sci. Technol.* 27, 2005-2014.
- del Castillo P., Chardon W.J., Salomons W. 1993. Influence of cattle-manure slurry application on the solubility of cadmium, copper, and zinc in a manured acidic, loamy-sand soil. *J. Environ. Qual.* 22, 689-697.
- Filius J.D., Hiemstra T. and van Riemsdijk W.H. 1997. Adsorption of small weak organic acids on goethite: Modeling of mechanisms. *J. Colloid Interf. Sci.* 195, 368-380.
- Fleer G.J., Cohen Stuart M.A., Scheutjens J.M.H.M., Cosgrove T., Vincent B. 1993. *Polymers at Interfaces*, Chapman & Hall, London.
- Franses E.I., Siddiqui F.A., Ahn D.J., Chang C-H. and Wang N-H.L. 1995. Thermodynamically Consistent Equilibrium Adsorption Isotherms for Mixtures of Different-Size Molecules. *Langmuir*, 11(8), 3177-3183.
- Geelhoed J.S., Hiemstra T. and van Riemsdijk W.H. 1997a. Phosphate and sulfate adsorption on goethite. *Geochim. Cosmochim. Acta* 61, 2389-2396.
- Geelhoed J.S., Hiemstra T. and van Riemsdijk W.H. 1997b. Competitive interaction between phosphate and citrate on goethite. *Environ. Sci. Technol.* 32(14), 2119.
- Goody D.C., Shand P., Kinniburgh D.G., van Riemsdijk W.H. 1995. Field-based partition coefficients for trace elements in soil solutions. *Eur. J. Soil Sci.* 46, 265-285.
- Gu B., Schmitt J., Chen Z., Liang L. and McCarthy J.F. 1994. Adsorption and Desorption of Natural Organic Matter on Iron Oxide: Mechanisms and Models. *Environ. Sci. Technol.* 28(1), 38-46.
- Gu B., Schmitt J., Chen Z., Liang L. and McCarthy J.F. 1995. Adsorption and desorption of different organic matter

## CHAPTER 4

- fractions on iron oxide. *Geochim. Cosmochim. Acta* 59(2), 219-229.
- Gu B., Mehlhorn T.L., Liang L. and McCarthy J.F. 1996. Competitive adsorption, displacement, and transport of organic matter on iron oxide: I. Competitive adsorption. *Geochim. Cosmochim. Acta* 60(11), 1943-1950.
- Hayes M.H.B., MacCarthy P., Malcolm R.L., Swift R.S. (Eds.), 1989. Humic Substances II: In Search of Structure, Wiley Interscience, New York.
- Hiemstra T. and van Riemsdijk W.H. 1996. A structural approach to ion adsorption: The charge distribution model. *J. Colloid Interface Sci.* 179, 488-508.
- Jardine P.M., Weber N.L., McCarthy J.F. 1989. Mechanisms of dissolved organic carbon adsorption on soil. *Soil Sci. Soc. Am. J.* 53, 1378-1385.
- Kim J.I., Delakowitz B., Zeh P., Probst T., Lin X., Ehrlicher U., Schauer C. 1992. Appendix I in: Colloid migration in groundwaters: geochemical interactions of radionuclides with natural colloids, 2nd progress report, RCM 00692, Technische universität münchen.
- Koopal, L.K., 1981. The effect of polymer polydispersity on the adsorption isotherm, *J. Colloid Interf. Sci.* 83(1), 116-129.
- McCarthy J.F., Williams T.M., Liang L., Jardine P.M., Jolley L.W., Taylor D.L., Palumbo A.V. and Cooper L.W. 1993. Mobility of Natural Organic Matter in a Sandy Aquifer. *Environ. Sci. Technol.* 4, 667-676.
- Ochs M., Čosović B., Stumm W. 1994. Coordinative and hydrophobic interaction of humic substances with hydrophilic  $Al_2O_3$  and hydrophobic mercury surfaces. *Geochim. Cosmochim. Acta* 58(2) 639-650.
- Parfitt R.L., Fraser A.R. and Farmer V.C., 1977. Adsorption on hydrous oxides III Fulvic acid and humic acid on goethite, gibbsite and imogolite. *J. Soil Sci.* 28, 289-296.
- Tipping E. 1981. The adsorption of aquatic humic substances by iron oxides. *Geochim. Cosmochim. Acta* 45, 191-199.
- Vermeer A.W.P. 1996. Interactions between humic acid and hematite and their effects on metal ion speciation. Ph.D. dissertation, Wageningen Agricultural University, The Netherlands.
- Wang L., Chin Y.-P. and Traina S.J. 1997. Adsorption of (poly)maleic acid and an aquatic fulvic acid by goethite. *Geochim. Cosmochim. Acta* 61(24) 5313-5324.



# Chapter 5

## **Modeling transport of a mixture of Natural Organic Molecules (NOM): effects of dynamic competitive sorption from particle to aquifer scale<sup>\*</sup>.**

### **Abstract**

Natural organic matter (NOM) can act as a carrier for contaminants. Therefore, it is of great importance to understand its adsorption/desorption and transport behavior. NOM is a mixture of organic molecules varying in chemical and physical properties. The heterogeneity of NOM will affect its adsorption and transport behavior. In this paper we describe sorption and transport of NOM in aquifer material in both laboratory columns and in the field. We use the NOMADS model of Van de Weerd *et al.* (1999) incorporated in the transport model COLTRAP (van de Weerd *et al.*, 1998). The NOMADS model has been used previously to describe adsorption/desorption of NOM to iron oxide. It is a relatively simple model taking into account nonlinear time-dependent competitive adsorption/desorption of a number of NOM subfractions. Together with the NOMADS model, a method to decrease the number of adaptable parameters is used. The model has been calibrated using independent batch adsorption data.

Both in the laboratory columns and in the field experiment, sorption and transport of NOM are well simulated. It is shown that the heterogeneity of NOM is an essential feature to understand NOM adsorption and transport. The breakthrough curves of different size fractions observed in the field (McCarthy *et al.*, 1996), varying largely in shape, can very well be simulated and understood with the NOMADS model. Simulation results show how experimental conditions like pore water velocity, transport distance and the presence and composition of sorbed NOM on the sorption complex influence the behavior and interaction of the subcomponents and also the shape of the breakthrough curves.

The adsorption/desorption of the high molecular weight (HMW) subfraction of NOM is found to be very slow, resembling irreversible adsorption. It is shown that under certain conditions, the adsorption sites occupied with HMW NOM can be considered to be blocked.

By simulating laboratory batch and column experiments, and a field experiment, it is shown that the process descriptions incorporated in NOMADS are valid over a wide range of temporal and spatial scales and mass to volume ratio's.

---

<sup>\*</sup>by H. van de Weerd, W.H. van Riemsdijk and A. Leijnse  
submitted to: Water Resources Research

## Introduction

Natural organic matter (NOM) is a mixture of complex organic molecules that vary in size and chemical composition. In natural porous media NOM is present in the solid phase as well as in solution. Transport of NOM is of interest because it can serve as a carrier for contaminants such as hydrophobic organic pollutants, radionuclides and heavy metals. Different types of contaminants bind to different fractions of the NOM (so-called subcomponents). Radionuclides and heavy metals were found to be associated with anionic organic molecules which comprise the hydrophillic (Hl) and the hydrophobic acid fractions (Champ *et al.*, 1984, Stevenson, 1982). Hydrophobic organic contaminants like PCB's and benzo(a)pyrene bind preferentially to hydrophobic (Hb) NOM (Kukkonen *et al.*, 1990). Both enhancement (e.g., Dunnivant *et al.*, 1992a; Magee *et al.*, 1991) and retardation (Totsche *et al.*, 1997) of contaminant transport due to the presence of aqueous NOM is reported. Whether enhancement or retardation occurs, depends on the mobility of this carrier. Modeling the transport behavior of NOM helps to understand the underlying processes.

The mobility of NOM in natural porous media depends on its reactivity with the solid matrix. In unsaturated porous media, sorption to the gas-water interface may play a role as well. Wan and Wilson (1994) show that retention of colloids increases with the gas content of a porous medium and that the degree of sorption increases with increasing colloid surface hydrophobicity. The mobility of NOM is further complicated by flocculation and precipitation reactions (Römken and Dolfing, 1998; Temminghoff *et al.*, 1997; 1998). These reactions occur at low pH and if high concentrations of polyvalent and potentially bridging ions, such as Ca, Al and Fe, are present in pore water. Further, also formation and degradation of mobile NOM may occur.

In soil and aquifer systems, the main components for adsorption of NOM are iron- and aluminum(hydr)oxides and clay minerals (Jardine *et al.*, 1989a, Sposito, 1984). The reactivity of NOM with the solid matrix depends on the affinity of NOM subcomponents for the reaction sites on the solid matrix and on the availability of these sites. The availability of sites is a function of the amount of reaction sites per unit mass of soil and the occupation of these reaction sites. The sorption affinity of NOM subcomponents depends on conditions influencing this affinity (such as pH and ionic strength). In soil and aquifer

systems these conditions can change in time (due to rainfall) and along the flow path of transport.

The reactivity of NOM with the solid matrix may further depend on hydrological properties of the system such as water saturation, porosity, presence of less permeable aggregates, and flow rate. These parameters influence the number of sorption sites per volume of water, the transport to these sites, and the contact time between NOM and sorption sites.

In this study we focus on transport and sorption of NOM in saturated systems with constant chemical conditions. We consider the behavior of a NOM mixture and NOM subcomponents in laboratory and in field experiments (different transport distances and flow velocities) and the modeling of this behavior.

Laboratory adsorption and adsorption/desorption studies give evidence for 1) nonlinear kinetic adsorption/desorption of NOM, 2) NOM consisting of subcomponents varying in sorption affinity and capacity and 3) competition between subcomponents (Ochs *et al.*, 1994; Wang *et al.*, 1997; Gu *et al.*, 1994, 1995, 1996). This suggests that the sorption of NOM should be described with a nonlinear, kinetic model that takes into account different organic species, which compete with each other for the same adsorption sites. Van de Weerd *et al.* (1999) developed a relatively simple model for competitive time dependent adsorption/desorption of a mixture of NOM subcomponents. Model parameters are the number of sorbing species (i.e., NOM subcomponents), adsorption and desorption rate constants and the sorption affinity and sorption capacity for each species. Using data and relations from literature, they defined six subcomponents varying in molecular weight and chemical characteristics and determined model parameters for these subcomponents. Using this model, dynamic competition between different subcomponents was simulated and experimental data showing apparent hysteresis could be adequately described.

Transport of NOM under saturated conditions is studied in both field and laboratory experiments (Jardine *et al.*, 1989b, McCarthy *et al.*, 1993; 1996, Dunnivant *et al.*, 1992b, Abdul *et al.*, 1990). Breakthrough curves of NOM can be characterized by a rapid breakthrough of part of the NOM (after around one pore volume) indicating inert transport of part of the NOM, followed by a decrease of the slope of the breakthrough curve and a slow approach to the influent concentration. Often extended tailing is observed. In the desorption phase of NOM transport experiments, the breakthrough curve often shows a steep decrease in concentration followed by a continuous slow decrease of a low

concentration of NOM (Dunnivant *et al.*, 1992b, McCarthy *et al.*, 1996).

Dunnivant *et al.* (1992b) show differences in shape between breakthrough curves of different NOM concentrations in comparable experiments, with the breakthrough of the higher concentration slightly earlier and approaching the influent concentration faster. Further, it is shown that subcomponents of NOM behave differently during transport both in field and column experiments (Dunnivant *et al.*, 1992b; McCarthy *et al.*, 1993; 1996) with the hydrophilic and low molecular weight (LMW) NOM subcomponents being more mobile than the hydrophobic and high molecular weight (HMW) subcomponents.

Experimental results of NOM transport through unsaturated soil columns (Totsche *et al.*, 1997) differ from results under saturated conditions. Totsche *et al.* (1997) found that an apparent equilibrium situation is reached after about three pore volumes at about 30% of the influent concentration at two different NOM concentration levels. They suggest this to be the result of selective retardation of the hydrophobic fraction.

Until now, models used to simulate NOM transport do not consider different behavior of subfractions of NOM but they do consider different types of sorption sites. Totsche *et al.* (1996) and Knabner *et al.* (1996) describe a two-site model for NOM adsorption. This model is not evaluated against NOM transport data. Jardine *et al.* (1992) compare data from displacement experiments of NOM through aquifer material with varying NOM influent concentration (Dunnivant *et al.*, 1992b) with modeling results. Modeling results are obtained using formulations of the convective-dispersive equation with different adsorption models assuming two types of adsorption sites and one adsorbing species. They used batch equilibrium and kinetic sorption studies with the same aquifer material to parameterize the transport models. The sorption parameters obtained from batch experiments could not be used to describe NOM transport data in column experiments. Furthermore, none of the transport models could successfully describe transport data at all influent NOM concentrations, even not after optimization on the data of the individual experiments. The description of both the initial rapid breakthrough and the tailing (at higher influent NOM concentrations) was a problem. NOM transport in a field experiment (McCarthy *et al.*, 1996) was simulated with a 2-site sorption model (Jardine *et al.*, 1992) included in a fully three dimensional flow model. Using this model, the shape of the measured breakthrough curves was reproduced reasonably well. However, differences between observed and simulated curves indicate that a single set of coefficients is not able to simulate the observed curves. The adsorption parameters seemed to change with time.

From this modeling exercise it was concluded that it is likely that the transport behavior of bulk NOM is due primarily to the multi-component nature of NOM and the large differences in the observed mobility of the NOM subcomponents. Moreover, from a fundamental chemical perspective the behavior of a chemically heterogeneous mixture cannot be mimicked by using a homogeneous model with average behavior (Van Riemsdijk *et al.*, 1986; van de Weerd *et al.*, 1999).

In this paper, we therefore consider different behavior of subfractions of NOM, in contrast with the transport models described above, assuming one "average" behavior of NOM molecules. We test whether, using this approach, results of NOM transport in natural media at different scales can be adequately described and understood. We assume the heterogeneity in surface sites to be negligible compared to the effect of the heterogeneity of the NOM mixture. The sorption model NOMADS (van de Weerd *et al.*, 1999), which is able to describe the dynamic competition between different NOM subcomponents, is incorporated in a 1-dimensional transport model for a saturated porous medium, COLTRAP (van de Weerd *et al.*, 1997; 1998). Using batch adsorption data of NOM to aquifer material, the NOMADS model is calibrated. Using this calibrated model, NOM transport in column experiments is predicted, transport of NOM subcomponents in a field experiment is simulated and features of NOM transport in the field are explained and predicted. Finally we discuss the expected impact of NOM on contaminant transport.

## **Models and model parameters**

### *Models*

We consider a system in which NOM subcomponents are present that vary in their reactivity with the solid matrix. The only interaction process considered is the competitive sorption of NOM subcomponents to the solid matrix. As we believe that the effect of heterogeneity in surface sites will be negligible compared to the effect of the heterogeneity of the NOM mixture, it is assumed that a limited number of homogeneous binding sites exist for NOM. Molecules of different NOM fractions may occupy a different number of these binding sites once they are bound (Van de Weerd *et al.*, 1999), and in this way the

different NOM subcomponents compete for the same NOM sites. Variable electrostatic potential effects and other interactions between adsorbed species are not modeled explicitly. Sorption reactions are described by a kinetic competitive Langmuir equation. The subcomponents (species  $i$ ) of NOM vary in their affinity, adsorption rate constant  $k_{ai}$ , desorption rate constant  $k_{di}$  and maximum mass adsorbed  $Q_{maxi}$ .

Describing the dispersive mass flux of all mobile species by a Fickian type relation and assuming constant porosity, velocity and dispersion coefficient, the one-dimensional mass balance equations for the mobile species can be written as:

$$\frac{\partial C_i}{\partial t} + v \frac{\partial C_i}{\partial x} - D \frac{\partial^2 C_i}{\partial x^2} = -\frac{\rho}{n} \frac{\partial Q_i}{\partial t} \quad (1)$$

where  $t$  is time (h),  $x$  is spatial position (cm),  $v$  (cm h<sup>-1</sup>),  $D$  (cm<sup>2</sup> h<sup>-1</sup>) are average velocity and dispersion coefficient of the mobile NOM species and  $\rho$  and  $n$  are the bulk density (kg·dm<sup>-3</sup>) and porosity (-), respectively.  $C_i$  is the aqueous concentration of NOM species  $i$  (mg·l<sup>-1</sup>) and  $Q_i$  is the amount of NOM species  $i$  sorbed (mg·kg<sup>-1</sup>). The mass of NOM is expressed as mass organic carbon. Further, we assume that the average velocity of all mobile NOM subcomponents equals the average velocity of water.

The mass balance equation for the NOM subcomponents bound to the solid matrix is given by:

$$\frac{\partial Q_i}{\partial t} = k_{ai}^* C_i (1 - \Theta) Q_{maxi} - k_{di} Q_i \quad (2)$$

where  $k_{ai}^*$  is the adsorption rate constant expressed in l·mg<sup>-1</sup>·h<sup>-1</sup> and  $k_{di}$  (h<sup>-1</sup>) is the desorption rate constant for species  $i$ ,  $Q_{maxi}$  is the maximum amount of species  $i$  adsorbed (mg·kg<sup>-1</sup>) and  $\Theta$  (-) is the fraction of sorption sites occupied, which is given by the sum of the occupations of the individual species  $\theta_i$ :

$$\Theta = \sum_{j=1}^{j=m} \theta_j = \sum_{j=1}^{j=m} \frac{Q_j}{Q_{maxj}} \quad (3)$$

where  $m$  is the number of species. The mass balance equations for the bound NOM subcomponents are coupled through this overall occupation  $\theta$  of the surface. The total mobile and bound NOM concentrations  $C$  and  $Q$  are given by respectively:

$$C = \sum_{i=1}^{i=m} C_i \quad (4)$$

$$Q = \sum_{i=1}^{i=m} Q_i \quad (5)$$

As we want to understand the behavior of NOM subcomponents at different scales and in different conditions we rewrite Equation 1 and 2 in dimensionless form. We define the following dimensionless variables:

$$C_{di} = \frac{C_i}{\Delta C_i} \quad x_d = \frac{x}{L} \quad t_d = \frac{t}{t_r} \quad Q_{di} = \frac{Q_i}{Q_{\max i}}$$

We define  $\Delta C_i$  to be equal to the influent concentration of species  $i$  and  $L$  to be the length of the domain. The reference time  $t_r$  is defined as  $L/v$ , which is the time needed to replace one pore volume in the domain with the influent solution. Using these dimensionless variables Equation 1 can be rewritten as:

$$\frac{\partial C_{di}}{\partial t_d} + \frac{\partial C_{di}}{\partial x_d} - \frac{D}{vL} \frac{\partial^2 C_{di}}{\partial x_d^2} = -\frac{\rho}{n} \frac{Q_{\max i}}{\Delta C_i} \frac{\partial Q_{di}}{\partial t_d} \quad (6)$$

Using the dimensionless variables Equation 2 can be rewritten as:

$$\frac{\partial Q_{di}}{\partial t_d} = k_{ai}^* \Delta C_i \frac{L}{v} C_{di} (1 - \Theta) - k_{di} \frac{L}{v} Q_{di} \quad (7)$$

where:

$$\Theta = \sum_{j=1}^{j=m} Q_{dj} = \sum_{j=1}^{j=m} \frac{Q_j}{Q_{\max j}} \quad (8)$$

From the dimensionless Equations 6 and 7 we can conclude that in situations with identical scaled initial and boundary conditions for all subcomponents and identical values of the following constants for all subcomponents:

$$\frac{D}{vL} = \frac{\alpha}{L} = \text{Pe} \quad (a) \quad \frac{\rho}{n} \frac{Q_{\max i}}{\Delta C_i} \quad (b) \quad \frac{L}{v} k_{ai}^* \Delta C_i \quad (c) \quad \frac{L}{v} k_{di} = \text{Da} \quad (d) \quad (9)$$

transport modeling of NOM subcomponents will lead to the same scaled results. The first and last constant are known as the Peclet (Pe) and Damkohler (Da) number respectively. The second constant is a ratio of the potentially available sites and the maximum change in concentration of a species (a ratio of the potential capacity of the solid matrix and of the solution for sorption). The last two constants are dimensionless adsorption and desorption rate constants. A combination of these constants gives a dimensionless equilibrium

constant. The dimensionless constants give insight in how the behavior of the NOM mixture depends on transport and sorption parameters. For example, larger transport distance or lower pore water velocity gives higher dimensionless adsorption and desorption rate constants which means that equilibrium conditions are approached more closely.

Note that dimensionless constants alone can never determine the total solution of a transport problem. Besides by the differential equation, the solution is also determined by initial and boundary conditions. Moreover, in a multi-component situation the behavior of the individual subcomponents depends on the occupation of the sorption complex with competing subcomponents that may change in time and place.

### *Program*

The adsorption/desorption equations (Equation 2) coupled by Equation 3 form the adsorption model NOMADS (van de Weerd *et al.*, 1999). The adsorption/desorption equations, together with the transport equations (Equation 1) for all NOM subcomponents form the set of mass balance equations that describe the dynamic adsorption/desorption and transport of a mixture of discrete fractions of NOM. These equations are incorporated in the program COLTRAP (Van de Weerd *et al.*, 1998). This program can solve a maximum number of 7 mass balance equations, which limits the maximum number of NOM species to 3. The governing equations are solved numerically by a Galerkin finite element method. A solution is obtained for the unknown concentration  $C_i$  and  $Q_i$ . Non-linearities are solved by a Newton-Raphson iteration scheme. In order to reduce round-off errors due to spatial discretization, an adaptive method is implemented, where the finite element grid is dynamically refined in areas with large concentration gradients.

### *Determination of model parameters*

To simulate transport of NOM subcomponents, we need to know transport parameters for the system considered, as well as parameters for adsorption/desorption of the individual NOM subcomponents.

In this paper we use batch data of NOM adsorption to aquifer material (Jardine *et al.*, 1992) to calibrate the adsorption/desorption model. This calibrated adsorption/desorption

model is then used to simulate NOM transport in laboratory and field experiments and to predict NOM transport behavior under field conditions. To determine the parameters for adsorption/desorption of the individual NOM subcomponents in the batch experiments and to reduce the number of parameters we use the same approach that was followed in Van de Weerd *et al.* (1999). We consider 6 NOM subcomponents and thus 18 model parameters ( $k_a$ ,  $k_d$  and  $Q_{max}$  for each fraction). However, the number of fitting parameters is reduced to 2, by using data and relations from literature. For the transport simulations the number of NOM fractions must be reduced to three. NOM fractions that show the most similar behavior (explained below) are combined using average properties.

Using the calibrated adsorption/desorption model we predict NOM transport data in a column experiment with the same NOM and aquifer material (Dunnivant *et al.*, 1992b). To simulate transport behavior of NOM under field conditions, calculations are done with lower pore water velocity, larger transport distances and with part of the sorption sites already occupied by NOM. The transport behavior of NOM in a field experiment (McCarthy *et al.*, 1996) is simulated as well using the calibrated adsorption/desorption model. In this experiment water is infiltrated and withdrawn with wells, resulting in a 3-D flow pattern between the wells. To simulate the flow pattern in this experiment a set of travel paths is determined (see explanation below). NOM transport is calculated along these travel paths.

Parameters for the adsorption/desorption model with 3 and 6 fractions are given in Table 1 and 2 respectively. Properties of the simulated column experiments are given in Table 3. Model parameters for calculation of NOM transport under field conditions are given in Table 4. Transport properties of the different travel paths and model parameters for simulation of NOM transport in the field experiment are given in Table 5 and 6. Below, the determination of the set of travel paths is explained. Further, the choice of boundary and initial conditions and the values of the model parameters are discussed.

#### *Determination of a set of travel paths*

The breakthrough curve of the tracer, as given by McCarthy *et al.* (1996), is analyzed in the ascending part, with a method described in Van de Weerd *et al.* (1991). The resulting travel time distribution and volume of travel paths are converted in 7 travel paths with a typical frequency, pore water velocity and travel path length (see Table 6). Lateral mixing between these travel paths will occur but is neglected here. Along these travel paths we performed 1-

D transport simulations of the tracer (CXTFIT) and of the NOM mixture (NOMADS/COLTRAP). The breakthrough curve of the tracer and of NOM (subcomponents) in the withdrawal well is calculated by:

$$C_i = \sum_{p=1}^{p=7} f_p C_{pi}(t, x=L) + f_o C_{bi} \quad (10)$$

In which  $C_{pi}$  is the concentration of species  $i$  in path  $p$  and  $C_{bi}$  and  $C_i$  are its background concentration and overall concentration in the withdrawal well respectively.  $f_p$  and  $f_o$  are the fractions of water in the withdrawal well coming from path  $p$  and from outside the area of travel paths delivering water from the infiltration well. Using this method, we do not intend to represent the actual flow field of water. However, we intend to approach the distribution of pore water velocity and travel distances of the withdrawn water. The breakthrough curve of the tracer using this approach shows good agreement with the tracer curve given by McCarthy *et al.*, (1996) (see the inset in Figure 8).

#### *Initial and boundary conditions*

For the mobile NOM subcomponents we use a no diffusion/dispersion boundary condition (Equation 11) at the end of the column and a prescribed flux boundary condition at the entrance of the column (Equation 12), in which  $C_{i^*}$  is the concentration of NOM species  $i$  at the inner boundary of the column and  $f_i$  is the fraction of the total NOM concentration ( $C$ ), consisting of species  $i$ .

$$\frac{\partial C_i}{\partial x}(L, t) = 0 \quad (11)$$

$$C_{i^*} - \frac{D}{nv} \frac{\partial C_{i^*}}{\partial x} \Big|_{x=0} = f_i C(t) \quad (12)$$

Initially organic matter (0.039%, Dunnivant *et al.*, 1992b) is present in the aquifer material used in both the batch and column experiments. As the nature and composition of the organic matter present is unknown, we assume that the organic matter already present is irreversibly bound and, beside blocking part of the adsorption complex, does not influence the binding of the "new NOM".

*Number of fractions and distribution of mass over fractions*

Dunnivant *et al.* (1992b) and Jardine *et al.* (1992) use both NOM from Hyde County, NC obtained from a stream channel adjacent to a peat deposit. The NOM is filtered through 0.8  $\mu\text{m}$ . Only the distribution of mass over the Hb and Hl fractions are known (69% Hb, 31% Hl). The distribution of mass over different MW fractions, within these "chemical" fractions, has to be considered as well. Therefore, we use this distribution from Van de Weerd *et al.* (1999) and we assume that it is also representative for the NOM used here. So six fractions (two chemical and three MW fractions) are distinguished. To each fraction an average MW is assigned. In the transport experiments we can only use 3 NOM fractions. To obtain 3 fractions, the < 3K fractions of Hl and Hb NOM and the 3-100 K and > 100 K fractions of Hl and Hb NOM respectively are joined together and their properties are averaged. These fractions showed the most similar behavior (results not shown). The 3-100 K and >100 K subcomponents of both the Hl and Hb NOM show similar adsorption and desorption behavior as a function of time and concentration. The <3K subcomponents of both Hl and Hb NOM reach equilibrium quite fast and have similar shapes of curves. In desorption simulations of the mixture, only the < 3K subcomponents desorb significantly.

*Q<sub>max</sub>*

For sorption of polymers, Cohen Stuart *et al.* (1980) have derived an empirical equation relating  $Q_{max}$  to molecular weight. For a good solvent this empirical equation can be simplified to:

$$Q_{max} = p / (1 + (MW/MW_0)^{-2b}) \quad (13)$$

where  $p$  is the maximum value of  $Q_{max}$  to which Equation 13 approaches at high MW and  $MW_0$  is the molecular weight at which the increase of  $Q_{max}$  as a function of molecular weight is maximal. The value of  $MW_0$  is chosen to be 1000 (Van de Weerd *et al.* 1999) and  $b$  is chosen to be 0.6 (a value taken from (Cohen-Stuart *et al.*, 1980)). In the adsorption experiment of Jardine *et al.* (1992) a maximum adsorption of 164 mg C/kg is reached. The isotherm is still increasing and using a Langmuir fit a  $Q_{max}$  of 245 mg C/kg is determined. We use this value as  $p$  for Hb NOM. We use the ratio between  $Q_{max}$  Hb and Hl as was found by Gu *et al.* (1995) (1.42:1) to determine the value for  $p$  for Hl NOM (172.54 mg/kg).

*Adsorption and desorption rate constants,  $k_a$  and  $k_d$*

High molecular weight NOM molecules adsorb preferentially over smaller ones at equilibrium and we assume that the affinity for Hb NOM is a factor 2 higher than the affinity of Hl NOM (see Van de Weerd *et al.*, 1999). To obtain dimensionless coefficients, relationships between MW and the affinity are expressed here in a different way than in earlier work:

$$\begin{aligned} \text{Hl NOM} & : k_{ai}/k_{di} = \kappa \frac{\text{MW}}{\text{MW}_0} K_0 \\ \text{Hb NOM} & : k_{ai}/k_{di} = 2\kappa \frac{\text{MW}}{\text{MW}_0} K_0 \end{aligned} \tag{14}$$

where  $\text{MW}_0$  ( $\text{g}\cdot\text{mol}^{-1}$ ) and  $K_0$  ( $\text{l}\cdot(\text{mg C})^{-1}$ ) are reference values for molecular weight and affinity of NOM respectively and  $\kappa$  (-) is a coefficient relating the affinity for Hl and Hb NOM to MW. For  $\text{MW}_0$  we again take the value of 1000 and the value of  $K_0$  is arbitrarily chosen to be 1. Using the data of Jardine *et al.* (1992)  $\kappa$  is fitted to be  $7.0\cdot 10^{-2}$ . Because both the affinity and the rate of diffusion and reformation affect the values of  $k_{ai}$  and  $k_{di}$ , these rate constants are assumed to be the product of a part determined by the affinity and a part determined by the rate of diffusion and reformation. The rate constant of diffusion and reformation is assumed to be inversely proportional with molecular weight. Furthermore it is also assumed that this rate constant is equal during adsorption and desorption and equal for the Hb and Hl fractions and that it can be given by  $\gamma \frac{\text{MW}_0}{\text{MW}}$  where  $\gamma$  (-) is a coefficient

relating the rate of diffusion and reformation during adsorption and desorption to MW. In contrast with the assumptions in Van de Weerd *et al.* (1999), we assume for the affinity that its effect is expressed evenly in the adsorption and desorption rate constant. The affinity factor is  $\sqrt{\kappa \frac{\text{MW}}{\text{MW}_0}}$  and  $\sqrt{2\kappa \frac{\text{MW}}{\text{MW}_0}}$  for the Hl and Hb fractions respectively. This

leads to the following relationship for  $k_{ai}$  and  $k_{di}$ :

$$\text{Hl NOM} : k_{ai} = \gamma \frac{MW_0}{MW} \sqrt{\kappa \frac{MW}{MW_0}} k_{ai_0} = \gamma k_{ai_0} \sqrt{\frac{\kappa MW_0}{MW}} \quad (15)$$

$$\text{Hb NOM} : k_{ai} = \gamma \frac{MW_0}{MW} \sqrt{2\kappa \frac{MW}{MW_0}} k_{ai_0} = \gamma k_{ai_0} \sqrt{\frac{2\kappa MW_0}{MW}}$$

$$\text{Hl NOM} : k_{di} = \gamma \frac{MW_0}{MW} \frac{1}{\sqrt{\kappa \frac{MW}{MW_0}}} k_{di_0} = \gamma k_{di_0} \sqrt{\frac{MW_0^3}{\kappa MW^3}} \quad (16)$$

$$\text{Hb NOM} : k_{di} = \gamma \frac{MW_0}{MW} \frac{1}{\sqrt{2\kappa \frac{MW}{MW_0}}} k_{di_0} = \gamma k_{di_0} \sqrt{\frac{MW_0^3}{2\kappa MW^3}}$$

in which  $k_{ai_0}$  ( $l \cdot (mg \ C) \cdot s^{-1}$ ) and  $k_{di_0}$  ( $s^{-1}$ ) are reference values for the adsorption and desorption rate constant with both a value of 1. Note that the part of  $k_a$  and  $k_d$  determined by the affinity are respectively divided and multiplied by the affinity factor indicating a higher probability of adsorption and a lower probability of desorption once a molecule is larger. Note that the overall adsorption rate decreases with MW. Using the data of Jardine *et al.* (1992)  $\gamma$  is fitted to have a value of  $1.75 \cdot 10^{-1}$ .

## Simulation results and comparison with experimental data

The NOMADS model describes adsorption/desorption processes of NOM subcomponents. In a previous publication (Van de Weerd *et al.*, 1999) it was shown that NOM adsorption/desorption phenomena observed in batch laboratory experiments with pure iron oxide could be described very well with the model. Because our final goal is to understand the sorption and transport behavior of NOM in natural systems (soils, aquifers), it is interesting to test the reliability of the model by applying it to describe NOM adsorption and transport in natural media in both the lab and in the field.

**Table 1** Properties of the discrete NOM fractions distinguished, and model parameters used for these discrete fractions for modelling the batch experiment<sup>a</sup>

fractions	MW (g·mol <sup>-1</sup> )	<i>f</i> (-)	<i>K</i> (l·mg C <sup>-1</sup> )	<i>k<sub>a</sub></i> (l·mg C <sup>-1</sup> ·h <sup>-1</sup> )	<i>k<sub>d</sub></i> (h <sup>-1</sup> )	<i>Q<sub>max</sub></i> (mg C·kg <sup>-1</sup> )
MW < 3·10 <sup>3</sup>						
HI	1.5·10 <sup>3</sup>	0.19	1.05·10 <sup>-1</sup>	3.78 10-2	3.60·10 <sup>-1</sup>	106.86
Hb		0.30	2.10·10 <sup>-1</sup>	5.35 10-2	2.55·10 <sup>-1</sup>	151.73
3·10 <sup>3</sup> < MW < 10 <sup>5</sup>						
HI	5.0·10 <sup>4</sup>	0.08	3.50·10 <sup>0</sup>	6.55 10-3	1.87·10 <sup>-3</sup>	170.99
Hb		0.36	7.00·10 <sup>0</sup>	9.26 10-3	1.32·10 <sup>-3</sup>	242.78
MW > 10 <sup>5</sup>						
( <i>d</i> < 0.8 μm)	5.0·10 <sup>5</sup>	0.04	3.50·10 <sup>1</sup>	2.07 10-3	5.92·10 <sup>-5</sup>	172.46
Hb		0.03	7.00·10 <sup>1</sup>	2.93 10-3	4.18·10 <sup>-5</sup>	244.86

<sup>a</sup> HI = Hydrophobic, HI = Hydrophilic, MW = molecular weight, *d* = diameter, *f* = weight fraction of total NOM consisting of subfraction.

**Table 2** Properties of the discrete NOM fractions distinguished, and model parameters used for these discrete fractions for modelling the transport experiments<sup>a</sup>

fractions	MW (g·mol <sup>-1</sup> )	<i>f</i> (-)	<i>K</i> (l·mg C <sup>-1</sup> )	<i>k<sub>a</sub></i> (l·mg C <sup>-1</sup> ·h <sup>-1</sup> )	<i>k<sub>d</sub></i> (h <sup>-1</sup> )	<i>Q<sub>max</sub></i> (mg C·kg <sup>-1</sup> )
MW < 3·10 <sup>3</sup>						
HI+Hb	1.50·10 <sup>3</sup>	0.49	1.69·10 <sup>-1</sup>	4.80·10 <sup>-2</sup>	2.84·10 <sup>-1</sup>	134.33
3·10 <sup>3</sup> < MW <i>d</i> < 0.8 μm	2.00·10 <sup>5</sup>	0.12	1.40·10 <sup>1</sup>	3.27·10 <sup>-3</sup>	2.34·10 <sup>-4</sup>	172.26
3·10 <sup>3</sup> < MW <i>d</i> < 0.8 μm	8.46·10 <sup>4</sup>	0.39	1.18·10 <sup>1</sup>	7.12·10 <sup>-3</sup>	6.01·10 <sup>-4</sup>	243.81

<sup>a</sup> HI = Hydrophobic, HI = Hydrophilic, MW = molecular weight, *d* = diameter, *f* = weight fraction of total NOM consisting of subfraction.

In this section simulation results are shown and compared with experimental data. First we discuss sorption and transport of NOM in the laboratory (small scale and often high pore water velocities), then we will focus on field situations and discuss the impact of initial conditions and larger spatial and temporal scales on simulation results. Finally, we simulate a field experiment. Here we have to deal with unknown initial conditions and a 3-D flow pattern of groundwater.

### *Simulation of laboratory experiments*

#### *Calibration of NOMADS to batch adsorption data*

Figure 1a and 1b show adsorption data as a function of NOM concentration and adsorption time measured by Jardine *et al.* (1992) together with the best fit (estimated by eye) simulation results using NOMADS. Adsorption data are obtained by adding known volumes of solution with known pH and ionic strength and different NOM concentration to an amount of aquifer material. After about 48 hours of shaking, the mixtures were centrifuged and filtered. The supernatant was analyzed for DOC. For the time-dependent adsorption of NOM the same experimental methods were used, only now the samples were analyzed at known times during their approach to equilibrium. For all adsorption experiments the solid to volume ratio was 0.129 kg/l, the pH 5.9, Ionic strength 0.025. Figures 1c and 1d show the contribution of the different species to the total organic carbon concentration in the aqueous phase for the experimental data points in Figure 1a and 1b, calculated with NOMADS.

Using the same set of parameters, assuming either 6 or 3 fractions of NOM (model parameters in Table 1 and 2, respectively), NOMADS describes both experimental data sets very well. Calculations using only one fraction with intermediate model parameters (not shown) did not result in a good description of the data. Especially the shape of the adsorption curve as a function of time with initially fast sorption and a slow approach to the adsorption maximum is very typical and could not be described with the one-species langmuir model. The model results using 6 and 3 fractions differ only slightly because the 3 fractions are chosen in such a way that the main difference in adsorption behavior of the subfractions is maintained.

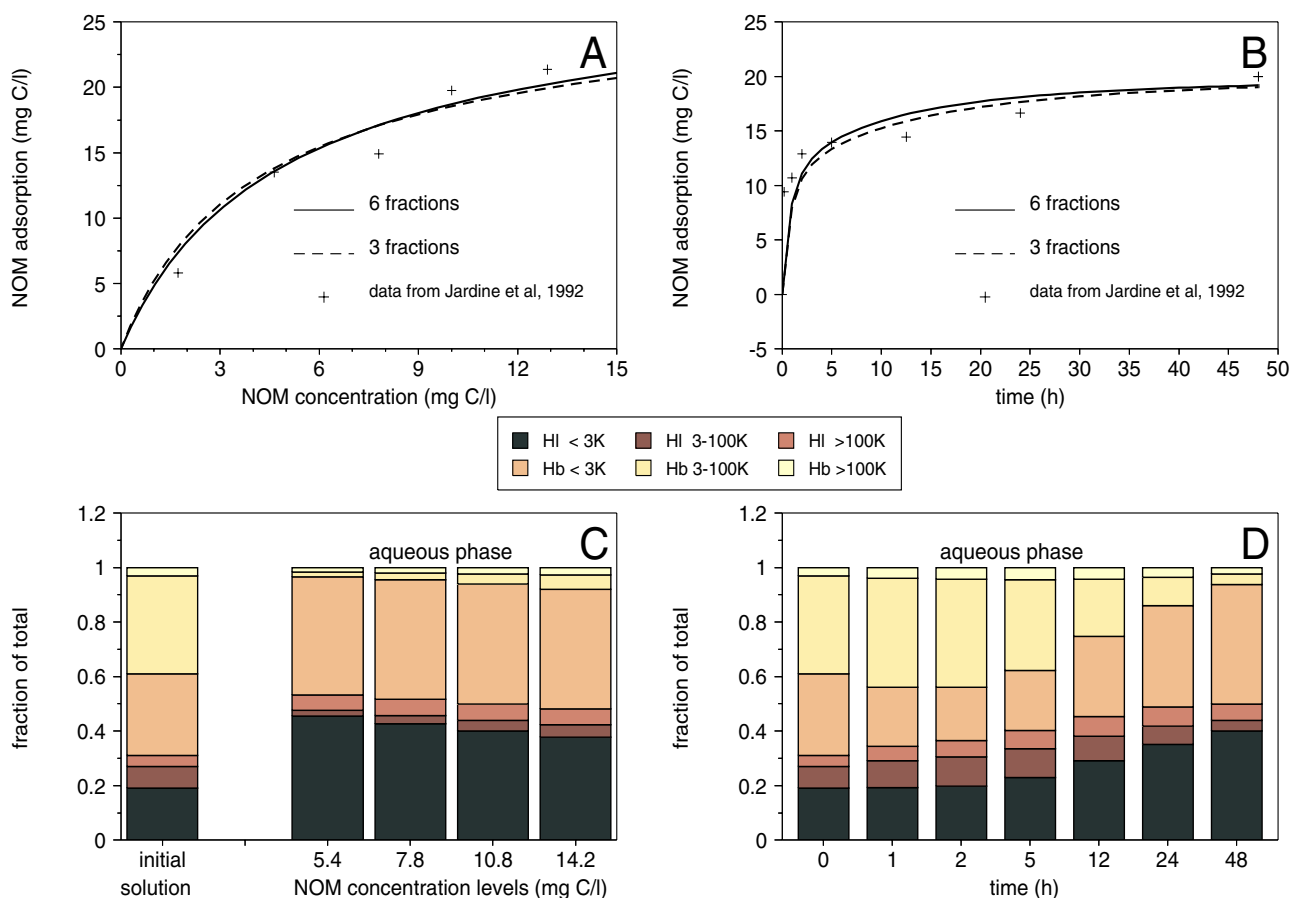


**Figure 1** Simulation and experimental results of adsorption of NOM to aquifer material at pH 5.9. (A) data and model simulations of adsorption as a function of NOM concentration measured after 48 h of equilibration. (B) data and model simulations as a function of equilibration time at a total NOM concentration level of 30 mg C/l. (C) initial fractionation of the NOM solution together with calculated fractionation in the aqueous phase at four NOM concentration levels representing roughly the experimental adsorption data in panel A. (D) Initial fractionation of the NOM solution ( $t = 0$  h) together with calculated fractionation in the aqueous phase after different times of equilibration, representing roughly the experimental adsorption data in panel B. HI = Hydrophilic, Hb = Hydrophobic, K = 1 Kilodalton = 1000 g/mol.

Figure 1c shows that the calculated composition of the NOM in the aqueous phase differs significantly from the initial composition. The low molecular weight (LMW) and Hydrophilic (HI) fractions are overrepresented in solution and the high molecular weight (HMW), intermediate molecular weight (IMW) and hydrophobic (Hb) fractions are underrepresented in solution and overrepresented on the adsorption complex (not shown). Model calculations show that with increasing NOM concentration, the composition of the NOM in solution changes in the direction of the initial composition of NOM. This is due to a decreasing influence of the amount adsorbed on the composition of the aqueous phase. On the sorption complex however (not shown), the overrepresentation of the Hb and the HMW and IMW fractions increases with increasing concentration.

From Figure 1b it is clear that adsorption is time dependent with fast initial adsorption and a slow approach to the adsorption maximum. The calculated composition as a function time in Figure 1d shows that mainly the LMW Hb and HI subfractions are responsible for this initial fast adsorption. Their relative aqueous concentration respectively decreases and stays constant with time in the first 2 hours of the experiment, while others increase. Between 2 and 5 hours of adsorption (the saturation of the sorption complex has reached a value of 0.6 then), their relative concentration starts to increase again, indicating exchange of sorbed LMW NOM with slower sorbing species with higher affinity from solution (mainly IMW NOM). This exchange causes the slow approach to the adsorption maximum.

### *Prediction of column experiments*

Figure 2 shows transport data of NOM measured by Dunnivant *et al.* (1992b) together with simulation results using the NOMADS equation in the COLTRAP model (parameters in Table 3). Column experiments were performed under the same conditions (pH, ionic strength) and with the same aquifer material and NOM as the batch experiments. Only the mass to volume ratio in the column experiments (varying between 3.92 to 4.12 kg/l) is about a factor 30 times the mass to volume ratio in the batch experiments (0.129 kg/l).

The sorption parameters obtained from the batch experiment (Table 2) are now used to predict the NOM transport data. Figure 2a shows that the very fast initial rise of the effluent concentration, followed by a much slower increase, which lasts several hundred pore volumes, is a general feature which is well described by the model. The quantitative agreement between data and prediction varies from very good to satisfactory. After 500 pore volumes of elution, the input to each column was changed to zero NOM concentration

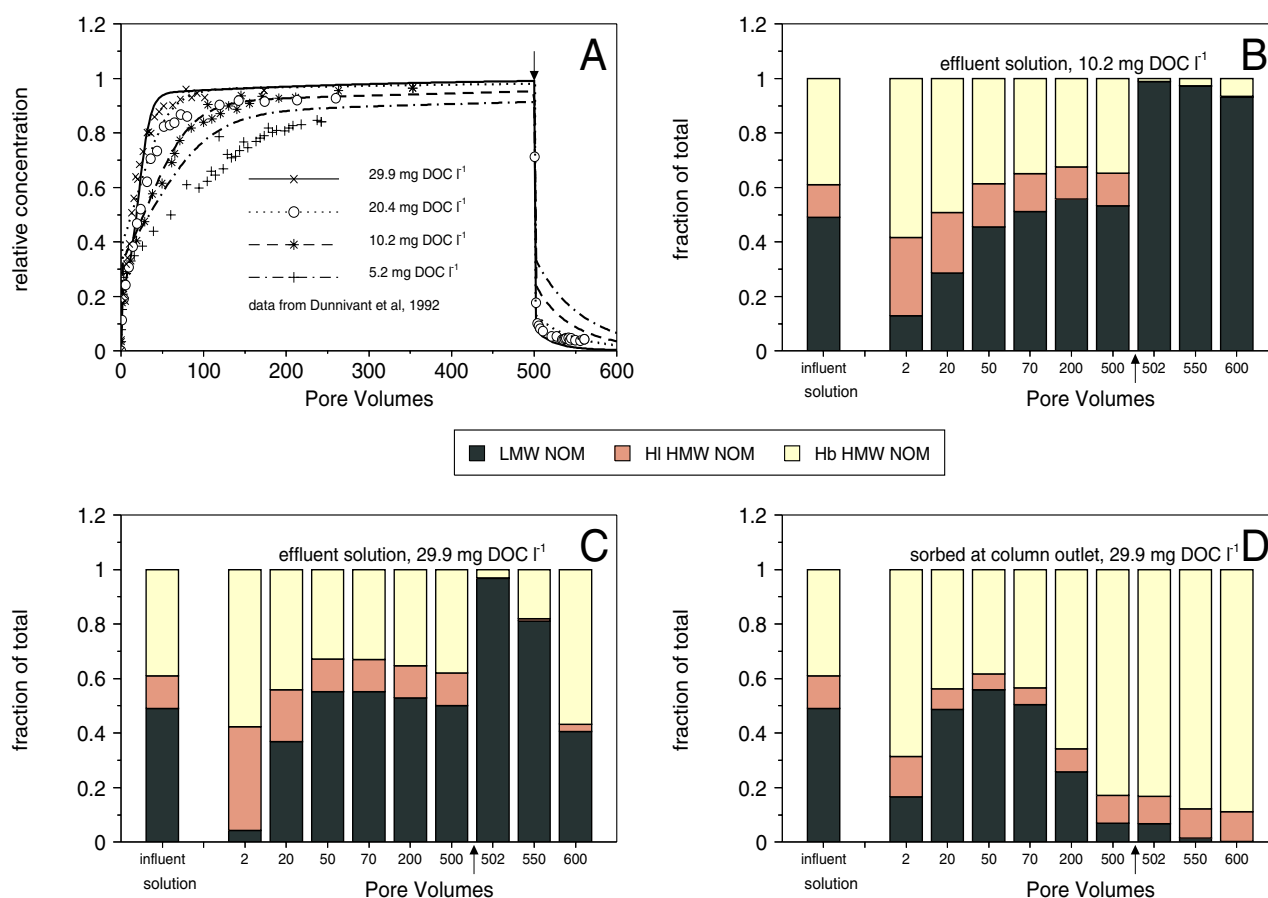
**Table 3** Properties of the simulated column experiments of Dunnivant *et al.*, (1992)<sup>a</sup> used for model calculations.

Simulation no.	$C$ (mg C·l <sup>-1</sup> )	$L$ (cm)	$\rho$ (g·cm <sup>-3</sup> )	$n$ (-)	$v$ (cm·h <sup>-1</sup> )	$D$ (cm <sup>2</sup> ·h <sup>-1</sup> )	$t_{pulse}$ (h)
1	5.15	7.95	1.66	0.423	79.5	10.52	50.00
2	10.19	7.95	1.64	0.400	79.6	11.70	49.94
3	20.40	8.00	1.61	0.409	98.7	12.88	40.53
4	29.9	14.5	1.59	0.386	87.7	6.9	82.67

<sup>a</sup>  $C$  = influent NOM concentration,  $L$  = column length,  $\rho$  = bulk density,  $n$  = (water filled) porosity,  $v$  = pore velocity,  $D$  = dispersivity ( $vL/P$ ),  $P$  = Peclet number,  $t_{pulse}$  = duration of the NOM injection

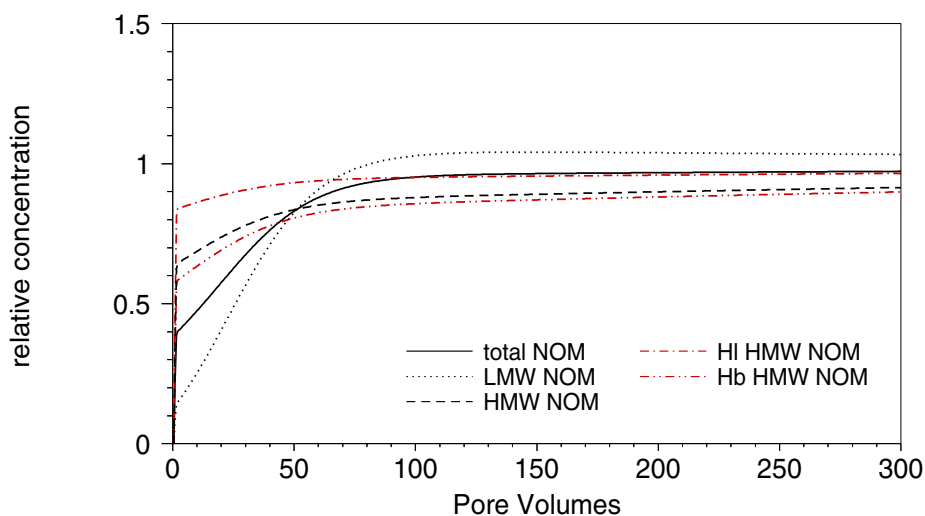
(indicated by the arrow). The desorption of NOM was followed in only one of the experiments. However, we predicted the desorption behavior of NOM for all experiments. In the desorption phase, the agreement between data and prediction is good. This suggests that the adsorption/desorption behavior of NOM in batch experiments (with varying adsorption time and concentration) as well as in column experiments, can be described with the same model, NOMADS, using the same set of parameters. This suggests that the description of the processes incorporated in NOMADS are valid over a large range of mass to volume ratios. Using one fraction of NOM with intermediate model parameters (not shown) does not lead to a reasonable prediction of the curves, not even if parameters are adapted. Using only one fraction, the slope of the simulated breakthrough curve changes gradually from steep to slowly approaching the maximum value. However, especially at high influent concentration, the data in Figure 2a show a large change in the slope of the breakthrough curves during only a few pore volumes.

Figure 2b to 2d show the simulated changes in the composition of the NOM adsorbed at the column outlet and in the effluent solution. As explained before, we use 3 fractions for simulation of NOM transport. We have only one LMW fraction and the IMW and HMW fraction together are the HMW fraction now. Note that the arrow indicates the beginning of the desorption phase. We first focus on the adsorption phase of the simulations. By following the relative amount of LMW NOM in the effluent solution as a function of pore volumes we see that it initially is lower than in the influent solution. There after it reaches a maximum value above the value in the influent solution (due to desorption) and decreases again in the direction of its value in the influent solution. This indicates that initially the adsorption of LMW NOM prevails. There after exchange of LMW with HMW NOM occurs. At an influent concentration of 29.9 mg DOC/l the maximum relative amount of LMW NOM is reached after elution of fewer pore volumes (70 PV) than at 10.2 mg DOC/l (200 PV). This difference is due to the higher dimensionless adsorption rates (constant 9c) at higher concentrations, which lead to a faster approach of equilibrium. After 500 PV of elution at all influent concentrations redistribution of NOM still occurs and equilibrium is not yet reached. In Figure 2d we see that initially, the relative amount of LMW NOM adsorbed at the column outlet, is lower than in the influent solution. This is due to the fact that the LMW NOM fraction at the column outlet is depleted due to sorption earlier in the column. However, comparison of the composition of the sorption complex and the effluent solution (Figure 2c) at the column



**Figure 2** Experimental results and model predictions of NOM adsorption/desorption and transport in laboratory columns with aquifer material at pH 5.9. (A) observed and predicted breakthrough curves for various influent NOM concentrations. The arrow indicates the change to zero NOM influent concentration after elution of 500 pore volumes. (B, C, D) Fractionation of NOM in the influent solution together with the calculated fractionation in the effluent solution (B, C) and sorbed at the column outlet (D) after different elution volumes at two influent NOM concentration levels. The course of the overall NOM concentration as a function of eluted volume is given by respectively the dashed (B) and solid line (C, D) in panel A. HI = Hydrophilic, Hb = Hydrophobic, LMW = low molecular weight, HMW = high molecular weight.

outlet after 2 pore volumes shows that the LMW NOM is overrepresented on the sorption complex. The amount of LMW NOM increases both in absolute value (not shown) and in relative value until a maximum is reached after 50 PV, after which the adsorbed LMW NOM decreases due to exchange with the HMW fractions. From the desorption phase of Figure 2b-c we can conclude that the LMW fraction is removed selectively from the sorption complex during desorption.



**Figure 3** Simulated breakthrough curves of different (combinations of) subcomponents at an influent concentration of 20.4 mg C/l. Each (combination of) subcomponent(s) is scaled with respect to its own influent concentration.

#### *Comparison of the behavior of individual subcomponents*

Figure 1 and 2 showed the contribution of the different subcomponents to the total mass of NOM. In this way we could see if any subcomponent dominated the behavior of the NOM mixture. In order to compare the transport behavior of the different subcomponents, the breakthrough curves for different (combinations of) subcomponents are given in Figure 3, for an influent concentration of 20.4 mg DOC/l. Note that each subcomponent is scaled with its own influent concentration.

Figure 3 shows that the main difference in behavior (different shape of curves) is between LMW and HMW NOM. The Hb and HI HMW fraction show similar behavior, with the HI HMW fraction being more mobile than the Hb HMW fraction due to its lower  $k_a$  value. The orders of magnitude of model parameters for these HMW fractions are comparable. The total HMW curve is only slightly higher than the Hb HMW curve because the HI HMW fraction represents only a small fraction of total HMW. Adsorption rates of the LMW NOM are roughly a factor 10 higher resulting in higher initial adsorption and a lower initial effluent concentration. The increase in effluent concentrations of all NOM subcomponents indicates that their adsorption along the column decreases. This is due to the increasing saturation of the adsorption complex. The BTC for LMW NOM even increases to a relative concentration above 1, which indicates that the effluent concentration exceeds the influent concentration. Due to its lower affinity for the aquifer material LMW NOM desorbs and exchanges with HMW NOM. This exchange between LMW and HMW NOM starts after 58 PV at the column entrance and after 98 PV at the column outlet in this

**Table 4** Properties of model calculations with simulation no 3 as a basis<sup>a</sup>.

Simulation no.	$Q_i(x, t=0)_{0 \leq x \leq L}$ (mg C · kg <sup>-1</sup> )			$\nu$ (cm·h <sup>-1</sup> )	$D$ (cm <sup>2</sup> ·h <sup>-1</sup> )	$t_{pulse}$ (h)
	LMW	HMW HI	HMW Hb			
3	0.	0.	0.	$9.87 \cdot 10^1$	$12.9 \cdot 10^1$	$4.05 \cdot 10^1$
5	0.	0.	0.	$9.87 \cdot 10^0$	$1.29 \cdot 10^0$	$4.05 \cdot 10^2$
6	63.5	0.	0.	$9.87 \cdot 10^0$	$1.29 \cdot 10^0$	$4.05 \cdot 10^2$
7	0.	24.6	80.3	$9.87 \cdot 10^0$	$1.29 \cdot 10^0$	$4.05 \cdot 10^2$
8	0.	0.	0.	$9.87 \cdot 10^{-2}$	$1.29 \cdot 10^{-2}$	$4.05 \cdot 10^4$
9	63.5	0.	0.	$9.87 \cdot 10^{-2}$	$1.29 \cdot 10^{-2}$	$4.05 \cdot 10^4$
10	0.	24.6	80.3	$9.87 \cdot 10^{-2}$	$1.29 \cdot 10^{-2}$	$4.05 \cdot 10^4$

<sup>a</sup>  $Q_i$  = amount sorbed of species  $i$ ,  $L$  = column length,  $\nu$  = pore velocity,  $D$  = dispersivity ( $\nu L/P$ ),  $P$  = Peclet number,  $t_{pulse}$  = duration of the NOM injection.

experiment (NOM concentration 20.4 mg/l). Figure 3 shows that between 58 and 98 PV the relative concentration in the effluent starts to exceed the value of 1.

Because of the similar behavior of Hb and HI HMW NOM, from now on, only total HMW and LMW NOM are represented and discussed. Further, all following simulations have simulation 3 as a basis. Only parameters differing from parameters of simulation 3 are given in Table 4.

### *Extrapolation of adsorption and transport behavior to field situations*

The final goal of our model development is to predict transport of NOM under field conditions. In aquifer systems the pore water velocity varies roughly between 0.1 cm/h and 10 cm/h. These are typical values for pore water velocities measured in shallow aquifers under natural conditions and near (about 10 m from) withdrawal wells. These pore water velocities are much smaller than the pore water velocities used in the column experiments of Dunnivant *et al.* (1992b). Also the distance over which one will predict the transport of NOM in the field will be larger, in the order of meters or tens of meters rather than centimeters. Moreover, the binding sites on the mineral surfaces in the field situation will be partly occupied by NOM derived from groundwater. Introduction of novel NOM with a

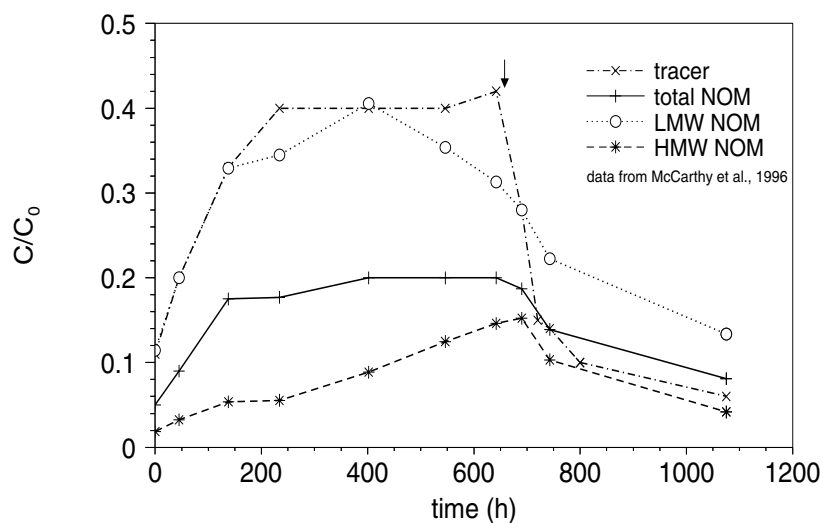


**Figure 4** Observed breakthrough curves of a tracer, total NOM and NOM subfractions at the withdrawal well of a field experiment. The withdrawal well is located 5 m from the infiltration well, pH ~ 8 and the average pore water velocity is 10 cm/h. Each subcomponent is scaled with respect to its own influent concentration.

different composition will result in competition between NOM subcomponents at the sorption complex and in solution.

McCarthy *et al.* (1996) performed a field experiment in which novel NOM was injected during 660 hours in an aquifer system. The injected NOM was monitored and withdrawn at a well at 5m distance. The average pore water velocity was about 10 cm/h. Results (presented in Figure 4) show that the breakthrough curves for the LMW and HMW subfractions deviate largely from each other and from the overall curve. The relative concentration of LMW NOM in the effluent reaches a maximum value and decreases again before percolation of NOM was stopped (indicated by the arrow). The curve of the HMW NOM however, slowly increases during the whole period of percolation. Using our calibrated model we will show some model calculations (see Table 4) with pore water velocities representative for field situations with and without sorption sites already occupied by NOM. In this way we will show the effect of dynamic adsorption/desorption of NOM subcomponents under aquifer conditions. Finally we will try to simulate, understand and explain the results found by McCarthy *et al.* (1996).

#### *Effect of pore water velocity*

Figure 5 shows the simulated effect of the pore water velocity on the breakthrough curves of NOM (subfractions) on the column scale (8 cm). The pore water velocity determines the residence time in the column and thus the reaction time of NOM with the solid matrix (see

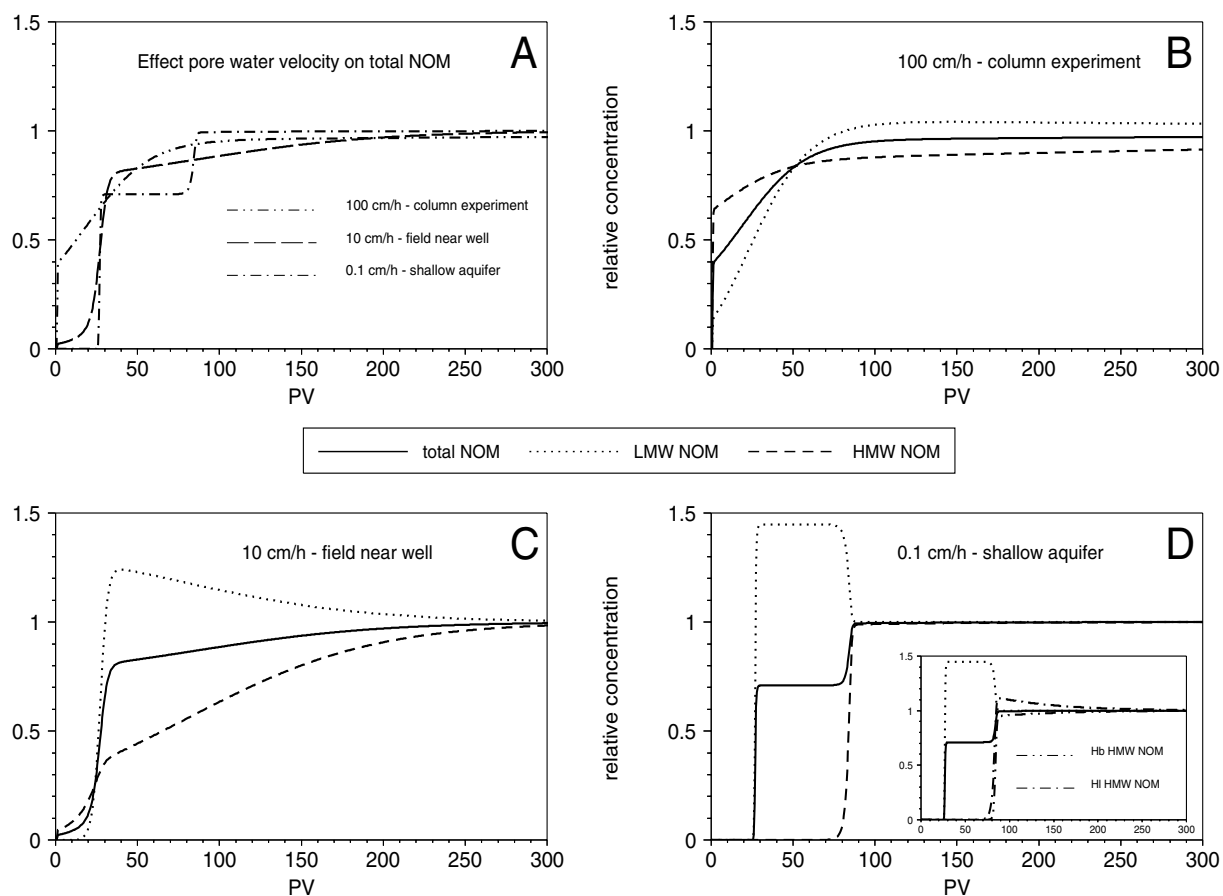


**Figure 5** Simulations showing the effect of the pore water velocity on the breakthrough curves of NOM (subfractions). (A) Breakthrough curves of total NOM at varying pore water velocities. (B-D) Breakthrough curves of NOM subfractions together with the curve of total NOM at the different pore water velocities from panel A. The total NOM breakthrough curve in each panel corresponds with one of the curves in panel A.

the dimensionless constants in section 2.1). Figure 5a shows simulations of the transport behavior of a NOM mixture with varying pore water velocities. The breakthrough curves change from a curve with an initial fast breakthrough slowly approaching the influent concentration at high pore water velocity, to a breakthrough curve with retarded breakthrough and two distinct fronts at the lowest pore water velocity. Figure 5b-d show the normalized breakthrough curves for the HMW and LMW subfractions together with the curve for the NOM mixture at the different pore water velocities. At pore water velocities corresponding to the column experiment (fig 5b = fig 3), none of the subfractions are in equilibrium and we see inert breakthrough of part of each subfraction. Adsorption of LMW NOM is fast due to its high  $k_a$  value. After a certain period of percolation (98 PV) exchange with the HMW NOM, which have a higher affinity for the surface, occurs along the whole column. The distance between the LMW and HMW NOM curves and the total NOM curve

indicates that we have significant exchange during percolation of several hundreds of pore volumes. At a pore water velocity corresponding with velocities in the field near withdrawal wells (fig 5c) we see a retarded breakthrough of the LMW fraction. Transport of a small part of the HMW fraction still is inert. Due to the higher residence time of the infiltrated water, the saturation of the sorption complex occurs after percolation of fewer pore volumes. Figure 5c shows a sharp increase of the effluent concentration in terms of pore volumes. Already after 36 PV exchange of LMW and HMW NOM occurs along the whole column. The amount of LMW exchanged in terms of pore volumes is large, resulting in LMW concentration up to 1.2 times the influent concentration and after already 300 PV equilibrium is approached. At pore water velocities typical for shallow aquifers, the breakthrough of both the LMW and HMW fractions is retarded. In Figure 5d we see two distinct fronts. The breakthrough of the LMW front occurs after about 27 PV of percolation and after 84 PV of percolation the breakthrough of the HMW fraction occurs. The results suggest that at this pore water velocity the adsorption of both LMW and HMW NOM is in equilibrium. However, the inset in Figure 5d, in which the breakthrough curves of the individual HMW fractions are shown, shows that the composition of the sorption complex and the effluent solution still change due to exchange between the Hl and Hb HMW subfractions.

The retardation of the fronts observed in Figure 5d, for the LMW and HMW subfractions are in agreement with retardation factors calculated for the equilibrium situation using parameters from Table 2 (calculations not shown). At equilibrium the breakthrough of the Hl and Hb HMW fraction occurs simultaneously. In situations where Hb HMW and Hl HMW travel independent from each other, the Hb HMW fraction is retarded less than the Hl HMW fraction. However, the coupled behavior of the HMW subcomponents in this system results in one front for HMW NOM with an average retardation factor.

From Figure 5 we can conclude that the pore water velocity has a large impact on the breakthrough of the NOM mixture and NOM subfractions as well as on the fractionation of NOM. With decreasing pore water velocity, both the sorption of HMW and LMW NOM approach more and more equilibrium and the multi-component features of the transport process become more apparent. The result is a shift in the breakthrough curves to lower concentrations and later times. Note that the calculated distinct fronts in Figure 5d are most likely not found in reality because, instead of describing NOM as a heterogeneous mixture

of molecules varying in MW and chemical composition, our model distinguishes only 3 NOM fractions.

#### *Effect of transport distance*

Figure 5 showed the simulated effect of the pore water velocity on the breakthrough curves of NOM (subfractions) at the column scale (8 cm). From the dimensionless constants in section 2.1 we can conclude that increasing the transport distance has the same effect on scaled breakthrough curves as decreasing the pore water velocity (if we assume that the dispersivity increases proportionally with transport distance). Therefore the results in Figure 5 with lower pore water velocity can also be interpreted as results with the same pore water velocity (100 cm/h) but with transport distances of 80 cm (5c) and 80 m(5d). The transport distance determines the duration of transport of a volume of water through a certain medium. The transport distance therefore determines the number of reaction opportunities of NOM with the solid matrix in the medium and thus the rate of adsorption in terms of pore volumes. Like the pore water velocity, also the transport distance has a large impact on the breakthrough of the NOM mixture and NOM subfractions as well as on the fractionation of NOM. With increasing transport distance, both the sorption of HMW and LMW NOM approach more and more equilibrium and the multi-component features of the transport process become more apparent.

#### *Effect of NOM on the sorption complex*

The presence and composition of NOM on the sorption complex will affect transport behavior of NOM subcomponents. Due to the dynamic competitive adsorption/desorption of subcomponents, the composition of the sorbed NOM will affect the transport behavior of the NOM mixture. To show these effects on NOM transport behavior, we performed model simulations with part of the sorption complex occupied with LMW and HMW, respectively. The initial conditions for these simulations are chosen in such a way that the initial saturation of the sorption complex ( $\Theta$ ) is equal and about 0.5 (see Table 4). Figure 6 and 7 show the simulation results at two pore water velocities typical for field situations. Note that they also represent simulation results with transport distances of 80 cm and 80 m respectively at a pore water velocity of 100 cm/h. Figure 6a and 7a show the effect of the presence of NOM at the sorption complex on the transport of the NOM mixture. Figure 6b-c and 7b-c show the breakthrough curves of the LMW and HMW subfractions together

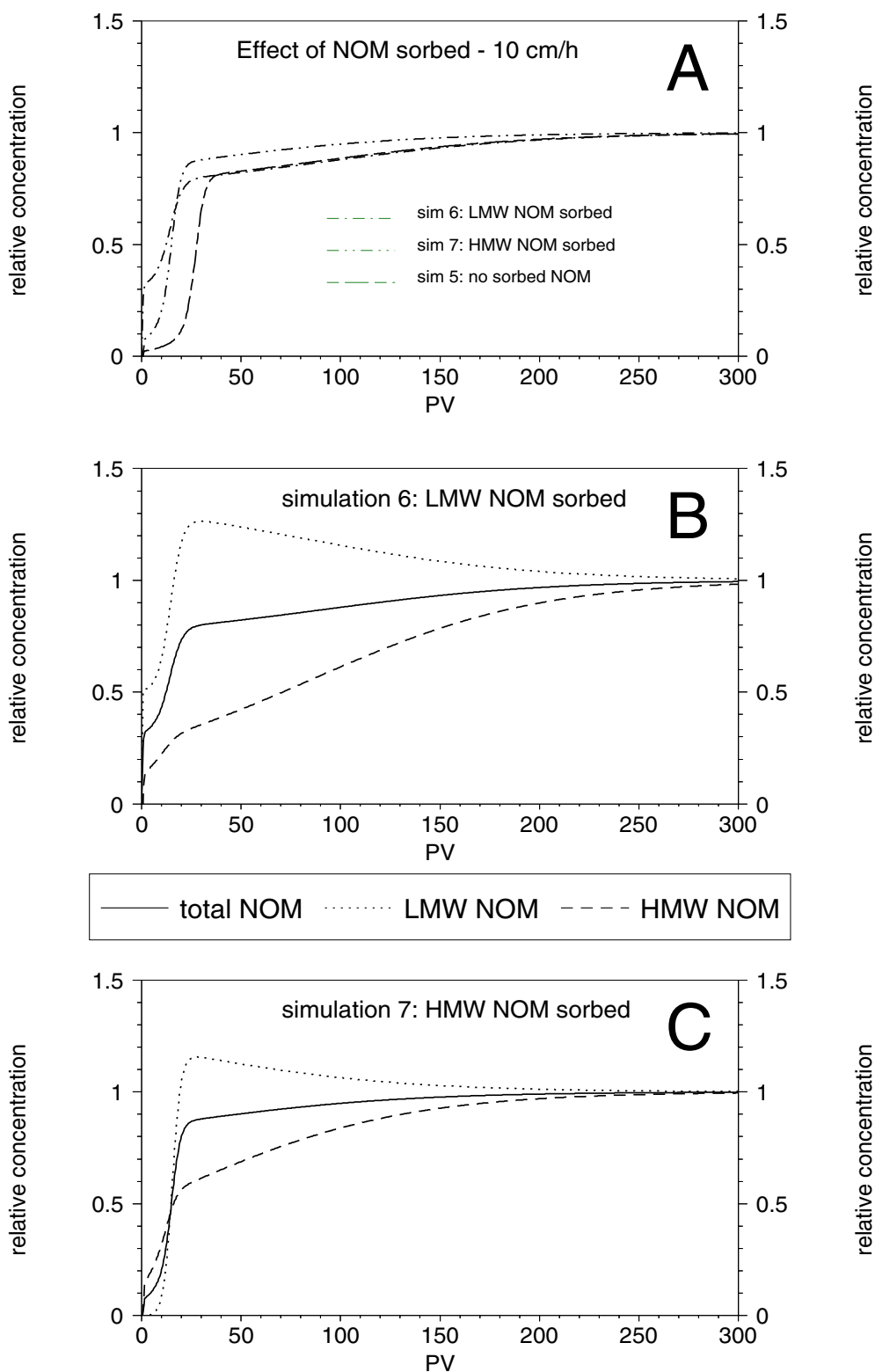


**Figure 6** Simulations showing the effect of the presence of NOM on the sorption complex on the breakthrough curves of NOM (subfractions) at a pore water velocity of 10 cm/h. (A) Breakthrough curves of total NOM while the sorption complex is empty and while part (about 50%) of the sorption complex is occupied with either LMW or HMW NOM. (B, C) Breakthrough curves of NOM subfractions together with the curve of total NOM while part of the sorption complex is occupied with LMW (B) or HMW (C) NOM

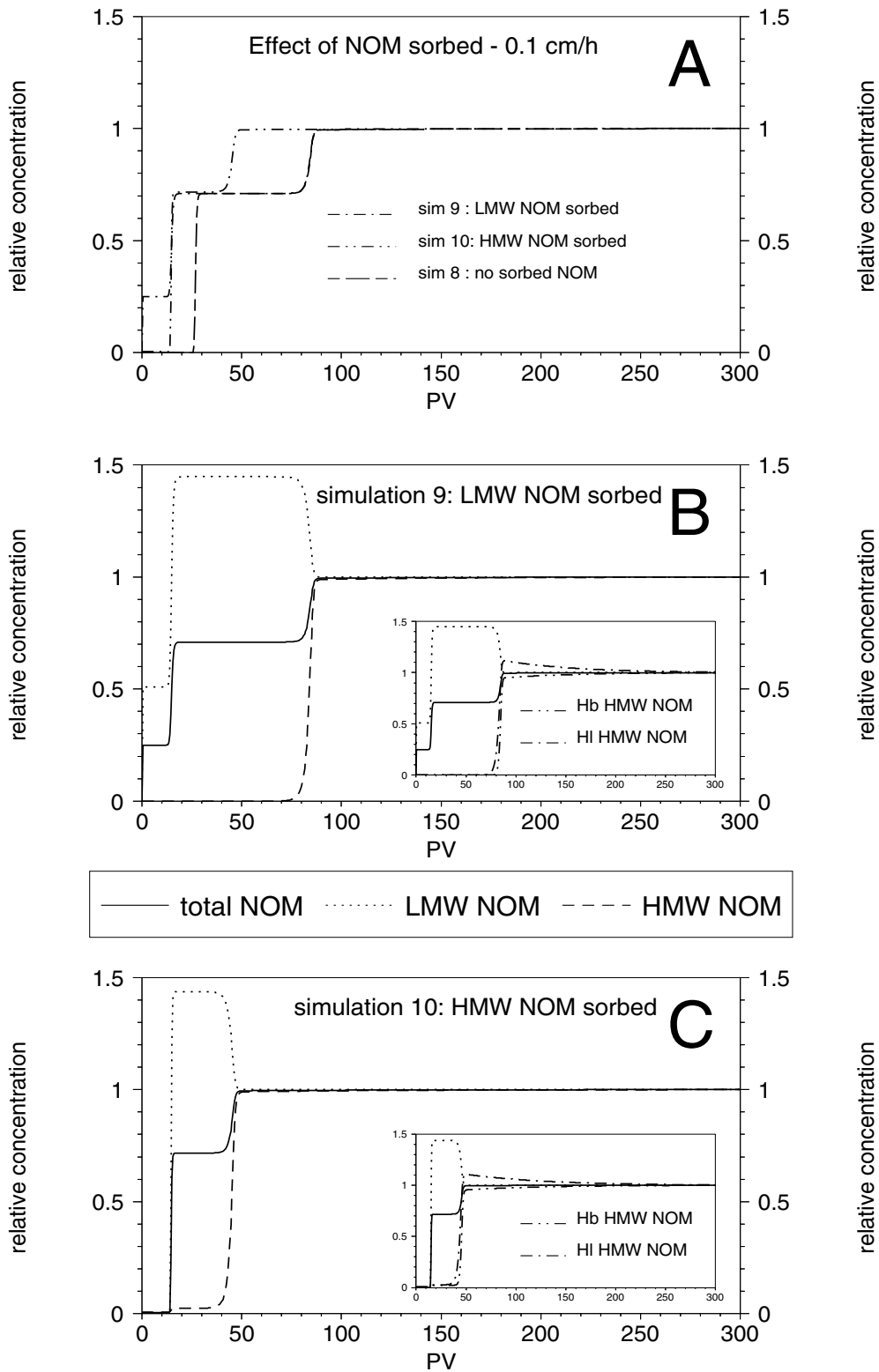
with the breakthrough curve of the NOM mixture for the simulations with part of the sorption complex occupied with NOM.

Figure 6a and 7a show that, due to the presence of NOM on the sorption complex, breakthrough of NOM occurs after fewer pore volumes. In these figures, the area above the breakthrough curves, bounded by a relative concentration of 1, is a measure for the amount of NOM, given in mg C/l, retained by the column. We see that the amount retained decreases in case part of the sorption complex is occupied. Note that there is a difference in the amount of NOM retained between the simulation with sorbed LMW and HMW NOM on the sorption complex. This difference is due to the different amount of NOM in terms of mg C/kg at equal saturation of the sorption complex (see Table 4).

The initial presence of LMW NOM has the largest impact on the shape of the breakthrough curve of the NOM mixture (see fig 6a,7a). By comparing Figure 6b with 5c and 7b with 5d we see that this is mainly due to the larger concentration of LMW NOM in the first pore volumes. From Equation 2 we can infer that this is due to the desorption of the LMW from the sorption complex and due to a decrease of the net adsorption due to the occupation of sorption sites. We further see a larger deviation of the curves of the individual subcomponents from the mixture curve. This indicates that in case of LMW NOM present on the sorption complex, more exchange will occur before equilibrium is reached.

The initial presence of HMW NOM does not influence the shape of the breakthrough curve of the NOM mixture dramatically (see fig 6a,7a). By comparing Figure 6c with 5c and 7c with 5d the main features drawing attention are the breakthrough after less pore volumes and the decrease in exchange before equilibrium is reached. Equation 2 and model simulations (not shown) indicate that due to its low desorption rates, the presence of HMW NOM on the sorption complex almost has the same effect as decreasing the adsorption capacity of the sorption complex. The main difference is that due to slow desorption of HMW NOM, the concentration of HMW NOM in the first pore volumes is somewhat higher. Figure 7c shows that the HMW NOM concentration between 0 and 15 PV is negligible and between 15 and 40 PV is almost negligible.

From Figure 6 and 7 we can conclude that the presence and the composition of NOM on the sorption complex affects the breakthrough of NOM. It results in an earlier breakthrough and less NOM retained by the column. If a mixture of NOM is infiltrated, the presence of LMW on the sorption complex results in an increase in exchange before



**Figure 7** Simulations showing the effect of the presence of NOM on the sorption complex on the breakthrough curves of NOM (subfractions) at a pore water velocity of 0.1 cm/h. (A) Breakthrough curves of total NOM while the sorption complex is empty and while part (about 50%) of the sorption complex is occupied with either LMW or HMW NOM. (B, C) Breakthrough curves of NOM subfractions together with the curve of total NOM while part of the sorption complex is occupied with LMW (B) or HMW (C) NOM.

equilibrium is reached. An important conclusion in understanding transport and fate of NOM is that the presence of HMW on the sorption complex almost has the same effect as decreasing the sorption capacity for all subcomponents. This implies that sorption sites occupied with HMW NOM can be considered as blocked.

### *Simulation of a field experiment*

McCarthy *et al.* (1996) performed a field experiment in which novel NOM was injected in an aquifer system with mainly LMW NOM in the aqueous phase. In the experiment, water is infiltrated and withdrawn with wells and the flow pattern is not 1-D. Experimental conditions are different from conditions in the simulated laboratory experiments (pH 8.0, Ionic strength 0.003 M). The composition of background NOM and the injected NOM in the field experiment differ, and is also different from the NOM used in the laboratory experiments. Further the initial composition of the sorption complex is unknown. The only information we have is that Langmuir  $Q_{max}$  parameters, estimated using laboratory batch experiments (pH 5.6 and an Ionic strength 0.001 M) with aquifer material from the major flow zone, are 131 and 231 mg C/kg (McCarthy *et al.*, 1993). These values represent the remaining (not the total) adsorption capacity at pH 5.6. What part of the sorption complex is already occupied and with what MW fraction is unknown. To simulate the field experiment we need to do some simplifying assumptions.

- We assume that the flow field is approximated by a previously determined set of travel paths (Table 5, see section 2.2). NOM transport is simulated along these travel paths.

**Table 5** Properties of travel paths obtained by analysis of the tracer curve<sup>a</sup>.

travel path no.	$v$ (m·h <sup>-1</sup> )	$D^b$ (m <sup>2</sup> ·h <sup>-1</sup> )	$L$ (m)	$L/v$ (h)	frequency (%)
1	1.00	$5.00 \cdot 10^{-2}$	5.00	5	10.5
2	$2.82 \cdot 10^{-1}$	$1.41 \cdot 10^{-2}$	5.30	19	6.3
3	$1.42 \cdot 10^{-1}$	$7.10 \cdot 10^{-3}$	5.62	40	6.3
4	$9.25 \cdot 10^{-2}$	$4.63 \cdot 10^{-3}$	5.93	64	6.7
5	$6.20 \cdot 10^{-2}$	$3.10 \cdot 10^{-3}$	6.42	104	11.1
6	$4.08 \cdot 10^{-2}$	$2.04 \cdot 10^{-3}$	7.14	175	14.0
7	$1.31 \cdot 10^{-2}$	$6.55 \cdot 10^{-4}$	7.82	597	2.9

<sup>a</sup>  $v$  = pore water velocity,  $D$  = dispersivity,  $L$  = length of the travel path,  $L/v$  = factor representing the duration of percolation of one pore volume. <sup>b</sup> assuming constant local dispersivity of 0.05 m (Yeh *et al.*, 1995).

- Despite the difference in the composition of background and injected NOM and the NOM in the laboratory experiments, we assume that the adsorption/desorption and transport behavior of NOM can be described using the same 3 subfractions as used for simulating the column experiment. We further assume the same mass distribution of Hl and Hb NOM within the HMW fraction.
- We assume that, except for the sorption capacity, the parameters for NOM adsorption/desorption used in the batch experiment, can be used for the field experiment. For  $Q_{max}$  we only adapt the absolute values, the ratio's between the  $Q_{max}$  values for the different fractions are kept constant.
- We assume that the aquifer material is in equilibrium with the background NOM. By using the background concentration of the individual fractions and the equilibrium constant ( $K$ ) for the individual fractions in the competitive Langmuir equation (Van de Weerd *et al.*, 1999), the composition of the sorption complex is calculated (8% LMW, 42% Hb HMW, 21% Hl HMW and 29% empty sites).
- We use the assumption of neglecting the sites occupied with HMW NOM (63% of the sites are considered to be blocked). In the simulations, we consider the non-blocked sites from which 22% is occupied with LMW NOM. As a first estimate for the  $Q_{max}$  of Hb HMW NOM, we use the lower value of the  $Q_{max}$ , estimated for the aquifer material of the field experiment at pH 5.6. Sorption studies of NOM to iron oxides (Filius *et al.*, 2000, Gu *et al.*, 1994, Tipping, 1981) show that ionic strength is not a major factor, however pH is an important factor controlling NOM adsorption. These studies show that the main effect of increasing pH (starting at about pH 4) is a decrease in the sorption capacity. Therefore, we

**Table 6** Model parameters and conditions for simulation of the field experiment<sup>a</sup>.

$t_{pulse}$	659	h		LMW	HMW Hl	HMW Hb	
$C_b$	1.8	mg C·l <sup>-1</sup>	$f_b$ <sup>b</sup>	0.90	0.03	0.07	-
$C$	33	mg C·l <sup>-1</sup>	$f$ <sup>b</sup>	0.35	0.15	0.50	-
$n$	0.3	-	$Q_{max}$ <sup>c</sup>	74.6 (27.6)	95.4 (35.3)	135.1 (50.0)	mg C·kg <sup>-1</sup>
$\rho$	1.86	kg·l <sup>-1</sup>	$Q_{ii}$ <sup>c</sup>	6.1	20.0 (0.0)	56.7 (0.0)	mg C·kg <sup>-1</sup>

<sup>a</sup>  $t_{pulse}$  = duration of the NOM injection,  $C_b$  = background NOM concentration before and after the NOM injection (659 h),  $C$  = concentration during the NOM injection,  $n$  = (water filled) porosity,  $\rho$  = bulk density,  $f_b$  = weight fraction of groundwater NOM (background concentration) consisting of subfraction,  $f$  = weight fraction of injected NOM consisting of subfraction,  $Q_{max}$  = model parameter,  $Q_{ii} = Q_i(x, t=0) 0 \leq x \leq L$  = initial amount sorbed of species  $i$ .  
<sup>b</sup> based on distribution given in McCarthy *et al.* (1996). <sup>c</sup> in parenthesis the value assuming the sites occupied with HMW NOM as blocked.

expect the initial estimate of  $Q_{max}$  for the aquifer material to be too high and we adapt it until we have a good fit of the data.

Figure 8 shows experimental data, together with the calculated breakthrough curves for the NOM mixture, the LMW and HMW NOM, constructed using Equation 9. Simulation results show a stepwise increase of the concentration of mainly the LMW NOM and the NOM mixture. After 659 h of percolation the NOM concentration in the injection solution is changed to background level and the concentrations of all subcomponents decrease. Simulation results describe the general pattern of the measured breakthrough of the NOM mixture and NOM subcomponents very well. The simulated curves show the deviation of the LMW and HMW NOM curves from the overall curves, the decrease in LMW NOM concentration before percolation was stopped (at the "plateaus"), and also the increase of HMW NOM during the whole period of percolation. Note that modeling results are adapted to the experimental data using only the absolute value of  $Q_{max}$ . All other modeling parameters are derived either from the batch experiment (Table 2), or from analysis of the tracer curve (Table 5) or from description of the field site (Table 6).

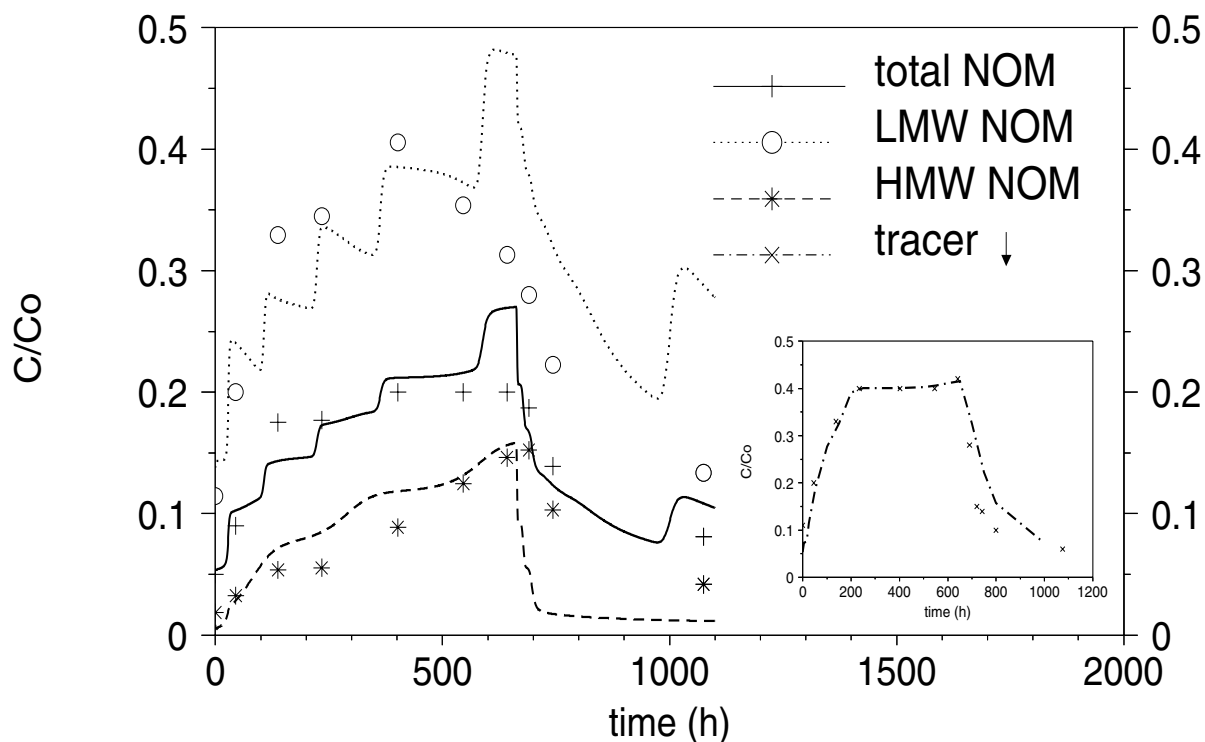


**Figure 8** Simulated and observed breakthrough curves of a tracer, total NOM and NOM subfractions at the withdrawal well of a field experiment. The withdrawal well is located 5 m from the infiltration well, pH  $\sim$  8 and the average pore water velocity is 10 cm/h. Each subcomponent is scaled with respect to its own influent concentration.

The best fit value for the adsorption capacity of the “non-blocked” sites for Hb HMW NOM ( $Q_{max}$  used in the simulation) was 50 mg C/kg. As expected, this value is significantly lower than the value determined at pH 5.6. The total adsorption capacity for the NOM subfractions is calculated as well (see Table 6). Using these values, simulation results (not shown) do not change significantly.

Simulation results in Figure 6b and 7b give an impression of the shape of the NOM breakthrough curves of the individual travel paths. The shape of the simulation results of the individual travel paths is mainly dependent on the ratio between  $L$  and  $v$  (the duration of the percolation of one pore volume). This ratio varies between 5 and 600 h (Table 5).  $L/v$  ratio's in Figure 6b and 7b are about 0.8 and 80 h respectively. In travel path 1 to 3 a distinct front of LMW NOM develops followed by a simultaneous gradual increase of HMW NOM and decrease of LMW NOM (not shown). In travel path 4 to 7, simulation results resemble results of Figure 7b, distinct fronts of both LMW and HMW NOM develop. The stepwise increase, shown in Figure 8, originates from the breakthrough of distinct fronts within the individual travel paths. The fact that this stepwise increase is not found in the experimental data may be due to the following reasons. 1) We consider only 3 fractions of NOM, instead of a heterogeneous mixture of NOM. 2) We consider transport of NOM along 7 travel paths without lateral interaction. In fact the flow field consists of a continuous distribution of flow paths with differences in length and flow velocity. Lateral interaction between these flow paths will result in smoothing of concentration differences.

## Discussion and Conclusions

In this paper, the dynamic adsorption/desorption behavior of NOM in batch and column experiments with aquifer material, and in a field experiment in a sandy aquifer, is described and explained with the model, NOMADS. This model has been used previously to describe the adsorption/desorption of NOM to iron oxides (Van de Weerd *et al.*, 1999). In this model NOM is described as a mixture of subcomponents that vary in their adsorption/desorption behavior while competing for the same sites. To reduce the number of adjustable parameters, we use simple relationships between molecular weight and model parameters (an affinity, adsorption rate constant and desorption rate constant). The relationships used

here are slightly different from the relationships used in an earlier paper (Van de Weerd *et al.*, 1999). The refinement in the relationships was necessary to describe adsorption data both as a function of time and concentration (Figure 1). Using the refined relationships, the adsorption/desorption data (Gu *et al.*, 1994) used in the earlier paper, could be adequately described as well.

Only the values of  $\gamma$  and  $\kappa$ , which are coefficients that relate respectively the affinity and the rate of diffusion and reformation to the molecular weight, are fitted using adsorption data of Jardine *et al.* (1992). The model NOMADS has been incorporated in a transport code. Using the set of parameters for NOM adsorption, derived from the batch data, it is possible to predict NOM transport in a set of column experiments, performed with the same aquifer material and under the same conditions as in the batch experiment. Moreover, transport of a different NOM mixture in a field experiment, with environmental conditions and aquifer material different from the batch experiment, can also be described well after adapting the value of  $Q_{max}$  only. Although only 3 NOM subcomponents are used, experimental results at different time and length scales and different mass to volume ratio's can be described well with NOMADS. This gives confidence that the model concepts and ideas incorporated in NOMADS include the main features that determine NOM adsorption/desorption behavior over a large range of mass to volume ratio's and over a large range of adsorption times (or pore water velocities) and transport distances, at least under aquifer conditions with relatively low concentrations of NOM, relatively constant environmental conditions and fully water saturated pores.

The factors controlling the behavior of NOM in NOMADS are nonlinear and time-dependent competitive adsorption/desorption, and the heterogeneity of the NOM mixture. Because adsorption parameters of subcomponents differ, sorption and transport of a NOM mixture is characterized by a complicated process of time dependent adsorption/desorption and redistribution between the subcomponents. Simulation results show how experimental conditions like pore water velocity, transport distance and the presence and composition of sorbed NOM on the sorption complex influence the behavior and interaction of the subcomponents and also the shape of the breakthrough curves for the different subcomponents.

Using our approach, in which NOM is described as a mixture of subcomponents, it is possible to simulate and explain experimental features like apparent hysteresis (Van de Weerd *et al.*, 1999), extended tailing, apparent irreversible sorption and concentration

dependency of scaled breakthrough curves. Attempts to describe the transport behavior of NOM assuming different types of sorption sites were not that successful (e.g. Jardine *et al.*, 1992).

Jardine *et al.* (1992) attributed the extended tailing of breakthrough curves for NOM to slow, time-dependent adsorption. We showed that additionally, this extended tailing is the result of slow redistribution of the subcomponents due to their different sorption behavior.

Calculations show that Hl NOM is more mobile than Hb NOM as has been observed also experimentally (Dunnivant *et al.*, 1992b, McCarthy *et al.*, 1996). Furthermore the mobility of LMW is found to be higher than that of HMW NOM. However, because time-dependent sorption is important at small temporal and spatial scales, inert transport of part of the NOM may occur resulting in higher relative concentrations of HMW NOM in the effluent solution.

Determination of the implications of the presence of NOM on contaminant transport is not straightforward. This work shows that some of the important factors determining the implications of NOM on contaminant transport can be, the mobility of the NOM fraction to which contaminants preferentially bind, the time and length scale over which transport occurs and the initial composition of the sorption complex.

In experiments with natural material, part of the sorption complex will be already occupied with NOM. However, in general it is unknown what the initial occupation of the sorption complex is. Indeed, Jardine *et al.* (1989a) show that the sorption capacity for NOM increases after removal of indigenous organic matter from soil. Our work shows that the adsorption/desorption of the HMW NOM is very slow compared to adsorption/desorption of LMW NOM. Model simulations show that under certain conditions it is a good assumption to neglect the desorption of HMW NOM and consider the adsorption sites occupied with HMW NOM to be blocked. This implies that in experiments with natural material, where the initial occupation of the sorption complex is unknown, the measured sorption capacity may represent a residual adsorption capacity of sites that are not blocked with HMW NOM, provided that the LMW molecules initially present have been removed by extensive washing. In these experiments it is often a reasonable assumption to consider the measured sorption capacity to be the total sorption capacity. This justifies the assumption we made (neglecting indigenous organic matter) in the simulation of the batch and column experiments. In field experiments the residual sorption capacity can be

determined in samples of the aquifer material. However, in the initial situation in the field also LMW NOM will be present on the sorption complex. We successfully applied an approach to estimate the occupation of the sorption complex with LMW NOM, by using the calculated occupation of the aquifer material in case of equilibrium with the background concentration of NOM. If an adsorption/desorption model with realistic adsorption/desorption rate constants is used, it is often a good assumption to consider the measured sorption capacity as the total sorption capacity.

Environmental conditions like pH and ionic strength will affect model parameters. In this paper we focused on situations with constant environmental conditions. Sorption studies of NOM to iron oxides (Filius *et al.*, 2000, Gu *et al.*, 1994, Tipping, 1981) show that ionic strength is not of major importance. However, these studies show that pH is an important factor controlling NOM adsorption. The main effect of increasing pH (starting at about pH 4) is a decrease in the sorption capacity.

In situations with high concentrations of NOM and/or high microbial activity, formation/degradation reactions and also flocculation reactions could be important. Under unsaturated conditions, sorption to the gas-water interface may play a role as an additional adsorption mechanism. This may explain the discrepancy between observations from unsaturated and saturated NOM transport experiments

In this paper we have shown that NOM transport must be understood in terms of the chemical heterogeneity of NOM. We have shown that sorption and transport of NOM can be described well with a relatively simple model integrating knowledge from polymer chemistry, environmental chemistry and hydrology. It allows illustrating and quantifying important features of sorption and transport of a mixture of NOM molecules. Experimental results at different time and length scales and mass to volume ratio's can be successfully described using the same set of model parameters. To simulate the field experiment, we had to deal with unknown initial conditions and a 3-D flow pattern of groundwater. Therefore it was necessary to do some initial assumption, and to fit one of the model parameters. Although the approach is rather crude and limited, using only 3 subcomponents and 7 travel paths, it shows clearly how information obtained at the particle scale (batch experiment) can be used in the field.

## Acknowledgment

Without the availability of extensive experimental data sets at different scales, it would have been impossible to develop this model. Mr. P. Jardine and Mr. J. F. McCarthy are greatly acknowledged for providing the NOM adsorption and transport data.

## References

- Abdul A.S., Gobson T.L. and Rai D.N. 1990. Use of humic acid solution to remove organic contaminants from hydrogeologic systems. *Environ. Sci. Technol.* 24, 328-333.
- Champ D.R., Young J.L., Robertson D.E. and Abel K.H. 1984. Chemical speciation of long-lived radionuclides in a shallow groundwater flow system. *Water Pollut. Res. J. Can.* 19, 35-54.
- Cohen Stuart M.A., Scheutjens M.M.H.M. and Fleer G.J. 1980. Polydispersity Effects and the Interpretation of Polymer Adsorption Isotherms. *J. Polym. Sci.* 18, 559-573.
- Dunnivant F.M., Jardine P.M., Taylor D.L. and McCarthy J.F. 1992a. Cotransport of Cadmium and Hexachlorobiphenyl by Dissolved Organic Carbon through Columns Containing Aquifer Material. *Environ. Sci. Technol.* 26(2), 360-368.
- Dunnivant F.M., Jardine P.M., Taylor D.L. and McCarthy J.F. 1992b. Transport of naturally occurring dissolved organic carbon in laboratory columns containing aquifer material. *Soil Sci Soc. Am. J.* 56(2) 437-444.
- Filius J.D., Lumsdon D.G., Meeussen J.C.L., Hiemstra T. and van Riemsdijk W.H. 2000. Adsorption of fulvic acid on goethite. *Geochim. Cosmochim. Acta* 64(1) 51-60.
- Gu B., Schmitt J., Chen Z., Liang L. and McCarthy J.F. 1994. Adsorption and Desorption of Natural Organic Matter on Iron Oxide: Mechanisms and Models. *Environ. Sci. Technol.* 28(1), 38-46.
- Gu B., Schmitt J., Chen Z., Liang L. and McCarthy J.F. 1995. Adsorption and desorption of different organic matter fractions on iron oxide. *Geochim. Cosmochim. Acta* 59(2), 219.
- Gu B., Mehlhorn T.L., Liang L. and McCarthy J.F. 1996. Competitive adsorption, displacement, and transport of organic matter on iron oxide: I. Competitive adsorption. *Geochim. Cosmochim. Acta* 60(11), 1943-1950.
- Jardine P.M., Weber N.L. and McCarthy J.F. 1989a. Mechanisms of dissolved organic carbon adsorption on soil. *Soil Sci. Soc. Am. J.* 53, 1378-1385.
- Jardine P.M., Wilson G.V., Luxmoore R.J. and McCarthy J.F. 1989b. Transport of inorganic and natural organic tracers through an isolated pedon in a forest watershed. *Soil Sci. Soc. Am. J.* 53, 317-323.
- Jardine P.M., Dunnivant F.M., Selim H.M. and McCarthy J.F. 1992. Comparison of models for describing the transport of dissolved organic carbon in aquifer columns. *Soil Sci Soc. Am. J.* 56(2) 393-401.
- Knabner P., Totsche K.U. and Kögel-Knabner I. 1996. The modeling of reactive solute transport with sorption to mobile and immobile sorbents. 1. Experimental evidence and model development. *Water Resour. Res.* 32(6) 1611-1622.
- Kukkonen J., McCarthy J.F. and Oikari A. 1990. Effects of XAD-8 fractions of dissolved organic carbon on the sorption and bioavailability of organic micropollutants. *Arch. Environ. Contam. Toxicol.* 19, 551-557.

- Magee B., Lion L.W. and Lemley A.T. 1991. Transport of dissolved organic macromolecules and their effect on the transport of phenanthrene in porous media. *Environ. Sci. Technol.* 25, 323-331.
- McCarthy J.F., Williams T.M., Liang L., Jardine P.M., Jolley L.W., Taylor D.L., Palumbo A.V. and Cooper L.W. 1993. Mobility of natural organic matter in a sandy aquifer. *Environ. Sci. Technol.* 27(4), 667-676.
- McCarthy J.F., Gu B., Liang L., Mas-Pla J., Williams T.M. and Yeh T.-C.J. 1996. Field tracer tests on the mobility of natural organic matter in a sandy aquifer. *Water Resour. Res.* 32(5), 1223-1238.
- Ochs M., Čosović B., Stumm W. 1994. Coordinative and hydrophobic interaction of humic substances with hydrophilic  $Al_2O_3$  and hydrophobic mercury surfaces. *Geochim. Cosmochim. Acta* 58(2), 639-650.
- Römkens P.F.A.M. and Dolfing J. 1998. Effect of Ca on the solubility and molecular size distribution of DOC and Cu binding in soil solution samples. *Environ. Sci. Technol.* 32, 363-369.
- Sposito G. 1984. *The Surface Chemistry of Soils*. Oxford Univ. Press.
- Stevenson F.J. 1982. *Humus Chemistry. Genesis, Composition, Reactions*. Wiley Interscience, New York.
- Temminghoff E.J.M., Van der Zee S.E.A.T.M. and De Haan F.A.M., 1997. Copper Mobility in a copper contaminated sandy soil as affected by pH, solid and dissolved organic matter. *Environ. Sci. Technol.* 31, 1109-1115.
- Temminghoff E.J.M., Van der Zee S.E.A.T.M. and De Haan F.A.M. 1998. Effects of dissolved organic matter on the mobility of copper in a contaminated sandy soil. *European. J. Soil. Sci.* 49, 617-628.
- Tipping E., 1981. The adsorption of aquatic humic substances by iron oxides. *Geochim. Cosmoch. Acta* 45(2) 191-199.
- Totsche K.U., Knabner P. and Kögel-Knabner I. 1996. The modeling of reactive solute transport with sorption to mobile and immobile sorbents. 2. Model discussion and numerical simulation. *Water Resour. Res.* 32(6), 1623-1634.
- Totsche K.U., Danzer J., and Kögel-Knabner I. 1997. Dissolved organic matter-enhanced retention of polycyclic aromatic hydrocarbons in soil miscible displacement experiments. *J. Environ. Qual.* 26, 1090-1100.
- Van de Weerd H. and Van der Linden A.M.A. 1991. Behaviour of pesticides in aquifer materials: Interpretation of an *in situ* experiment: Bilthoven RIVM report nr. 725502004.
- Van de Weerd H. and Leijnse A. 1997. Assessment of the effect of kinetics on colloid facilitated radionuclide transport in porous media. *J. Contam. Hydrol.*, 26, 245-256.
- Van de Weerd H., Leijnse A., and Van Riemsdijk W.H. 1998. Transport of reactive colloids and contaminants in groundwater: effect of nonlinear kinetic interactions. *J. Contam. Hydrol.*, 32, 313-331.
- Van de Weerd H., Van Riemsdijk W.H. and Leijnse A. 1999. Modelling the dynamic adsorption/desorption of a NOM mixture: Effects of physical and chemical heterogeneity. *Environ. Sci. Technol.* 33(10) 1675-1681.
- Van Riemsdijk W.H., Bolt G.H., Koopal L.K. and Blaakmeer J. 1986. Electrolyte adsorption on heterogeneous surfaces: adsorption models. *J. Colloid interface Sci.* 109 219-228.
- Wan J. and Wilson J.L. 1994. Colloid Transport in unsaturated porous media. *Water. Resour. Res.* 30(4), 857-864.
- Wang L., Chin Y.-P. and Traina S.J. 1997. Adsorption of (poly)maleic acid and an aquatic fulvic acid by goethite. *Geochim. Cosmochim. Acta* 61(24) 5513-5324.
- Yeh, T.-C.J., Mas-Pla J., Williams T.M. and McCarthy J.F. 1995. Observation and three-dimensional simulation of chloride plumes in a sandy aquifer under forced-gradient conditions. *Water Resour. Res.* 31(9), 2141-2157.

# Chapter 6

## Summary and conclusions

Transport of contaminants constitutes a potential threat for public health and ecosystems. One of the potential pathways for contaminant transport is transport with carriers. To assess the potential role of reactive carriers on contaminant transport in groundwater systems, we need to find the relevant mechanisms determining the transport of such carriers and contaminants in this system. The central aim of this study was to find and describe these relevant mechanisms by a process of model development, model application and model evaluation. Emphasis was put on the behavior of natural organic matter as a carrier for contaminants. In Chapter 2 to 5, the main part of this study is described in separate articles. In this chapter, the results of the individual articles are summarized, integrated and are presented together with their implications. This chapter is divided in a short summary and concluding paragraphs on the relevant mechanisms found, the modeling approach used and the implications of results for transport of reactive carriers and contaminants, and for risk assessment.

### Summary

#### *Behavior of contaminants in a system with carriers*

The first part of this thesis considers the behavior of contaminants in a system with a constant concentration of carriers (steady state). Equilibrium has been reached between the solid matrix and “one carrier”. Using a model for coupled carrier and contaminants transport (COLTRAP) the effect of reaction rates and non-linearity on contaminant transport is studied. Varying the reaction rates of carrier-solid matrix and contaminant-carrier reactions, it is shown that a range of reaction times exists in which time dependent reactions determine the transport of contaminants. Transport processes within this range can only be described and understood using models considering dynamic sorption, like

COLTRAP. Transport at and beyond the limits of this range can be calculated with equilibrium models. Simulation of a column experiment under natural conditions shows that time dependent contaminant-carrier and carrier-solid matrix interactions are important under these conditions. In this experiment, transport of a radioactive contaminant (americium) is dramatically increased due to the presence of mobile NOM. Both desorption of Am from NOM and interaction between mobile and immobile NOM are found to be time dependent (slow).

### *Behavior of carriers*

The second part of this thesis considers the behavior of NOM in more detail. As mobile NOM is a mixture of molecules varying from simple small molecules like citric acid to complicated large molecules like humic acid, its adsorption behavior cannot be fully understood from mono-component adsorption models. The NOMADS model (NOM adsorption) is developed in order to describe the dynamic competitive adsorption/desorption of NOM subcomponents on a homogeneous surface. Furthermore, a method to minimize the number of adaptable parameters is developed. The model allows illustrating and quantifying important features of sorption and transport of a mixture of NOM molecules, like apparent adsorption/desorption hysteresis, slow increasing sorption maxima and large tailing of NOM breakthrough curves. It is shown that experimental results over a large range of temporal and spatial scales and surface to volume ratio's can be successfully described using the same set of model parameters. The behavior of NOM is described in laboratory batch experiments with a few grams of soil and some tens of milliliters of water and also in a field experiment with large travel times, distances of some meters and large volumes of soil.

## **Relevant mechanisms**

### *Time dependent sorption reactions*

For contaminants that are present in relatively low concentrations, it is generally accepted that adsorption is the concentration regulating process in subsurface environments. In Chapter 3, 4 and 5 it is shown that the behavior of NOM under constant aquifer conditions

can be described also with adsorption equations, indicating that under these conditions adsorption is the concentration regulating process for NOM as well.

If the duration of an experiment is longer than reaction times in the system, all reactions in the system will be in equilibrium. In case of transport, non-equilibrium effects of adsorption can be ignored in systems where reaction times are significantly smaller than solute travel times. Solute travel times depend on flow velocity and on the distance over which transport is studied. It is often assumed that in groundwater systems with small water velocities non-equilibrium effects can be ignored. However, some evidence exists that contaminant-carrier and carrier-solid matrix interactions are slow relative to other interactions in natural systems. To study the relevance of time dependent sorption reactions it is interesting to relate the degree of equilibrium observed with solute travel times in the systems studied. Typical solute travel times over a distance of 1 meter in natural aquifer systems vary between 10 h and 1000 h (more than one month).

In Chapter 3 it is shown that, in an experiment under aquifer conditions with a solute travel time of 10h, time dependent sorption is important for both contaminant-carrier and carrier-solid matrix reactions. This implies that under aquifer conditions time dependent sorption may play a role.

In Chapter 5 it is shown that beyond solute travel times of 80 h total equilibrium between a NOM mixture and aquifer material has still not been reached. Due to their difference in reaction time, different subcomponents reach equilibrium at different travel times. Figure 5 of this chapter shows that at a solute travel time around 1 h, equilibrium between the relatively fast reacting low molecular weight NOM and aquifer material is almost reached. At a solute travel time of 80 h all NOM subcomponents seem to be in equilibrium. However, this is not really the case because still very slow redistribution of subcomponents occurs. Total equilibrium or a steady state situation, is only reached after the slowest subcomponent has reached equilibrium. In Figure 4 of Chapter 4, the same phenomena are described in a batch experiment.

Figure 4 of Chapter 4 also reveals that due to competition total equilibrium is reached much slower than expected on the basis of the reaction rate constants of the slowest subcomponent. In case of more competition (at higher concentration), the reaction rates of the slowest subcomponents decrease considerably. From Equation 2 in Chapter 5 we can conclude that according to the model, the adsorption rate of a subcomponent among others is determined by the fraction of sorption sites occupied. In case of multi-component

sorption, the presence of competing subcomponents will therefore decrease adsorption rates. This effect will be more pronounced for slow subcomponents, because all other subcomponents will occupy sorption sites faster.

In Chapter 5 it is shown that in some situations sorption of NOM can be considered to be irreversible. It is shown that at solute travel times of 80 h, desorption of the relatively slow reacting high molecular weight (HMW) NOM that is initially present at aquifer surfaces can be neglected. Sorption sites already occupied with HMW NOM can be considered as blocked sites.

This study showed that time dependent adsorption reactions of both reactive carriers and contaminants are relevant, even under aquifer conditions. However, knowledge of adsorption and desorption rates, and the factors determining these rates are limited. Time dependent sorption of contaminants by reactive colloids may change their mobility dramatically. Therefore, to assess risks better, we need more information on the time dependent sorption of contaminants by reactive colloids.

### *Competitive sorption of a heterogeneous carrier mixture*

In Chapter 4 and 5 we showed that the behavior of a NOM mixture can only be understood if its heterogeneous nature is taken into account. The behavior of NOM subcomponents is described using a dynamic competitive adsorption/desorption model. The different subcomponents considered, vary in their affinity, their reaction rate constants and their adsorption maximum. Therefore, sorption and transport of a NOM mixture is characterized by a complicated process of time dependent adsorption/desorption and redistribution between the subcomponents. Because time dependent sorption and heterogeneity cannot be considered separately, part of the observed features are described already together with time dependent sorption.

In Chapter 4 it was shown that in a multicomponent system at equilibrium, the distribution of NOM subcomponents between the sorption complex and the aqueous phase depends on the total sorption capacity, the S/V ratio, and the total amount of NOM added to a system.

In Chapter 5, it is shown that with increasing solute travel time, non-equilibrium effects disappear more and more and the multi-component transport features of the NOM mixture become more apparent. Simulated breakthrough curves of subcomponents, after introduction of a NOM mixture, show that every time a new subcomponent breaks through,

the equilibrium composition of the effluent changes.

This study showed that the heterogeneity of a NOM mixture is an important property determining its adsorption behavior. As a result of this, heterogeneity will also affect the mobility of contaminants and NOM in groundwater systems. Other types of carriers most likely are heterogeneous mixtures as well. Therefore, the phenomena observed here may be (partly) applicable for carriers in general, provided that adsorption is the concentration regulating process.

## **Modeling approach**

The modeling approach applied in this study revealed two main relevant features: time dependent reactions and the heterogeneity of carriers resulting in competitive sorption behavior. The understanding of both contaminant and carrier transport behavior in the laboratory and the field is significantly increased.

Using this modeling approach it was possible to go from the particle scale (in laboratory batch experiments) to the field. Ideally, one wants to understand, describe and predict the behavior of contaminants and carriers in the field with phenomena observed in laboratory experiment. Laboratory experiments are rather fast and easy in comparison with field experiments. In these experiments it is relatively easy to control certain conditions. However the time and length scale and sometimes also the surface to volume ratio in laboratory experiments differs from field conditions. Therefore, the observed processes should be described in such a way that it is possible to get a correct description for situations that vary widely in temporal and spatial scale. In Chapter 4 and 5 a model is developed for dynamic competitive adsorption and transport behavior of a NOM mixture. In the laboratory it was shown that the model was appropriate at different time and length scales and at different solid to volume ratios'. This gives confidence that the underlying processes occur in reality and are relevant over a range of scales. Finally, using the model, phenomena observed in a field experiment could be described well. Apparently the process descriptions and assumptions made are also valid in the field and are not overruled by other processes. However, to describe the behavior in the field experiment, extra complicating factors did arise. It was necessary to deal with the mixture of water that has traveled over

varying distances and with varying velocities. This was taken into account by assuming a number of flow paths. Further, the initial occupation of the sorption complex was unknown. This was taken into account by assuming equilibrium with the background NOM present.

In Chapter 4 and 5 NOM is described as a mixture of discrete subcomponents. Due to this discrete approach, the number of unknown parameters is large. Therefore, a method was developed to reduce the number of adaptable parameters. This was done by defining relationships between the discrete entities (subcomponents) and parameters that influence modeling results. These relationships were based on observations and trends observed in literature. This approach proved to be successful. Relations were defined between on one hand the sorption maximum, the affinity and the reaction rate constants and on the other hand MW. Between the affinity for hydrophobic and hydrophobic NOM a constant ratio was assumed. The empirical relations between the properties of NOM subfractions and model parameters are interesting starting points for further research. One of the relations was already refined because a new experiment revealed more information about the occurring processes.

### **Implications for transport of reactive carries and contaminants in groundwater systems**

With respect to the transport of NOM two situations can be distinguished. In “Steady state” situations, total equilibrium has been reached between the NOM mixture and the aquifer system. In transient state situations, the composition or concentration of NOM varies.

#### *Steady state*

This type of situation is studied in Chapters 2 and 3. In this situation the transport of all NOM subcomponents is apparently inert. The term apparently is used because redistribution still occurs but in terms of the concentrations of NOM subcomponents there is no effect. However, in Chapter 3 we saw that when NOM "spiked" with a contaminant enters the system this redistribution has an effect in terms of the concentration of the contaminant. The contaminant may be immobilized due to this redistribution. Depending on the subcomponents to which the contaminant precedently binds, and the occupation of the

sorption complex (see above), the rate of this redistribution may vary. In Chapter 3 the observed rates are very slow. After the pulse of americium has passed, redistribution of mobile and immobile NOM results in a supply of a very low concentration of americium during a long period.

In the model applied in Chapter 3, NOM is considered as "one species". The adsorption and transport behavior could be simulated quite well. This might indicate that in case total equilibrium exists between NOM and aquifer material, the multi-component features of NOM adsorption can be neglected.

#### *Transient state*

In this situation disequilibrium exists between the NOM mixture and aquifer system, due to introduction of a NOM mixture with a different composition or concentration. In this situation the composition of the mixture may change during transport, due to the differences in transport behavior of the subcomponents. This also means that the properties for contaminant transport of the NOM mixture will change.

In Chapter 5, the breakthrough of a NOM mixture was studied in a system with initially no, or only a little NOM present. It is shown that HMW NOM is sorbed strongly while LMW NOM is more mobile. It was shown that interpreting the behavior of a NOM mixture as "one species" with average properties will lead to incorrect results. The behavior of the mixture is characterized by small retardation but large loss of mass. The large loss of mass is determined by the sorption of HMW NOM. The small retardation however, is determined by the LMW NOM.

Because the transport behavior of NOM subcomponents differ, the transport behavior of contaminants will be determined by their distribution over the different NOM fractions. This is an interesting subject for more research. Further the multicomponent adsorption processes observed for NOM may also be significant for contaminated sites, like waste disposal sites. Here, transport of mixtures of different kinds of more or less toxic (organic) molecules occur together with transport of NOM. In these situations, possibly (a part of) the organic molecules may behave like NOM. They may compete for the same aquifer sites and also may act as carriers for contaminants.

## **Implications for risk assessment**

The two main relevant mechanisms found in this research are time dependent sorption reactions (sorption dynamics) and the dynamic competitive sorption of a heterogeneous carrier mixture. These mechanisms determine main features of contaminant and carrier transport in groundwater systems and therefore also determine potential risks for public health and ecosystems

The main conclusion from this study is that due to the mechanisms found in this research, the transport of contaminants and therefore the risks for public health and ecosystems, in specific situations are much larger than expected if these mechanisms are neglected. For example, the radionuclide americium, which is strongly sorbed to NOM and desorbs only slowly, will move unretarded through the subsoil in natural situations with relatively high flow velocities and relatively much competition with other (natural) organic molecules. Therefore, in this situation, the risk that this highly toxic contaminant reaches a certain place is very large due to the mechanisms described in this thesis.

## SUMMARY AND CONCLUSIONS

# Samenvatting

## Achtergrond en doel

Een van de door menselijke activiteit ontstane problemen is de aanwezigheid en het brengen van verontreinigingen in de bodem en ondergrond. Als gevolg hiervan kan er transport van verontreinigingen optreden naar plekken waar hun aanwezigheid risico met zich meebrengt. Om de volksgezondheid en ecosystemen te beschermen is het van belang om de mobiliteit van verontreinigingen te voorspellen. Pogingen om de mobiliteit van verontreinigingen te beschrijven en voorspellen kunnen alleen slagen wanneer er rekening gehouden wordt met de belangrijkste manieren van transport en met de mechanismen die hierbij van belang zijn. Een van de mogelijke manieren van transport, waar tot op heden weinig rekening mee gehouden wordt, is het “meeliften” van verontreinigingen met zogenaamde dragers die aanwezig zijn in het bodem- of grondwater.

De mobiliteit van verontreinigingen is afhankelijk van hun verdeling over de immobiele vaste fase en de mobiele waterfase van de bodem en ondergrond. Veel verontreinigingen adsorberen (binden zich) sterk aan reactieve oppervlakken van de immobiele vaste fase en worden daarom vaak verondersteld weinig mobiel te zijn. De mobiele waterfase bevat echter ook reactieve oppervlakken in de vorm van kleine deeltjes, colloïden en grote moleculen. Verontreinigingen kunnen zich binden aan deze zogenaamde “dragers” en op deze manier kan hun mobiliteit sterk veranderen.

Het is niet gemakkelijk om te ontdekken of, en in welke omstandigheden dragers een belangrijke manier zijn voor transport van verontreinigingen. Verontreinigingen binden zich aan dragers, maar doordat de dragers zelf ook reactief zijn verdelen zij zich ook over de mobiele waterfase en de immobiele vaste fase. Verder binden verontreinigingen zich ook nog aan de vaste fase. We hebben dus te maken met een gecompliceerd systeem. Om de mobiliteit van verontreinigingen te kunnen voorspellen is er meer kennis nodig van het gedrag van dragers en van het gedrag van verontreinigingen in een systeem waar dragers aanwezig zijn.

Het doel van dit onderzoek was om mechanismen die van belang zijn bij het transport van reactieve dragers en verontreinigingen in grondwater systemen te bepalen en te beschrijven. Dit is gedaan door middel van een proces van modelontwikkeling,

modeltoepassing en modevaluatie..

In dit onderzoek is de nadruk gelegd op het gedrag van mobiel natuurlijk organisch materiaal (NOM). Dit is een veel voorkomende drager in bodem- en grondwater. Mobiel NOM, ook wel opgelost organisch materiaal genoemd, is een mengsel van verschillende moleculen. Het kunnen simpele kleine organische zuren zijn, zoals citroenzuur, tot grote ingewikkelde humusmoleculen.

### **Het gedrag van verontreinigingen in een systeem met dragers**

In het eerste deel van dit proefschrift (hoofdstuk 2 en 3) is het gedrag van verontreinigingen bestudeerd in een systeem met een constante concentratie van dragers. Er is evenwicht bereikt tussen de vaste fase van het systeem en “één type drager” (steady state). Zoals al geschetst hebben we te maken met een gecompliceerd systeem waarin verschillende interacties van belang kunnen zijn. Hierdoor is het moeilijk om te ontdekken waardoor het gedrag van verontreinigingen bepaald wordt. Om hier meer zicht op te krijgen werd een model ontwikkeld dat zowel het transportgedrag van dragers als van verontreinigingen beschrijft. Met behulp van dit model werd het gedrag van verontreinigingen bestudeerd.

Met behulp van modelsimulaties is het effect van reactiesnelheidsconstanten en niet-lineariteit op het gedrag van verontreinigingen bestudeerd (Hoofdstuk 2). Door de reactiesnelheidsconstanten van verontreiniging-drager en van drager-vaste fase reacties te variëren werd getoond dat voor beide reacties een gebied van reactietijden bestaat waarin tijdsafhankelijke reacties het gedrag van verontreinigingen bepalen. Om transportprocessen in dit gebied te beschrijven is het nodig om modellen te gebruiken die dynamische sorptieprocessen meenemen, zoals COLTRAP. Transport op en voorbij de grenzen van dit gebied kan met evenwichtsvergelijkingen worden berekend.

Met behulp van het model werd ook een experiment geïnterpreteerd dat is uitgevoerd onder grondwatercondities (Hoofdstuk 3). In dit experiment werd het transport van een radionuclide (americium) gebonden aan natuurlijk organisch materiaal (NOM) gevolgd in een kolom met aquifer materiaal. Het transport van americium in dit experiment was bijna ongeretardeerd en de doorbraak van de americium piek werd gevolgd door een lage concentratie van americium gedurende een lange tijd. Dit resultaat kon alleen maar

worden gesimuleerd wanneer zowel langzame adsorptiesnelheidsconstanten tussen americium en NOM en tussen NOM en de vaste fase werden aangenomen. Alle andere parameters waren vast. Dit geeft aan dat tijdsafhankelijke adsorptiereacties daadwerkelijk belangrijk zijn onder aquifer condities.

## Het gedrag van dragers

In het tweede deel van dit proefschrift werd aandacht besteed aan het adsorptiegedrag van NOM. Dit is een veel voorkomende drager in bodem- en grondwater. In het eerste deel (hoofdstuk 2 en 3) werden situaties beschreven waarin er evenwicht is ontstaan tussen dragers en de vaste fase. Echter, toepassing van het model voor het transport van NOM in situaties waar deze “steady state” verstoord was leverde problemen op. Uit de literatuur bleek verder dat het adsorptiegedrag van een NOM mengsel niet adequaat beschreven en begrepen kan worden met behulp van simpele evenwichtsmodellen, zoals het Langmuir model. Daarom is extra aandacht besteed aan het adsorptiegedrag van NOM.

Een aantal potentieel optredende mechanismen werden onderzocht en het bleek dat alleen het meenemen van de heterogeniteit van het NOM mengsel een verklaring opleverde voor geobserveerde verschijnselen zoals schijnbare hysteresis en een zeer langzaam toenemend adsorptiemaximum.

De heterogeniteit van NOM beïnvloedt het adsorptiegedrag van het mengsel als geheel. NOM bestaat uit verschillende moleculen met verschillend adsorptiegedrag. Doordat de moleculen op dezelfde plaatsen op het oppervlak kunnen binden, vindt er competitie plaats en is hun gedrag dus gekoppeld. Kleine moleculen zullen maar een of een paar plaatsen bezetten. Grote moleculen, echter, kunnen een groot deel van het oppervlak bedekken. De grote moleculen kunnen zich ook gedeeltelijk in de oplossing uitstrekken en zogenaamde lussen en staarten vormen.

Ook voor het gedrag van NOM is een model ontwikkeld (hoofdstuk 4). Hierin werd het competitieve tijdsafhankelijke adsorptie/desorptie gedrag van een NOM mengsel op een homogeen oppervlak beschreven. Het NOM mengsel werd verondersteld te bestaan uit een aantal subcomponenten. Om te voorkomen dat voor elke individuele subcomponent modelparameters bepaald en bijgesteld moesten worden, werd een methode ontwikkeld om

## SAMENVATTING

het aantal te schatten parameters van het model te beperken. Deze methode gaat ervan uit dat er relaties bestaan tussen de karakteristieken van de individuele NOM moleculen, zoals molecuulgewicht en hydrofobiteit, en modelparameters.

Met behulp van het ontwikkelde model en de relaties was het mogelijk om het adsorptiegedrag van een NOM mengsel aan een kunstmatig oxide oppervlak te beschrijven in een set van experimenten, zonder dat modelparameters werden aangepast. Door het gebruik van bovengenoemde relaties hoefde er maar 2 coëfficiënten gefit te worden aan de beschreven experimenten. Alle andere waarden konden onafhankelijk worden geschat. Ook was het mogelijk om eigenschappen van NOM adsorptie en desorptie geobserveerd in de literatuur te begrijpen.

Het ontwikkelde model werd toegepast in verschillende experimenten met natuurlijk aquifer materiaal om te testen of het geschikt is om het gedrag van een NOM mengsel te beschrijven in grondwatersystemen, wanneer er ook transport is en wanneer dit transport plaatsvindt over grote tijd en lengte schalen (door een groot volume grond) zoals gevonden wordt in het veld (hoofdstuk 5).

Het model werd gekalibreerd met behulp van laboratorium batch experimenten met aquifer materiaal. De adsorptie van een NOM mengsel als functie van de concentratie en van tijd werd goed beschreven in batch. Met behulp van het gekalibreerde adsorptie model geïncorporeerd in een transport model kon het transport van NOM in kolomexperimenten goed worden voorspeld.

Omdat de omstandigheden in de kolomexperimenten niet representatief zijn voor een veldsituatie werd het gedrag van NOM onder veldomstandigheden gesimuleerd met behulp van het gekalibreerde model. Variaties in watersnelheid en de afstand van transport bleken de vorm van de gesimuleerde NOM doorbraakcurves sterk te beïnvloeden doordat zij bepalen in hoeverre evenwicht benaderd wordt in de gesimuleerde tijdschaal. Naarmate evenwicht meer bereikt werd, werden de multicomponent eigenschappen van NOM transport steeds meer zichtbaar. Aanwezigheid van NOM op het sorptiecomplex bleek versnelde doorbraak tot gevolg te hebben. Aanwezigheid van LMW NOM op het sorptiecomplex beïnvloedde voornamelijk de omwisseling van NOM subcomponenten. Adsorptieplaatsen bezet met HMW NOM verminderde de adsorptiecapaciteit, doordat HMW niet significant desorbeert en dus adsorptieplaatsen blokkeert.

Uiteindelijk werd NOM transport in een veldexperiment gesimuleerd met behulp van het model. Om dit te kunnen doen werd het 3-D stroompatroon in het veldexperiment

benaderd met een aantal stroombanen, zodat simulatie met behulp van een 1-D transportmodel mogelijk was. Verder was het nodig om een aantal aannames te doen voor de initiële toestand in het veld. Het verloop van de gemeten doorbraakcurves van zowel het NOM mengsel als de NOM subcomponenten in het veldexperiment konden goed worden beschreven met behulp van het model. Het binnenkomend HMW NOM bleek zich sterk aan het aquifer materiaal te binden terwijl er zelfs LMW NOM van het aquifer materiaal vrij kwam.

Het model ontwikkeld in hoofdstuk 4 bleek dus bruikbaar te zijn voor de beschrijving van adsorptie/desorptie gedrag aan natuurlijke media in zowel transport experimenten in het lab en het veld. Het model is geschikt om adsorptie/desorptie van NOM te beschrijven over grote tijd en ruimteschalen en is dus bruikbaar in praktijksituaties. De dynamische competitieve sorptieprocessen beschreven in het model blijken relevant te zijn zowel in laboratorium batch experimenten uitgevoerd met een paar gram grond en enkele tientallen milliliters water, als in het veld met lange reistijden, grote volumes grond en over afstanden van enkele meters.

## **Tijdsafhankelijke sorptie**

Als de duur van een experiment langer is dan de reactietijden in het systeem dan zullen alle reacties in evenwicht zijn. Dit geldt ook voor transport. Wanneer in een systeem de reistijd van verontreinigingen of dragers langer is dan hun reactietijd, dan zal er evenwicht bereikt worden en kan de tijdsafhankelijkheid van reacties verwaarloosd worden in dit systeem. De reistijd van een stof wordt bepaald door de watersnelheid en de lengte waarover transport wordt bestudeerd. Voor grondwatersystemen wordt vaak aangenomen dat niet evenwichtseffecten verwaarloosd kunnen worden omdat de watersnelheden over het algemeen laag zijn. Typische reistijden in grondwater over een afstand van 1 meter variëren tussen 10 en 1000 uur (meer dan een maand).

In hoofdstuk 3 zagen we dat in een experiment onder aquifer condities met een reistijd van 10 uur, tijdsafhankelijke sorptie een belangrijke rol speelt voor zowel de reactie tussen verontreiniging en drager en voor de reactie tussen drager en vaste fase. Dit geeft aan dat onder aquifercondities tijdsafhankelijke sorptie wel degelijk van belang kan zijn.

In hoofdstuk 5 zagen we dat bij reistijden van 80 uur nog steeds geen totaal evenwicht bereikt werd tussen een NOM mengsel en aquifer materiaal. Door hun verschillende reactietijden bereiken verschillende subcomponenten evenwicht na verschillende reistijden. In Figuur 5 van dit hoofdstuk zien we dat bij reistijden van 1 uur evenwicht tussen de relatief snel reagerende NOM met een laag molecuul gewicht (LMW) bereikt wordt. Bij reistijden van 80 uur lijken alle subcomponenten in evenwicht. Toch vindt er nog zeer langzame redistributie plaats van subcomponenten doordat de relatief langzaam reagerende NOM met een hoog molecuul gewicht (HMW) nog steeds geen volledig evenwicht hebben bereikt. Totaal evenwicht en dus een “steady state” situatie wordt pas bereikt wanneer de langzaamste subcomponent in evenwicht is met het aquifer materiaal. Figuur 4 van Hoofdstuk 4 laat dezelfde fenomenen in een batchexperiment zien.

Figuur 4 laat ook zien dat door competitie totaal evenwicht veel langzamer bereikt wordt dan verwacht op basis van de reactiesnelheidsconstanten van de langzaamste subcomponent. Wanneer er meer competitie is (bij de hogere totaal concentratie van NOM) verminderen de reactiesnelheden van de langzaamste subcomponenten aanzienlijk. Met behulp van Vergelijking 2 in Hoofdstuk 5 kan dit verklaard worden. Uit deze vergelijking blijkt dat de adsorptiesnelheid van een subcomponent onder andere bepaald wordt door de fractie van bezette adsorptieplaatsen. Wanneer er sprake is van multi-component sorptie zal de aanwezigheid van concurrerende subcomponenten daardoor de adsorptiesnelheden verkleinen. Dit effect zal het grootst zijn voor de langzame (HMW) subcomponenten omdat alle andere subcomponenten het sorptiecomplex sneller bezetten.

In hoofdstuk 5 zien we ook dat langzame desorptiereacties een rol spelen. In sommige situaties kan adsorptie van NOM zelfs als onomkeerbaar beschouwd worden. Bij reistijden van 80 uur kan de desorptie van het relatief langzaam reagerende HMW NOM, dat initieel op het aquifer materiaal aanwezig is, verwaarloosd worden. Adsorptieplaatsen die al bezet zijn met HMW NOM kunnen dan worden gezien als geblokkeerd.

In dit proefschrift is dus aangetoond dat tijdsafhankelijke sorptiereacties van zowel reactieve verontreinigingen als reactieve dragers relevant zijn, zelfs onder aquifer condities. De kennis van adsorptie en desorptie snelheden en de factoren die deze snelheden bepalen is echter gelimiteerd. Tijdsafhankelijke desorptie van aan dragers gebonden verontreinigingen kan de mobiliteit van deze verontreinigingen aanzienlijk veranderen. Om risico's beter in te kunnen schatten is er meer onderzoek nodig op dit gebied.

## **Multicomponent sorptie**

In hoofdstuk 4 en 5 hebben we laten zien dat het gedrag van een NOM mengsel alleen maar begrepen kan worden wanneer het heterogene karakter van dit mengsel wordt meegenomen. De verschillende subcomponenten van het mengsel zullen verschillen in hun affiniteit, hun reactiesnelheidsconstanten en hun adsorptiemaxima. Daardoor wordt adsorptie en transportgedrag van een NOM mengsel gekarakteriseerd door een gecompliceerd proces van tijdsafhankelijke adsorptie/desorptie en redistributie tussen de verschillende subcomponenten. Omdat tijdsafhankelijke sorptie en heterogeniteit van het mengsel niet apart van elkaar kunnen worden gezien zijn een deel van de eigenschappen hierboven al beschreven onder het kopje tijdsafhankelijke sorptie. In langdurige experimenten of bij lange reistijden zullen de verschillende subcomponenten uiteindelijk allemaal evenwicht bereikt hebben en kan het multicomponent gedrag apart bestudeerd worden.

In hoofdstuk 4 wordt getoond dat door het multicomponent karakter van NOM adsorptie de verdeling van het NOM subcomponenten over vaste en waterfase afhankelijk is van de oppervlakte/volume verhoudingen, de totale hoeveelheid NOM toegevoegd aan het systeem en van de totale adsorptiecapaciteit.

In hoofdstuk 5, Figuur 5 is het duidelijk dat bij toename van de reistijden de niet-evenwicht eigenschappen steeds meer verdwijnen en de multi-component transport eigenschappen van het NOM mengsel steeds duidelijker zichtbaar worden. De gesimuleerde doorbraakcurves van de subcomponenten laten zien dat na de introductie van een NOM mengsel, de evenwichtssamenstelling van het effluent telkens verschuift.

Het is gebleken dat de heterogeniteit van NOM het adsorptiegedrag van NOM sterk bepaald. De heterogeniteit van NOM kan hierdoor ook de mobiliteit van verontreinigingen en NOM in grondwatersystemen beïnvloeden. Andere typen dragers zijn hoogstwaarschijnlijk ook heterogene mengsels. Daardoor kunnen de hier geobserveerde fenomenen (deels) ook geldig zijn voor dragers in het algemeen, aannemende dat adsorptie het concentratie regulerende proces voor deze dragers is.

## **Modelleeraanpak**

Met behulp van de modelleeraanpak in dit proefschrift konden 2 belangrijke relevante mechanismen onderscheiden worden: tijdsafhankelijke adsorptie van zowel verontreinigingen als dragers en de tijdsafhankelijke multicomponent sorptie van een dragers veroorzaakt door hun heterogene karakter. Door het meenemen van deze mechanismen in modellen is het begrip van het transport van verontreinigingen en dragers in zowel het lab als het veld aanzienlijk vergroot

Met behulp van de hier gebruikte modelleeraanpak was het mogelijk om van de laboratoriumschaal naar het veld te gaan. Het zou ideaal zijn als het gedrag van verontreinigingen en dragers begrepen, beschreven en voorspeld zou kunnen worden met behulp van laboratoriumexperimenten. Laboratorium experimenten zijn namelijk redelijk snel en minder complex dan experimenten in het veld. Verder is het in deze experimenten relatief gemakkelijk om de experimentele condities te controleren. Echter de tijd- en ruimteschaal en soms ook de oppervlakte/volume verhouding in laboratorium experimenten zijn vaak anders dan in het veld. Daarom moeten de geobserveerde processen zo beschreven worden dat ze geschikt zijn om situaties te beschrijven die sterk variëren in schaal. In hoofdstuk 5 werd getoond dat het in dit proefschrift ontwikkelde model toegepast kon worden in sterk variërende omstandigheden. Blijkbaar zijn de procesbeschrijvingen en aannames ook geldig in het veld en worden ze niet door andere processen overvleugeld. Om het veldexperiment te beschrijven moesten er wel extra complicerende factoren worden meegenomen. We moesten een oplossing vinden voor het beschrijven van de samenstelling van een mengsel van water dat over verschillende afstanden en met verschillende snelheden gereisd had. Dit hebben we gedaan door transport langs een aantal stroombanen te veronderstellen en te simuleren. Verder moest de initiële bezetting van het adsorptiecomplex worden ingeschat. Hiervoor hebben we aangenomen dat er evenwicht bestond tussen NOM gebonden aan de aquifer en in het grondwater.

In hoofdstuk 4 en 5 werd een methode toegepast om het aantal onbekende parameters te verminderen. Er werden relaties gedefinieerd tussen de subcomponenten en de parameters die het modelresultaat beïnvloeden. Deze relaties werden gebaseerd op observaties en trends uit de literatuur. Dit bleek een succesvolle aanpak. In dit onderzoek werden relaties gedefinieerd tussen enerzijds het adsorptiemaximum, de affiniteit en de

reactiesnelheidsconstanten en aan de andere kant het molecuulgewicht. Tussen de affiniteit van hydrofoob en hydrofiel NOM werd een constante verhouding verondersteld. Deze empirische relaties tussen de eigenschappen van NOM subcomponenten en modelparameters zijn interessante uitgangspunten voor verder onderzoek.

## **Implicaties voor het transport van verontreinigingen en dragers in grondwatersystemen**

Met betrekking tot het transport van NOM kunnen 2 situaties onderscheiden worden. Situaties waarin totaal evenwicht is bereikt tussen NOM in oplossing en gebonden aan de vaste fase waardoor er een “steady state” situatie is ontstaan en situaties waarin dit niet het geval is.

### *Steady state*

Dit type situatie wordt bestudeerd in hoofdstuk 2 en 3. Wanneer er evenwicht bestaat tussen NOM gesorbeerd aan de vaste fase en NOM in oplossing vertonen alle NOM species hetzelfde schijnbaar inerte transportgedrag. Het transportgedrag is schijnbaar inert omdat er nog steeds uitwisseling plaatsvindt tussen NOM in oplossing en NOM geadsorbeerd. De uitwisseling van HMW NOM moleculen zal relatief langzaam zijn en mogelijk zelfs verwaarloosbaar, terwijl de uitwisseling van LMW NOM relatief snel kan zijn. In termen van NOM concentratie is het netto resultaat van de uitwisseling nihil. Echter, wanneer er NOM met verontreinigingen (gelabeld NOM) het systeem binnen komt, heeft deze uitwisseling uitgedrukt in de concentratie van de verontreiniging wel degelijk invloed. Het in hoofdstuk 3 beschreven experiment illustreert dit duidelijk. Hoewel er hier evenwicht bestaat tussen mobiel en immobiel NOM, veroorzaakt de langzame uitwisseling tussen mobiel en immobiel NOM een nalevering van een zeer lage concentratie americium gedurende een zeer lange periode.

In hoofdstuk 3 werd maar 1 NOM specie verondersteld. Het transportgedrag van de verontreiniging kon hiermee naar tevredenheid beschreven worden. Dit zou er op kunnen wijzen dat in gevallen van evenwicht tussen mobiel en immobiel NOM het niet nodig is om NOM als een mengsel te beschouwen.

### *Geen “steady state”*

Wanneer er geen evenwicht bestaat tussen NOM in oplossing en gesorbeerd aan de vaste fase, dan zal de samenstelling van het NOM mengsel dat het systeem binnen komt veranderen gedurende transport. Dit betekent ook dat de eigenschappen voor transport van verontreinigingen zullen variëren in de tijd en afstand langs stroombanen. Afhankelijk van de samenstelling van het binnenkomende NOM en de NOM aan het complex kunnen er verschillende dingen gebeuren.

In hoofdstuk 5 is gekeken naar de doorbraak van een NOM mengsel in een systeem met weinig of geen NOM aanwezig. We zien hier dat HMW NOM sterk aan het aquifer materiaal gebonden wordt terwijl LMW in mindere mate gebonden wordt aan het aquifer materiaal. In het veldexperiment komt er zelfs LMW NOM van het aquifer materiaal vrij. Interpretatie van het gedrag van het NOM mengsel opgevat als het gedrag van één gemiddelde specie zou dit kunnen leiden tot verkeerde conclusies en een verkeerde beschrijving van bijvoorbeeld het gedrag van verontreinigingen gebonden aan dit NOM mengsel. Het gedrag van het mengsel wordt gekarakteriseerd door weinig retardatie en een groot verlies aan massa. Het grote verlies in massa wordt in sterke mate bepaald door het gedrag van HMW NOM. De weinige retardatie echter wordt voornamelijk bepaald door LMW NOM.

Door het verschil in transportgedrag van de NOM subcomponenten kan de verdeling van verontreinigingen over verschillende NOM subcomponenten ook bepalend zijn voor hun transport gedrag. Dit is een interessant onderwerp voor verder onderzoek. Verder kunnen de multicomponent adsorptieprocessen gevonden voor NOM ook significant zijn voor verontreinigde locaties, zoals locaties waar afval is gedumpt. Hier vindt transport van mengsels van verschillende soorten meer of minder toxische (organische) moleculen plaats gelijktijdig met het transport van NOM. In deze situaties is het mogelijk dat (een deel van ) de organische moleculen zich als NOM gedragen. Zij kunnen concurreren voor dezelfde adsorptieplekken op het oppervlak en kunnen ook als drager voor verontreinigingen fungeren.

## **Implicaties voor het bepalen van risico's**

De twee belangrijkste relevante mechanismen in dit onderzoek zijn de tijdsafhankelijke adsorptie en de dynamische competitieve sorptie van een heterogeen drager mengsel. Deze mechanismen beïnvloeden het transport van verontreinigingen en dragers in grondwatersystemen en beïnvloeden daardoor ook het risico voor de volksgezondheid en voor ecosystemen.

De belangrijkste conclusie die we uit dit onderzoek kunnen trekken is dat door de mechanismen gevonden in dit onderzoek, het transport van verontreinigingen en daardoor de risico's voor de volksgezondheid en voor ecosystemen in bepaalde situaties veel groter zijn dan wordt verwacht als je deze mechanismen verwaarloost. Een radionuclide, zoals americium, dat sterk gebonden is aan NOM en dat maar langzaam desorbeerd (zie hoofdstuk 3), kan in natuurlijke situaties ongeremd door de bodem bewegen, wanneer de watersnelheden relatief hoog zijn en er sprake is van veel competitie met andere (natuurlijke) organische moleculen. In deze situatie is als gevolg van de in dit proefschrift beschreven mechanismen het risico dat deze sterk toxische stof een bepaalde plek bereikt zeer groot.



# Nawoord

Mijn proefschrift is af! Het is het resultaat van jaren werk. Maar het is geen weergave van deze periode. Daarom wil ik in dit nawoord een kijkje achter de schermen geven, en natuurlijk ook een aantal mensen die van belang waren in het tot stand komen van dit proefschrift bedanken.

In 1995 liep mijn contract bij het RIVM af. De projecten waaraan ik werkte waren afgerond. Een logisch vervolg zou het zoeken van een nieuwe baan zijn. Of toch niet? Na lang overwegen werd mijn weg duidelijk. Ik zou de plannen die ik had om te promoveren op het onderzoek bij het RIVM doorzetten. Ik heb het onderzoek voortgezet op de vakgroep Bodemkunde en Plantenvoeding van de Landbouwniversiteit.

De afgelopen jaren waren een intensieve en vruchtbare periode. Zowel in mijn werkzaamheden, in mijn onderzoek als in mijn leven. De geboorte van Rianne, Wouter en Mirjam waren de hoogtepunten van deze periode.

De dagen van mijn onderzoek werden voornamelijk gevuld met literatuur lezen, interpreteren van experimenten, programmeren, simuleren en schrijven. Lange periodes van uitproberen en aanpassen waren geen uitzondering. En dan opeens, ..., inspiratie, inzicht, nieuwe ideeën. Ja, het valt op z'n plek. Hier voor u ligt het resultaat.

Mijn beide promotoren hebben een belangrijke rol gespeeld in mijn onderzoek. Toon, ik dank je voor de geweldige stimulans en het plezier dat je me in het onderzoek gegeven hebt. Ik heb op velerlei vlak veel van je geleerd. Willem, ik dank je voor je scherpzinnigheid. In je zoektocht naar helderheid hielp je mij om mijn ideeën helder te verwoorden. Zonder jouw steun en hulpvaardigheid in praktische zaken had ik dit onderzoek nooit kunnen afronden.

Mijn collega's dank ik voor de prettige werkomgeving. In het bijzonder wil ik Jeroen noemen. Je was een gezellige kamergenoot. We hebben veel gepraat, soms over wetenschap, meestal over andere dingen. Onze wekelijkse wandeling door het Arboretum is inmiddels een traditie geworden.

Hoewel het grootste deel van mijn onderzoek in werktijd is gedaan, had het proefschrift niet op deze manier voor u gelegen als ik niet de steun had gehad van een aantal vrienden en familieleden: MaPa, Rianne (tante), Ralf en Kitty bedankt. MaPa, jullie hebben me de mogelijkheid gegeven en me gestimuleerd om te gaan studeren. Arnold, ik

dank jou voor wie je bent en voor al de ruimte die je geeft. Je bent een stille helper aan de zijlijn. Jouw kritische vragen hielpen me om op het goede spoor te blijven. Rianne, Wouter en Mirjam, door wie jullie zijn, hielpen jullie me om mijn onderzoek te relativeren.

Terugkijkend is het een goede en leerzame periode geweest. Ik heb mijn eigen creativiteit ontdekt en heb geleerd om mijn weg te blijven volgen. Ik draag het boekje op aan mijn grootste Inspiratiebron.

*Rilke*

## **The River**

(Victoria Shaw, Garth Brooks)

You know a dream is like a river  
Ever changin` as it flows  
And a dreamer's just a vessel  
That must follow where it goes  
Trying to learn from what's behind you  
And never knowing what's in store  
Makes each day a constant battle  
Just to stay between the shores

Too many times we stand aside  
And let the waters slip away  
'Til what we put off 'til tomorrow  
Has now become today  
So don't you sit upon the shoreline  
And say you're satisfied  
Choose to chance the rapids  
And dare to dance the tide

I will sail my vessel  
'Til the river runs dry  
Like a bird upon the wind  
These waters are my sky  
I'll never reach my destination  
If I never try  
So I will sail my vessel  
'Til the river runs dry

And there's bound to be rough waters  
And I know I'll take some falls  
But with the good Lord as my captain  
I can make it through them all



# Curriculum vitae

Rikje (Hendrika) van de Weerd werd op 27 november 1966 geboren in Heteren. Na het doorlopen van de lagere school in Oosterbeek behaalde ze het VWO diploma in 1985 aan het van Lingen college te Arnhem. In September 1985 begon ze aan de studie Milieuhygiëne aan, toen nog, de Landbouwhogeschool te Wageningen. In 1991 rondde zij deze studie af met afstudeervakken hydrogeologie en bodemhygiëne en -verontreiniging en een praktijktijd bij het RIVM. Tijdens deze praktijktijd deed zij onderzoek naar het adsorptie- en transportgedrag van pesticiden in aquifer materiaal.

Vanaf 1991 tot 1995 werkte zij op het Laboratorium voor Bodem- en Grondwateronderzoek (LBG) van het RIVM binnen 2 internationale projecten. Zij werkte aan de modellering van de vorming en de verandering van uraniumerts in de ondergrond van een locatie in Australië met geohydrologische, geochemische en stoftransport modellen. Verder werkte ze aan de ontwikkeling van een model voor simultaan transport van verontreinigingen en colloïden met alle mogelijke interacties. Dit laatste onderwerp vormde de basis voor haar promotieonderzoek.

Van 1995 tot 2000 werkte zij aan haar promotieonderzoek op de vakgroep Bodemkunde en Plantenvoeding van de Landbouwuniversiteit Wageningen. Gedurende deze periode bepaalde en beschreef ze belangrijke mechanismen bij het transport van reactieve dragers en verontreinigingen met behulp van modellen en simulaties van reeds uitgevoerde experimenten. De belangrijkste resultaten van dit promotieonderzoek zijn vastgelegd in dit proefschrift.

In 1996 en 1997 was zij 12 maanden aangesteld als toegevoegd onderzoeker. In deze periode deed zij onderzoek naar het belang van opgeloste organische stof voor het transport van verontreinigingen in de Nederlandse praktijk. In 1998 was zij 7 maanden aangesteld als projectmedewerker onderwijs. In deze periode werkte ze aan het opzetten van een via internet toegankelijke cursus ECOSAT bestaande uit met behulp van de computer opgenomen instructiefilmpjes.

In januari 1996, augustus 1997 en juli 1999 werd zij moeder van achtereenvolgens Rianne, Wouter en Mirjam.



# List of publications

- Van de Weerd H., van Riemsdijk W.H. and Leijnse A. 2000. Modelling transport of a mixture of Natural Organic Molecules (NOM): effect of dynamic competitive sorption from particle to aquifer scale. submitted to *Water Resour Res.*
- Leijnse A., van de Weerd H. and Hassanizadeh S.M. 2001. Modelling of radionuclide transport in Koongarra, Australia: The effect of a moving weathering zone. *Math. Geol.* 33 (in press)
- Van de Weerd H., van Riemsdijk W.H. and Leijnse A. 1999. Effect of Physical and chemical heterogeneity on the adsorption desorption behaviour of NOM. *Environ. Sci. Technol.* 33(10), 1675-1681.
- Van de Weerd H. and Temminghoff E.J.M. 1999. Spaghetti als vervoermiddel voor verontreinigingen? Verspreiding niet in the schatten met standaard Kd-waarde. *Bodem*, 9(1), 41-43.
- Van de Weerd H., Leijnse A. and van Riemsdijk W.H. 1998. Transport of reactive colloids and contaminants in groundwater: effect of non-linear kinetic interactions. *J. Contam. Hydrol.*, 32, 313-331.
- Van de Weerd H. and Leijnse A. 1998. Development of a model for coupled colloid and contaminant transport (COLTRAP). Bilthoven, RIVM rapport nr. 715401002.
- Van de Weerd H. and Leijnse A. 1997. Assessment of the effect of kinetics on colloid facilitated radionuclide transport in porous media. *J. Contam. Hydrol.*, 26, 245-256.
- Van de Weerd H. and Leijnse A. 1997. Development of a model for coupled colloid and contaminant transport. In: Development of a model for radionuclide transport by colloids in the geosphere, Van der Lee et al. EUR 17480, 123-180.
- Van de Weerd H. and Leijnse A. 1996. Parameter estimation for kinetic interactions during colloid-facilitated transport in a porous medium. In: Calibration and Reliability in Groundwater Modelling, Kovar, K and P. van der Heijde (eds). IAHS Publication No. 237.
- Van der Toorn R..A. and van de Weerd H. 1995. Transport of pollutants through porous media facilitated by colloids: Mathematical analysis of the case without diffusion and dispersion (Hyperbolic case). Bilthoven, RIVM rapport nr. 715203001.
- Van de Weerd H., Leijnse A., Hassanizadeh S.M. and Richardson-van der Poel M.A. 1994. INTRAVAL phase 2, test case 8 - Alligator Rivers Natural Analogue - Modelling of uranium transport in the weathered zone at Koongarra (Australia), final report; Bilthoven, RIVM rapport nr. 715206005.
- Van de Weerd H. and Fraters B. 1994. General knowledge of groundwater colloids. In: A bibliographical review of colloid transport through the geosphere. EUR 15481, 3-11.
- Richardson-van der Poel M.A., van de Weerd H. and Hassanizadeh S.M. 1994. In: Fifth CEC Natural Analogue Working Group meeting and Alligator Rivers Analogue Project (ARAP) final workshop. Proceedings of an international workshop held in Toledo, Spain from 5 to 9 October 1992. H. von Maravic and J. Smellie (eds). EUR 15176, 365-372.
- Van de Weerd H., Hassanizadeh S.M. and Richardson-van der Poel M.A. 1993. INTRAVAL phase 2, test case 8 - Alligator Rivers Natural Analogue - Modelling of uranium transport in the weathered zone at Koongarra (Australia), progress report; Bilthoven, RIVM rapport nr. 725206010.
- Wijland G.C., Bockting G.J.M. and van de Weerd H. 1992. INTRAVAL test case 8 – Geochemical modelling of the Uranium mobility in the weathered zone of the Alligator Rivers Koongarra Ore deposit (Australia); Bilthoven, RIVM rapport nr. 725206006.
- Van de Weerd H. and van der Linden A.M.A. 1991. Behaviour of pesticides in aquifer materials: interpretation of an *in situ* experiment; Bilthoven, RIVM rapport nr. 725502004.